

**The functional characterization of AtStr5, a  
member of the sulfurtransferase/rhodanese  
family of *Arabidopsis thaliana*, and its arsenic  
phytoremediation studies**

Von der Naturwissenschaftlichen Fakultät  
der Gottfried Wilhelm Leibniz Universität Hannover  
zur Erlangung des Grades

**Doktorin der Naturwissenschaften**

Dr. rer. nat.

**genehmigte Dissertation**

**von**

**Most. Shanaj Parvin, M. Sc. (The Netherlands)**

geboren am 10.02.1981 in Panchagarh, Bangladesh

**2018**

Referentin: Prof. Dr. rer. nat. Jutta Papenbrock

Korreferent: Prof. Dr. rer. Bernd Huchzermeyer

Tag der Promotion: 27.09.2018

## ERKLÄRUNG

aus:

Gemeinsame Ordnung für die Promotion zur Doktorin der Naturwissenschaften oder zum Doktor der Naturwissenschaften (Dr. rer. nat.) an der Gottfried Wilhelm Leibniz Universität Hannover (25.03.2013), § 8 Dissertation, (3):

**A:**

„[...]<sup>2</sup> Es ist eine ausführliche Darstellung voranzustellen, die eine kritische Einordnung der Forschungsthemen und wichtigsten Erkenntnisse aus den Publikationen in den Kontext der wissenschaftlichen Literatur zum Thema vornimmt [...]“

**Die voranzustellende ausführliche Darstellung ist in dieser Arbeit aufgeteilt in die Kapitel 1 und 6.**

**B:**

„[...] sowie die individuellen eigenen Beiträge und ggf. die Beiträge weiterer Autoren an den jeweiligen Publikationen darlegt.“

**Chapter II:** Most, P., & Papenbrock, J. (2015): Possible roles of plant sulfurtransferases in detoxification of cyanide, reactive oxygen species, selected heavy metals, and arsenate. *Molecules*, 20(1), 1410-1423.

The structure of the review was designed by J. Papenbrock. In all other aspects, both authors contributed equally to this article.

**Chapter III:** Characterization of group III *Arabidopsis* sulfurtransferase 5 proteins

The comprehensive idea and the design of the experiment were developed by J. Papenbrock. The experiments were conducted by Most. Parvin as well as the data analysis. The chapter was written by Most. Parvin and reviewed by J. Papenbrock.

**Chapter IV:** Simultaneous overexpression of *Arabidopsis* sulfurtransferases AtStr5, AtStr17a, and the phytochelatin synthase protein AtPCS1 in *Arabidopsis thaliana*, an approach to improve arsenic phytoremediation

The general idea of the experiments was developed by Most. Parvin and J. Papenbrock. The experimental methods were illustrated by Most. Parvin and J. Papenbrock. The experiments were conducted by Most. Parvin. The chapter was written by Most. Parvin and reviewed by J. Papenbrock.

**Chapter V:** Heterologous overexpression of AtStr5 and AtStr17a in rolB-AtPCS1 overexpressing *Nicotiana tabacum* for arsenic phytoremediation study

The experimental idea and the detail design of the experiment were developed by J. Papenbrock and Most. Parvin. The experiments were conducted by Most. Parvin. The chapter was written by Most. Parvin and reviewed by J. Papenbrock.

## SUMMARY

The AtStr5 shares the similar structural association with the enzyme families of phosphatase and arsenate reductase and thus arises the functional conflation of this protein. The result showed in the present study is the first attempt to functionally and biochemically characterized the AtStr5 protein and decode its role, whether it is phosphatase (Arath; CDC25) or arsenate reductase (AtACR2). For enzymatic characterization, the single rhodanese domain carrying AtStr5 protein was overexpressed in *Escherichia coli*. In enzymatic determination, the AtStr5 protein showed phosphatase activity over sulfurtransferase. Despite its ability to catalyze the phosphate-rich substrates, such as 3-OMFP and pNPP, the kinetic parameters ( $K_m$ ,  $k_{cat}$ , and  $k_{cat}/K_m$ ) of AtStr5 were shown remarkably lower values than the human CDC25B protein. Therefore the mitotic inducer role (as Arath; CDC25) of AtStr5 is questionable. To analyze the *in vivo* function of AtStr5 in *Arabidopsis* and to obtain more information about its putative substrate localization in the metabolic network, one full-length and two truncated versions of AtStr5 was fused both the 5' and 3' end of GFP. Transient expression of fusion constructs with the GFP in *Arabidopsis* protoplasts indicated localization of truncated AtStr5 fusion proteins are in the cell cytoplasm, whereas the localization of full-length AtStr5 has not been transparent. To elucidate the biological function of the AtStr5/AtACR2 protein *in vivo*, the overexpressing lines of this gene were produced. In parallel, the overexpressing lines of AtStr17a were also developed, since it has been identified as *High Arsenic content 1* (HAC1) or *Arsenic tolerance QTL 1* (AtATQ1) gene in *Arabidopsis* recently. Furthermore, the attempt has been taken to develop the co-overexpressing lines of *Arabidopsis phytochelatin synthase* (AtPCS1) gene with AtStr5/AtACR2 and AtStr17a/HAC1/ATQ1 genes to obtain maximum benefit from of the As phytoremediation process. To further explore the potentiality of ARs genes in the As phytoremediation process, the effort has been conducted to overexpress the AtStr5/AtACR2 and AtStr17a/HAC1/ATQ1 genes in AtPCS1 overexpressing *Nicotiana tabacum*. The transgenic *N. tabacum* overexpressing AtStr5/AtACR2<sup>oe</sup>-AtPCS1<sup>oe</sup> and AtStr17a/HAC1/ATQ1<sup>oe</sup>-AtPCS1<sup>oe</sup> genes can be directly used for As phytoremediation purposes.

**Keywords:** Sulfurtransferase; arsenate reductase; CDC25 phosphatase; *Arabidopsis thaliana*; *Nicotiana tabacum*

## ZUSAMMENFASSUNG

Das AtStr5-Protein teilt strukturelle Eigenschaften mit den Enzymfamilien der Phosphatasen, der Sulfurtransferasen und der Arsenat-Reduktasen, was zu Schwierigkeiten in der funktionellen Einordnung dieses Proteins führt. Die vorliegende Studie zeigt den Versuch, die Funktion dieses Proteins zu entschlüsseln, sei es als Phosphatase (Arath; CDC25), Arsenat-Reduktase (AtACR2) oder Sulfurtransferase. Für die enzymatische Charakterisierung wurde das AtStr5-Protein, das nur eine Rhodanese-Domäne enthält, in *Escherichia coli* überexprimiert. Enzymatische Bestimmungen zeigen, dass das AtStr5-Protein eine Phosphatase-Aktivität, aber keine Sulfurtransferase-Aktivität besitzt. Trotz seiner Fähigkeit die Phosphat-haltigen Substrate wie 3-OMFP und pNPP umzusetzen, zeigen die kinetischen Parameter ( $K_m$ ,  $k_{cat}$ , and  $k_{cat}/K_m$ ) der AtStr5 deutlich niedrigere Werte als das menschliche CDC25-Protein. Daher bleibt die Rolle von AtStr5 als mitotischem Induktor Arath;CDC25 fraglich. Informationen über die Lokalisierung des AtStr5-Proteins in der Zelle aufzuzeigen, wurden die Sequenzen codierend für das gesamte AtStr5-Protein sowie zwei am 5'-Ende verkürzte Sequenzen mit dem 5'-Ende der GFP-Sequenz fusioniert. Zur Lokalisierung der Fusionsproteine wurden die GFP-Fusionskonstrukte transient in *Arabidopsis*-Protoplasten exprimiert. Die Fusionsproteine mit verkürztem N-terminalen Ende wurden im Cytoplasma detektiert, während die Lokalisierung des vollständigen AtStr5-Proteins nicht eindeutig gezeigt werden konnte. Um die biologische Funktion des AtStr5/AtACR2-Proteins *in vivo* zu erhellen, wurden überexprimierende Pflanzen dieses Gens von *Arabidopsis* und *Nicotiana tabacum* hergestellt. Parallel wurden auch überexprimierende Pflanzen von AtStr17a produziert, da dieses Protein mit Sulfurtransferase-Domäne als *High Arsenic content 1 (HAC1)*- oder *Arsenic tolerance QTL 1 (AtATQ1)*-Gen vor kurzem in *Arabidopsis* identifiziert wurde. Außerdem wurde der Versuch unternommen, ko-überexprimierende Linien des *Phytochelatine Synthase (AtPCS1)*-Gens aus *Arabidopsis* und den Genen AtStr5/AtACR2 oder AtStr17a/HAC1/ATQ1 von *Arabidopsis*- und *Nicotiana tabacum*-Pflanzen zu erzeugen, um optimierte Pflanzen für die As-Phytoremediation zu entwickeln. Die transgenen *N. tabacum*-Pflanzen, die AtStr5/AtACR2<sup>oe</sup>-AtPCS1<sup>oe</sup> und AtStr17a/HAC1/ATQ<sup>oe</sup>-AtPCS1<sup>oe</sup> überexprimieren, könnten direkt in der As-Phytoremediation eingesetzt werden.

**Stichwörter:** Sulfurtransferase; Arsenate Reduktase; CDC25 Phosphatase; *Arabidopsis thaliana*; *Nicotiana tabacum*

## ABBREVIATIONS

3-MP	3-mercaptopyruvate
3-OMFP	3-O-methylfluorescein-phosphate
aa	amino acid (s)
ACR2	plant arsenate reductase
AR	arsenate reductase
AsrC	bacterial arsenate reductase
<i>A. thaliana</i>	<i>Arabidopsis thaliana</i>
AtStrs	<i>Arabidopsis thaliana</i> sulfurtransferase(s)
BCIP	5-bromo-4-chloro-3-indolyl-phosphate
BSA	bovine serum albumin
CDC25	cell division cycle 25
CDKs	cyclin-dependent kinases
Cys	cysteine
db	database
DDT	dichlorodiphenyltrichloroethane
DNA	deoxyribonucleic acid
dNTPs	deoxy nucleotide triphosphates
<i>E. coli</i>	<i>Escherichia coli</i>
EDTA	ethylenediaminetetraacetic acid
exp	experimental
GFP	green fluorescent protein
His	histidine
ID	identification
IPTG	isopropyl- $\beta$ -D-galactoside
kDa	kilo Dalton
LB	Luria Bertani
LP	long pass
M	DNA marker
MAP	mitogen-activated protein
MT	mitochondrial
MoCo	molybdenum cofactor
mRNA	messenger ribonucleic acid
MS	Murashige & Skoog (medium)
MW	molecular mass
NBT	nitroblue tetrazolium
no.	number
OD	optical density
PAGE	polyacrylamide gel electrophoresis
PCR	polymerase chain reaction
pNPP	para- nitrophenyl phosphate
PRF	persulfide dioxygenase rhodanese fusion protein
pred	predicted
Rhd	rhodanese(s)
Rhd-S	sulfur-substituted rhodanese

---

ABBREVIATIONS

RNA	ribonucleic acid
RNAi	ribonucleic acid interference
rpm	rounds per minute
SDS	sodium dodecyl sulfate
sp.	species
SP	signal peptide
Str	sulfurtransferase(s)
T-DNA	transfer deoxyribonucleic acid
Thr	threonine
TP	targeting peptide
TS	thiosulfate
Tyr	tyrosine
UV	ultra violet
WT, wt	wild-type



# Contents

<b>ERKLÄRUNG</b> .....	<b>I</b>
<b>SUMMARY</b> .....	<b>III</b>
<b>ZUSAMMENFASSUNG</b> .....	<b>IV</b>
<b>CHAPTER I</b> .....	<b>1</b>
1 GENERAL INTRODUCTION.....	1
1.1 Arsenic and its consequence to the environment .....	1
1.2 Plant-arsenic biochemistry .....	2
1.3 Arsenic-phytoremediation (potential solution) .....	2
1.4 Arsenate reductases (ARs) in plant and possibilities for phytoremediation.....	4
1.5 Role of phytochelatin (PCs) in As stress .....	5
1.6 Role of sulfur in the plant under As-stress .....	6
1.7 General information about CDC25 dual-specificity tyrosine phosphatase .....	7
1.8 General aspects of the rhodanese/sulfurtransferase family .....	10
1.8.1 Sulfurtransferases in <i>Arabidopsis thaliana</i> .....	11
1.8.2 Biological functions of Strs in the organisms .....	14
1.8.3 The structural relationship among rhodanases, CDC25 phosphatases, and arsenate reductases .....	15
1.8.4 <i>Arabidopsis thaliana</i> sulfurtransferase 17a (AtStr17a or At2g21045 or AtARQ1 or HAC1).....	16
1.8.5 Overexpression of <i>Arabidopsis</i> AR ( <i>AtStr5</i> and <i>AtStr17a</i> ) in <i>Nicotiana tabacum</i> 17	
1.9 Aims of the project.....	18
<b>CHAPTER II</b> .....	<b>19</b>
REVIEW PAPER .....	19
<b>CHAPTER III</b> .....	<b>34</b>
CHARACTERIZATION OF GROUP III <i>ARABIDOPSIS</i> SULFURTRANSFERASE 5 PROTEINS .....	34
Abstract.....	34
1 Introduction .....	35
2 Material & methods.....	37
2.1 <i>In vitro</i> biological function elucidation for recombinant AtStr5 (At5g03455) protein.....	37
2.1.1 DNA cloning techniques .....	37
2.1.1.1 Cloning into a pGEM®-T cloning vector.....	37
2.1.1.2 Cloning into a pQE-30 expression vector .....	39
2.1.2 Expression, extraction, and purification of AtStr5 proteins from transformed <i>E. coli</i> .....	40
2.1.3 SDS-PAGE and Western blot analysis.....	41
2.1.4 Enzyme activity measurement.....	41
2.1.4.1 Phosphatase assay with para-nitrophenyl phosphate ( <i>pNPP</i> ).....	41
2.1.4.2 Phosphatase assay with 3-O-methylfluorescein-phosphate (3-OMFP)42	
2.1.4.3 Sulfurtransferase assay .....	43
2.2 Determination of the intracellular localization of AtStr5 .....	43
2.2.1 Plant material and growth conditions .....	43
2.2.2 Cloning into a pGEM®-T cloning vector.....	43
2.2.3 Cloning into pBSK based GFP-C/-N vectors for localization study .....	44
2.2.4 Transient transformation of GFP fusion construct into <i>Arabidopsis</i> protoplasts.....	45
2.2.5 Microscopic analysis .....	46
2.2.6 Miscellaneous .....	46

3 Results.....	47
3.1 Expression, extraction, and purification of AtStr5 proteins from transformed <i>E. coli</i> .....	47
3.2 Results of the phosphatase assays.....	50
3.3 Results of the sulfurtransferase assays .....	53
3.4 Subcellular localization of AtStr5 .....	56
4 Discussion.....	62
<b>CHAPTER IV .....</b>	<b>68</b>
<b>SIMULTANEOUS OVEREXPRESSION OF ATSTR5, ATSTR17A, AND THE PHYTOCHELATIN SYNTHASE PROTEIN ATPCS1 IN <i>ARABIDOPSIS THALIANA</i>, AN APPROACH TO IMPROVE ARSENIC PHYTOREMEDIATION .....</b>	<b>68</b>
Abstract.....	68
1 Introduction .....	69
2 Material & Methods .....	70
2.1 DNA isolation and cloning .....	70
2.1.1 Cloning into plant expression vectors (pBinAR and pBin-Hyg-TX).....	74
2.1.2 Cloning into <i>Agrobacterium tumefaciens</i> (strain GV3101) .....	74
2.2 Plant preparation and transformation to generate stable transformants .....	75
2.2.1 Seeds sterilization for primary transformants.....	76
2.2.2 PCR analysis of T1 primary overexpressing transformants .....	76
2.3 Southern blotting.....	78
2.3.1 Restriction enzyme selection and digestion for Southern blot analysis .....	78
2.3.2 DIG probe synthesis .....	79
2.3.3 Hybridization with DIG-labeled probes .....	80
2.3.4 Colorimetric detection with NBT/BCIP .....	81
2.4 Gene expression study by Genevestigator.....	81
2.5 Northern blotting and RNA extraction.....	82
2.5.1 Detection by CDP-Star .....	83
2.6 Construction of dual genes overexpressing transgenic lines .....	83
3 Results.....	83
3.1 DNA cloning technique .....	83
3.2 Plant transformation and selection.....	88
3.3 Southern blot analysis .....	91
3.4 Gene expression analysis by Genevestigator program .....	96
3.5 Northern analysis of the T2 overexpressing lines .....	99
4 Discussion.....	101
<b>CHAPTER V .....</b>	<b>105</b>
<b>HETEROLOGOUS OVEREXPRESSION OF ATSTR5 AND ATSTR17A IN ROLB-ATPCS1 OVEREXPRESSING <i>NICOTIANA TABACUM</i> FOR ARSENIC PHYTOREMEDIATION STUDY .....</b>	<b>105</b>
Abstract.....	105
1 Introduction .....	106
2 Material & methods.....	109
2.1 Plant material.....	109
2.2 <i>Agrobacterium</i> strains and culture.....	109
2.3 Preparation of the bacteria .....	109
2.4 Transformation, co-cultivation, and regeneration medium .....	110
2.5 Molecular analysis .....	111
2.5.1 DNA isolation.....	111
2.5.2 PCR amplification and screening of transformed regenerates by analyzing the presence of <i>AtStr5/AtACR2</i> and <i>AtStr17a/ATQ1/HAC1</i> gene .....	111

---

2.6 Southern blotting.....	112
3 Results.....	112
4 Discussion.....	118
<b>CHAPTER VI.....</b>	<b>120</b>
1 General discussion.....	120
1.1 Sulfurtransferase activity of AtStr5.....	120
1.2 Phosphatase activity of AtStr5.....	121
1.3 Subcellular localization of AtStr5.....	123
1.4 Simultaneous overexpression of <i>AtStr5/AtACR2-AtPCS1</i> and <i>AtStr17a/HAC1/ATQ1-AtPCS1</i> in <i>A. thaliana</i> for arsenic phytoremediation study...	125
1.5 Overexpression of <i>AtStr5/AtACR2</i> and <i>AtStr17a/HAC1/ATQ1</i> in <i>rolB-AtPCS1</i> overexpressing <i>N. tabacum</i> for arsenic phytoremediation study.....	126
2 Future prospects.....	127
<b>REFERENCES.....</b>	<b>128</b>
<b>ACKNOWLEDGMENTS.....</b>	<b>145</b>

# CHAPTER I

## 1 General introduction

### 1.1 Arsenic and its consequence to the environment

Arsenic (As) toxicity has become one of the crucial global concerns in the twenty-first century, as it clandestinely contaminated in soil and groundwater, ultimately resulted in a deposition in many crops species (Bhattacharya et al. 2010; Schoof et al. 1999). As belongs to group V<sub>A</sub> element and it is a ubiquitous metalloid having the characteristics of both metal and non-metals (Bondada and Ma 2003). As is classified as the number one of hazardous substances by the United State Agency for Toxic Substances and Disease Registry that exhibits toxic effect depending on the type of exposure. The metalloid (As) can enter in the agricultural system through a variety of means such as natural geochemical process, and microbial activities which enhance the mobilization of As into the environment (Duker et al. 2005). Furthermore, human action exacerbated the problem namely; using As based pesticides, mining operations, irrigation with As contaminated groundwater, and fertilization with municipal solid wastes (Meharg et al. 2009). Arsenic contamination of the human food chain is a worldwide concern that is not restricted by physical boundaries. Nevertheless, severe As contamination occurred in an area where rice is the staple food for most of the population, for instance in South East Asia such as West Bengal, Bangladesh, China, Vietnam, Thailand, and Taiwan. As contaminated drinking water is not the only primary source of As to the diet in that area, further extensive use of contaminated groundwater to irrigate the paddy field led to an elevated level of As in rice grain (Meharg and Rahman 2003). It has been reported that rice grain can accumulate up to 2 mg kg<sup>-1</sup> As and in rice straw up to 92 mg kg<sup>-1</sup> (Williams et al. 2005). Therefore, As polluted rice consuming population is under the threat of As contamination which can pose health risk significantly. As exposure can cause a variety of health problems including anaemia, neuropathies, hyperpigmentation, skin irritation and several respiratory problems (Helleday et al. 2000; Sheena et al. 2009). Prolonged exposure can also cause skin lesions and can intensify the chances of cancer development, especially the possibilities of development of skin, lung, and bladder cancer (Sheena et al. 2009). The extensive

contamination of As in the environment and its carcinogenic toxicity to human and animal, alarming the urgent elimination of As from its contaminated sites.

## **1.2 Plant-arsenic biochemistry**

Plant response to As stress vastly depends on the type of plant species, soil physical and chemical characteristics, environmental conditions and the bioavailability of As. In the terrestrial environment, As may present in the different oxidation state; semi-metallic element [As (0)], arsenate [As (V<sup>+</sup>)], arsenite [As (III<sup>+</sup>)], and arsine [As (III<sup>-</sup>)], and they can be interchangeable by different chemical and biological reactions that are common in the environment. However, the typical oxidation state of inorganic As in soil, water and living cells are [As (V)] and [As (III)]. Of the two inorganic forms, the highly oxidized [As (V)] predominates in an aerobic environment, while the highly reduced [As (III)] is the predominant form in an anaerobic environment such as flooded rice paddy field (Zhu et al. 2008). Regardless of the fate of inorganic As in living cells, both forms can interrupt biological functions differently. Nevertheless, [As (III)] is considered to be 100-fold more toxic than the [As (V)] (Cervantes et al. 1994; Mishra and Dubey 2006) which binds to proteins with sulfhydryl groups and interferes with their functions (Leonard and Lauwerys 1980). It inhibits respiration by binding to vicinal thiols in pyruvate dehydrogenase and 2-oxoglutarate dehydrogenase. Although [As (III)] does not act directly as a mutagen, but it induces intra-chromosomal homologous recombination which could cause tumorigenesis (Helleday et al. 2000). Besides, it could generate reactive oxygen species to induce lipid peroxidation that causes plant death (Chou et al. 2004). Conversely, [As (V)] interferes with oxidative phosphorylation and ATP synthesis (Carbonell et al. 1998).

## **1.3 Arsenic-phytoremediation (potential solution)**

Unlike the toxic organic compounds, the threats of these heavy metals or metalloid like As cannot be degraded from the environment by chemical and biological transformation. Conventional methods of metal remediation like leaching, solidification, vitrification, electro-kinetical treatment, chemical oxidation or reduction, excavation, and off-site treatment are expensive, disturb soil structure and fertility and are limited to relatively small areas (Luo et al. 2000; Wu et al. 2010).

Against the backdrop, the “phytoremediation” mechanism has been adopted by the plants to mitigate the As pollution. It offers an environment-friendly approach in which the

unwanted and hazardous heavy metals are contained and controlled (Desbrosses-Fonrouge et al. 2005). As a fact, plants to be useful in phytoremediation must produce a significant amount of harvestable biomass that contains high concentrations of pollutants. Several hyper-accumulator plants, for instance, *Pteris vittata* and *Pityrogramma calomelanos* are well known for As phytoremediation. However, the fact is most known hyper-accumulators tend to grow slowly and produce relatively low biomass (Cunningham et al. 1995). Hence, to overcome this limitation, genetic and molecular investigations of plant defense mechanisms involved in the heavy metal detoxification process have been underway to improve the efficiency of phytoremediation. The way plant accumulates As and detoxifies this toxicant through the phytoremediation process is demonstrated in **Figure 1**.

In anoxic soil condition the major part of As occurs in soil in the [As (V)] form as  $\text{FeAsO}_4$  (Ducleff and Terry 2002) and due to its analogy with phosphate, the [As (V)] can rapidly enter into plant root through phosphate uptake transporter (Meharg and Macnair 1992; Ullrich-Eberius et al. 1989; Wu et al. 2011). After uptake, the reduction of intracellular [As (V)] into [As (III)] occurs by arsenate reductases (ARs) (Bleeker et al. 2006; Dhankher et al. 2006). Conversely in submerged soil the leading bioavailable form of As is [As (III)] (Stroud et al. 2011) and it can enter into the plant root by using plant aquaporin like channel (Bienert et al. 2008; Isayenkov and Maathuis 2008; Ma et al. 2008; Meharg and Jardine 2003). Subsequently, [As (III+)] can detoxify through thiol-rich peptides or effluxes out of the cell (Liu et al. 2010). [As (III+)]-thiol-rich peptide complex formation and subsequent storage in vacuoles in the root consequently make lower efflux rate and long-distance transport to other, thus completing the As phytoremediation process (Liu et al. 2010).

Therefore, to engineer plants for phytoremediation, one must be considered to manipulate the target genes that are involved in As detoxification process (Li et al. 2005; Li et al. 2004; Picault et al. 2006). Several genes are participating in this process, for instance, As uptake and reduction, translocation from root to shoot, chelation and vacuolar transportation and aspect of phosphorus and sulfur metabolism. Manipulation of a single gene is, therefore, unlikely to yield considerable progress in developing hyper-accumulating plants. An integrated approach is essential to optimize the various aspects of plant As tolerance and accumulation. Suitable plants include As hyper-accumulating ferns and aquatic plants capable of decreasing As levels from the soil by reducing [As (V)] to

[As (III+)], [As (III+)]-PC complexation, and vacuolar compartmentalization of complexed or inorganic As and thus can bring about As phytoremediation.

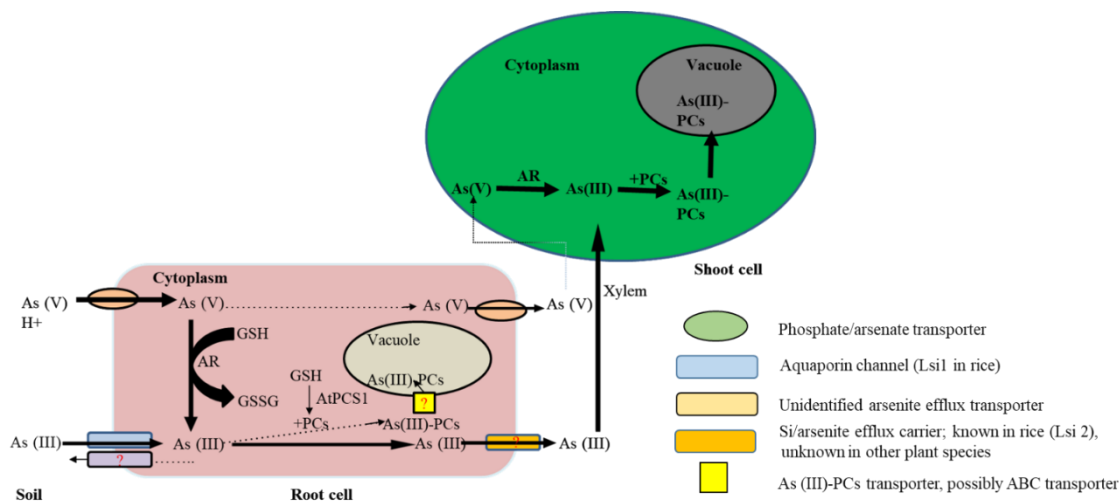


**Figure 1.** Mechanism of As uptake and metabolism in roots and shoots cell in hyper-accumulators species, modified from Zhao et al. (2009). Line thickness related to flux rate, with the dotted line indicating the slowest rate. Question marks indicate major knowledge gaps; GSSG oxidized glutathione; GSH, glutathione; Lsi, Si influx transporter; PC, phytochelatin.

#### 1.4 Arsenate reductases (ARs) in plant and possibilities for phytoremediation

The first step after As intake into the plant followed by [As (V)] reduction, which is catalyzed by AR (*ACR2*). The first AR gene and its mechanism were reported in bacteria and later observed in yeast (Gladysheva et al. 1994; Ji et al. 1994; Mukhopadhyay et al. 2000) (Ghosh et al. 1999; Mukhopadhyay and Rosen 2002; Mukhopadhyay et al. 2000; Shi et al. 1999). This enzyme family arose at least three times independently by convergent evolution. The first family of AR includes *Escherichia coli* plasmid R773 ArsC that uses glutaredoxin (Grx) and glutathione (GSH) as reductants. A second family of AR also widely distributed in bacteria is called ArsC found on the *Staphylococcus aureus* plasmid pI258 and uses thioredoxin (Thx) instead of Grx as reductant (Ji et al. 1994). The *S. aureus* plasmid pI258 encoding the ArsC protein contains a pair of cysteine (Cys) residues (that are essential to its catalytic action), one of which is a part of a highly conserved sequence: [Cys-(X)<sub>5</sub>-Arg] (Ji et al. 1994; Messens et al. 1999). The mechanism of enzymatic reduction by AR involves in the formation of a thioester bond between the Cys and [As (V)], and the arginine residue assists in the stabilization of the intermediate. The reduced

form of AR is its active form which is generated by a reductant either Thx or Grx. Interestingly, ArsC from pI258 is related to low-molecular-weight protein tyrosine phosphatases (LMW-PTPases) and exhibits low-level phosphatase activity (Zegers et al. 2001). The third family of AR is similar to protein tyrosine phosphatases, although to a family of phosphatases different from that of pI258 ArsC. To date, several members of this family have been characterized for example *ScACR2p* from yeast, *AtACR2* in *Arabidopsis thaliana* (Dhankher et al. 2006), *HlACR2* in *Holcus lanatus* (Bleeker et al. 2006), *OsACR2* in *Oryza sativa* (Duan et al. 2007) and *PvACR2* in *P. vittata* (Ellis et al. 2006) and *High As content 1 (HAC1)* or *As tolerance QTL-1(ATQ1)* from *A. thaliana* (Chao et al. 2014; Sánchez-Bermejo et al. 2014) which does not belong to the plant ACR2 group of AR. The plant ACR2 enzyme uses GSH and Grx as the electron donor (Ellis et al. 2006; Duan et al. 2007), indicating that the catalytic cycle includes the formation of a mixed disulfide between ACR2 and GSH that is solved by Grx (Mukhopadhyay et al. 2000). Nevertheless, most of these studies are focused on heterologous functional assays either in *E. coli* or yeast, which may not represent the planta *in vivo* functions. Additionally, the mechanism of catalytic reaction of these ACR2 in the plant has not been illustrated as like in bacteria and yeast. Therefore this work focuses on the characterization of AtStr5/AtACR2 protein and unravels its contribution in the As reduction process.

## 1.5 Role of phytochelatins (PCs) in As stress

Phytochelatins (PCs) are enzymatically synthesized Cys-rich peptides having a general structure  $(\gamma\text{Glu-Cys})_n\text{-Gly}$ , where n equals 2–11 and play a vital role in metals and semimetals homeostasis and detoxification (Rauser 1990). These peptides are rapidly synthesized in plants in response to various metals and semimetals at a toxic level (Cobbett 1999; Zenk 1996). PCs form stable complexes with heavy metals in the cytosol, and these metal-PC complexes are subsequently sequestered into the vacuole (Cobbett and Goldsbrough 2002; Cobbett 1999; Grill et al. 1985; Steffens 1990; Zenk 1996). They are synthesized from reduced glutathione catalyzed by the enzyme phytochelatin synthase (PCS), a glutamyl-Cys dipeptidyl transpeptidase (EC 2.3.2.15) (Cobbett 2000; di Toppi et al. 2012). Genes encoding PC synthase have been cloned from *A. thaliana* (*AtPCSI*), wheat (*TaPCSI*), *Schizosaccharomyces pombe* (*SpPCSI*), *Caenorhabditis elegans* (*CePCSI*), and other species (Clemens et al. 1999; Clemens et al. 2001; Ha et al. 1999; Vatamaniuk et al. 2001; Vatamaniuk et al. 1999).



These genes were successfully overexpressed in tobacco plants (Pomponi et al. 2006; Shukla et al. 2012; Wojas et al. 2008). Overexpression of *PCS* gene leads to increased production of PCs, with a general increment of plant Cadmium (Cd)-detoxification when the metal was supplied at specific concentrations (Brunetti et al. 2011; Pomponi et al. 2006). Also, exogenous GSH application enhances the Cd detoxification process of those overexpressing lines (Pomponi et al. 2006). Although the importance of PCs under Cd stress was extensively studied, less information is available about As accumulation and detoxification. It has been shown that tobacco overexpressing *AtPCS1* gene exposed to As, and Cd plus As enhance As, and As and Cd accumulation and detoxification (Zanella et al. 2016). For As phytoremediation study one has to be considered that As the need to be reduced from [As (V)] form to [As (III)] in the presence of AR and subsequently that [As (III)] can be bind with PCs for complex formation and sequestration into the vacuole. So only overexpression of *AtPCS1* might not be an efficient technique for As-phytoremediation. Therefore, it might be a promising approach to overexpress both AR and PCS genes in the same transgenic plant.

## **1.6 Role of sulfur in the plant under As-stress**

Sulfur is a crucial element for plant growth, which plays a vital role in regulating As tolerance through complexation of As by sulfur-containing ligands (GSH, PCs and GSH oligomers) (Mishra et al. 2013; Raab et al. 2005; Srivastava and D'souza 2009). Subsequently, the As-thiol complexes are transferred to vacuoles, and this process is known as As-detoxification (Song et al. 2010). It is known that As-complexation affects the transportation of As by decreasing either its translocation from root to shoot or its efflux from root to the medium (Liu et al. 2010). Studies showed that sulfur supply has an influence to As uptake, translocation, and accumulation in rice plants (Dixit et al. 2015; Zhang et al. 2011). For example, the concentration of PCs negatively correlates to grain As accumulation in rice (Duan et al. 2011).

Furthermore, the As levels in shoots were decreased with increasing doses of sulfur sources ( $\text{SO}_4^{2-}$  or  $\text{S}_0$ ) (Hu et al. 2007). This phenomenon was elucidated by the sulfur-induced formation of iron plaque, which has been suggested to act as a barrier to As entry into the roots through As sequestration. Conversely, other studies propose that iron plaque to work as a buffer and increase the As concentration in plants (Tripathi et al. 2014). Thus, the function of iron plaque in the regulation of As level in plants is still arguable. High

sulfate pretreated rice plants showed reduced ability to transfer As from root-to-shoot and ascribed this effect to increase the complexation of As in roots (Zhang et al. 2011). Thus, high sulfur supply significantly decreased translocation factor of As compared to treatment without sulfur supply and they conclude that excessive sulfur increased the formation of iron plaque. The phenomenon of sulfur supply and iron plaque formation was further explained that excessive sulfur supply induced iron plaque formation, in consequence, increased As concentration in roots (Tripathi et al. 2014), while decreasing As concentration in shoots might be the result of higher As complexation in roots in more sulfur available conditions (Zhang et al. 2011). Additionally, excessive sulfur treatment led increase As accumulation in roots with a sequential decline in root-to-shoot translocation factor of As and attributed the fact the induced synthesis of thiols and consequent higher As complexation in roots (Dixit et al. 2015). Therefore, the role of sulfur in As uptake and translocation in plants needs to be studied further.

Indeed suitable plants for phytoremediation have to be able to transfer a substantial amount of As either [As (V)] or [As (III)] form into shoot part and after that increased complex formation have to be demanded. Hence, it is essential to understand the impact of sulfur under As stress (Lei et al. 2013) analyzed the effects of sulfur metabolism on As stress in As hyper-accumulator *P. vittata*, and found that sulfur assimilation inhibitor buthionine sulfoximine (BSO) markedly inhibited As reduction, and thus decreased As the movement to aboveground tissues by 47%. Therefore it is essential to understand the sulfur significance under As-stress to obtain the maximum benefit from phytoremediation.

## **1.7 General information about CDC25 dual-specificity tyrosine phosphatase**

The CDC25 is a dual specificity phosphatase (DS-PTPase) under the sub-class of protein tyrosine phosphatases, and it is involved in the de-phosphorylation of CDKs (Cyclin-Dependent Kinases) for the progression of the cell cycle (Pines 1999). The CDC25 is also the critical component of a checkpoint pathway that becomes activated during the event of DNA damage (Mailand et al. 2000; Niida and Nakanishi 2006; Xiao et al. 2003; Zhao et al. 2002). CDC25 phosphatases were found in all eukaryotic organisms except plants (Boudolf et al. 2006). The CDC25 initially discovered in the fission yeast *Schizosaccharomyces pombe* (*SpCDC25*) as a critical regulator for G2/M phase transition of the cell division cycle (Russell and Nurse 1986). In humans, three CDC25 isoforms

(huCDC25A, huCDC25B, and huCDC25C) were reported (Galaktionov and Beach 1991; Nagata et al. 1991; Sadhu et al. 1990). Each isoform of huCDC25 is periodically activated and controlled the CDK/ cyclin complex of the cell cycle (G1-S-G2-M) (Hoffmann et al. 1993; Jinno et al. 1994; Lammer et al. 1998) through the dephosphorylation of threonine (Thr14) and tyrosine (Tyr15) residues of that complex (Kumagai and Dunphy 1991). To date, CDK-cyclin is the only known substrate for CDC25 (Kristjansdottir and Rudolph 2004), and CDC25 can itself get phosphorylated with its substrate CDK during cell cycle that enhances its phosphatase activity (Izumi et al. 1992).

All species contain CDC25 composed of at least two specific regions, a highly conserved C-terminal domain that includes a catalytic active Cys residue, and a vast, diverse N-terminal region with no sequence conservation between species. Very few information is found about the N-terminal region of CDC25 which possesses a regulatory residue and is thought to be involved in the determination of subcellular localization (Boutros et al. 2007). The phosphorylation of the N-terminal regulatory domains by several kinases, including the CDK–cyclin complexes themselves, have been reported to regulate the activities of the CDC25 phosphatases (Karlsson-Rosenthal and Millar 2006; Mailand et al. 2002).

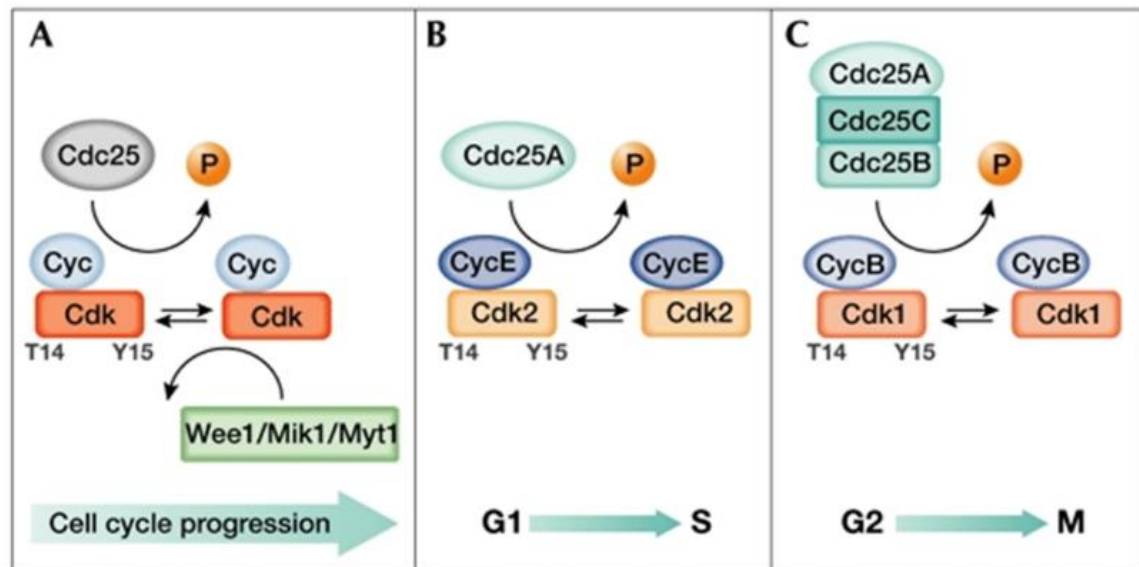
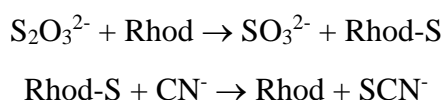


**Figure 2.** Regulation of cell cycle process by different CDC25 in a mammalian cell retrieved from (Donzelli and Draetta 2003). Both phosphatases and kinases regulate the activity of Cdks during cell cycle progression (A) The Wee1/Mik1/Myt1 protein kinase phosphorylated Thr 14 (T14) and Tyr 15 (Y15) residues of Cdks and maintained in an inactive state. The CDC25s (DS-PTPases) dephosphorylates of these residues from Cdks and thereby activated the cell cycle process, (B) CDC25A regulates Cdk2-cyclin E complex during G1 and S phase. (C) CDC25A, CDC25B, and CDC25C control Cdk1-cyclin B complex during G2 and M phase.

Whereas the C terminal domain of the CDC25 protein is holding the catalytic Cys residues that remain in a short loop with the tyrosine phosphatase signature motif [His-Cys-(X)<sub>5</sub>-Arg]. Except for this motif, the CDC25s do not show any sequence and other structural similarities with other protein tyrosine phosphatases, for instance, LMW-PTPases or DS-PTPases. The CDC25 catalyzes or dephosphorylates their substrate in a two-step mechanism, in the first step they formed phosphocysteine intermediate and which is subsequently hydrolyzed to give inorganic phosphate and free enzyme in the second step of the reaction (Fauman et al. 1998). The crystallographic investigation of the catalytic domain of the huCDC25A and huCDC25B are shown to contain the rhodanese-like 3D fold (Fauman et al. 1998; Hofmann et al. 1998; Reynolds et al. 1999). The CDC25 protein family forms a distinct clade in a neighbor-joining tree analysis (generated by CLUSTALW) representing the rhodanese superfamily; it also includes yeast *ScACR2p* (Bordo and Bork 2002).

## 1.8 General aspects of the rhodanese/sulfurtransferase family

Rhodanases (Rhds) are ubiquitous and multifunctional enzymes that prevalent in all living organisms including bacteria and mammals. The name ‘rhodanese’ of the enzyme comes from the German name for thiocyanate (Rhodanid), and the actual name is thiosulfate: cyanide sulfurtransferase or TST (EC 2.8.1.1). The enzyme is also known as mercaptopyruvate: cyanide sulfurtransferase or MST (EC 2.8.1.2) as it catalyzes the similar reaction using 3-mercaptopruvate (3-MP) as a sulfur donor. The bovine Rhd is perhaps the most studied and best characterized Str (thiosulfate: cyanide Str, EC 2.8.1.1) of this protein superfamily, which catalyzes *in vitro* the transfer of a sulfane sulfur atom from thiosulfate (TS) to cyanide, leading to the formation of sulfite and thiocyanate (Westley 1973). The overall accepted mechanism can be explained corresponding to the following scheme.



**Equation 1:** Reaction mechanism of thiosulfate: cyanide Str (EC 2.8.1.1)

According to the generally accepted reaction mechanism, the catalytic cycle of Strs involves two half reactions. In the first, the sulfur is transferred from donor to an active site Cys to form a covalent enzyme-sulfur intermediate (Rhd-S). In the second half reaction, the outer sulfur from Rhd-S intermediate is transferred to a thiophilic acceptor to regenerate the free enzyme. Crystallographic investigations have shown that the Rhd-S intermediate is characterized by a persulfide bond at the sulfhydryl group of the essential Cys residue 247 in the active-site (Gliubich et al. 1996; Ploegman et al. 1979; Russell et al. 1978). The Strs or Rhd-like domains (RLDs) often share only low amino acid sequence homology among each other but display highly conserved structural criteria (Ploegman et al. 1978; Ploegman et al. 1979). The substrate specificity and catalytic activity of the RLDs is dependent on the composition of the active site center which holds with either a conserved CRXGX(T/R) motif in the case of TSTs (EC 2.8.1.1), or a more defined CG(S/T)GV(T/S) motif in the case of MSTs (Bordo and Bork 2002; Nagahara et al. 1995).

The Rhd superfamily members are distinguished by a basic module with an  $\alpha/\beta$  topology in which  $\alpha$ -helices surround a central five stranded  $\beta$ -sheet core (Ploegman et al. 1978). At

least three variations of the Rhd domain are found in family members (Bordo and Bork 2002). The Rhd domain can appear in a single or tandem repeat in a protein with Str activity (Adams et al. 2002; Bordo et al. 2000; Burow et al. 2002; Colnaghi et al. 2001; Papenbrock and Schmidt 2000b; Spallarossa et al. 2001). Alternatively, Rhd domains can be fused to other protein domains as in CDC25 phosphatase (Bordo and Bork 2002) or the persulfide dioxygenase rhodanese fusion protein (PRF) and copper-sensing operon repressor-like sulfurtransferase operon (CstB) proteins (Motl et al. 2017; Shen et al. 2015). Analysis of all known members of Str family has revealed that only the C terminal domain anchors the catalytic Cys residue as a single domain or concerted with multi-domain protein families (Mueller et al. 2001; Palenchar et al. 2000; Schultz et al. 1998). The counterpart of the Cys residue in the N-terminal domain occupied by the aspartic (Asp) residue which is not essential for catalysis. The two amino acid sequence patterns recognized at inactive N-terminal region ([F/Y]-X<sub>3</sub>-H-[L/I/V]-P-G-A-X<sub>2</sub>-[L/I/V/F]) and at active C-terminal region ([A/V]-X<sub>2</sub>-[F/Y]-[D/E/A/P]-G-[G/S/A]-[W/F]-X-E-[F/Y/W]) are called as Rhd signatures (Cipollone et al. 2007). Analysis of the amino acid sequences of Rhd superfamily proteins indicates the heterogeneity of the superfamily, despite the conservation of the Rhd signatures. The variability among the members arise at different levels, for instance, the active site loop length, the presence of catalytic Cys residues, and domain arrangement.

### 1.8.1 Sulfurtransferases in *Arabidopsis thaliana*

In the *Arabidopsis* genome, 20 genes encoding Strs and Str-like proteins (AtStrs), have been identified by database mining and each contains at least one Rhd domain (Bartels et al. 2007; Bauer and Papenbrock 2002). These proteins are classified into six groups by conservation of the active site Cys, the Rhd signature sequence and further 12 conserved amino acids (**Table 1**). Some of them were characterized by previous members of the working group (Bartels et al. 2007; Bauer et al. 2004; Bauer and Papenbrock 2002; Papenbrock and Schmidt 2000a, b). Among those, two two-domain AtStrs protein have shown 3-MP affinity over TS as a sulfur donor (Nakamura et al. 2000; Papenbrock and Schmidt 2000a, b), and two single domain proteins which contain the catalytic Cys at the C-terminal prefer TS over 3-MP as their sulfur donor *in vitro* (Bauer and Papenbrock 2002). So far *in vivo*, biological substrates for most members of the Str family have remained unknown, and it seems unrealistic that these substrates are those identified by the

*in vitro* reaction (Nandi et al. 2000; Ray et al. 2000b). Rhd domain is the versatile sulfur carrier that has adapted its function to meet the demand for reactive sulfur in distinct metabolic and regulatory pathways, and substrate specificity of a protein depends on the size and composition of amino acids on the catalytic loop (Bordo and Bork 2002). Therefore, the putative AtStr proteins may use not only substrates containing sulfur but also substrates containing phosphorous, As or selenium.

**Table 1. Overview of the 20 putative Str in *Arabidopsis thaliana*.** The protein name, gene identification, number of amino acids, predicted or experimentally shown localization and remarks on different aspects are summarized including the respective references. The programs Predotar, PSORT, and TargetP, were used for the localization prediction (<http://www.expasy.ch/tools>). The respective probabilities are given. Abbreviations: aa, amino acids; CP, chloroplast; DB, database; ER, endoplasmatic reticulum; exp, experimental; ID, identification; kDa, kiloDalton; MT, mitochondrial; MW, molecular mass; no., number; PER, peroxisome; pred, predicted (Bartels 2006).

	AGI ID	Amino acids	Localization (pred/exp)	Reference for localization	Putative <i>in vivo</i> or <i>in vitro</i> enzyme activity	Reference
<b>Group I</b>						
1	At1g79230	322	MT (exp)	Bauer et al. 2004 Heazlewood et al. 2004 Nakamura et al. 2000	TS Str 3-MP Str	Papenbrock and Schmidt 2000a, b Hatzfeld and Saito 2000 Nakamura et al. 2000
2	At1g16460	318	Cyt (exp)	Bauer et al. 2004 Hatzfeld and Saito 2000 Nakamura et al. 2000	TS Str 3-MP Str	
<b>Group II</b>						
3	At5g23060	387	MT (exp)	Heazlewood et al. 2004	similar to unknown protein	db annotation
4	At4g01050	457	CP, thylakoid membrane (exp)	Peltier et al. 2004	hydroxyproline-rich glycoprotein	db annotation
4a	At3g25480	264	CP, thylakoid membrane (exp)	Peltier et al. 2004	hypothetical protein	db annotation
<b>Group III</b>						
5	At5g03455	132 146	Cyt Not identified	This study	dual-specificity tyrosine phosphatase Acr2 AR	Landrieu et al. 2004 Duan et al. 2005
6	At1g09280	581	Cyt (pred/exp)	www.expasy.ch	Unknown protein	db annotation
7	At2g40760	522	MT (pred)	www.expasy.ch	unknown protein	db annotation
8	At1g17850	366	CP/ER (pred)	www.expasy.ch	contains rhodanese-like PF00581 domain	db annotation
<b>Group IV</b>						
9	At2g42220	234	CP, thylakoid membrane (exp)	Peltier et al. 2004 Bartels 2006	<i>Datura innoxia</i> homolog Cd <sup>2+</sup> induced	Louie et al. 2003
10	At3g08920	214	MT (pred/preliminary exp)	Bartels 2006	unknown protein	db annotation
11	At4g24750	260	CP/Per (pred/preliminary exp)	Bartels 2006	putative protein	db annotation
<b>Group V</b>						
12	At5g19370	309	CP/MT (pred)	www.expasy.ch	putative peptidyl-prolyl cis-trans isomerase	db annotation Zhao et al. 2003
13	At5g55130	464	CP/Cyt (pred)	www.expasy.ch	molybdopterin synthase sulfurylase	db annotation
<b>Group VI</b>						
14	At4g27700	237	CP (exp)	Bauer et al. 2004 Peltier et al. 2004	hypothetical protein	db annotation
15	At4g35770	182	CP, thylakoid membrane (exp)	Bauer et al. 2004	AtSen1, senescence association, dark-induced, MoCo synthesis TS Str	Oh et al. 1996 Schenk et al. 2005 Papenbrock, unpublished
16	At5g66040	120	CP (exp)	Bauer et al. 2004	senescence-associated protein sen1-like protein; ketoconazole resistance protein-like TS Str	db annotation Bauer and Papenbrock 2002
17	At2g17850	150	Nu (pred)	www.expasy.ch	putative senescence-associated rhodanese protein; similarity to Ntdin homology to defense and stress associated <i>Cucurbita</i> proteins	Yang et al. 2003 Walz et al. 2004
17a	At2g21045	169	Nu/Cyt	Sanchez-Bermejo et al. 2014	Arsenate reductase protein	Chao et al. 2014 Sanchez-Bermejo et al. 2014
18	At5g66170	136	Cyt (exp)	Bauer et al. 2004	senescence-associated protein sen1-like protein TS Str	db annotation Bauer and Papenbrock 2002



### 1.8.2 Biological functions of Strs in the organisms

The ubiquity of Strs in all living organisms suggests that they have a distinct physiological role in the cellular process. Several studies in many different organisms proposed several functions, though the identification of natural substrate is still elusive. A range of function for Strs has been suggested, including, in a mammal, Strs are involved to eliminate the toxic cyanogenic compound (Nagahara et al. 1999; Vennesland et al. 1982), while cyanide detoxification role in the plant is insignificant (Meyer et al. 2003) but cannot be excluded. Detoxification of reactive oxygen species in aerobic tissues (Nandi et al. 2000) and formation of prosthetic iron-sulfur proteins (Pagani et al. 1984), sulfate assimilation (Donadio et al. 1990), selenium metabolism (Ogasawara et al. 2001), thiamine biosynthesis (Palenchar et al. 2000) and synthesis of Molybdenum cofactor (Leimkühler and Rajagopalan 2001; Matthies et al. 2004) have also been suggested. The *AtStr1* and *AtStr2* have shown increased expression and enhanced Str activity during the senescence stage of *Arabidopsis*, hence the involvement of these Str proteins in the sulfur transport process during senescence was proposed (Papenbrock and Schmidt 2000b). Additionally, it has been reported that single domain AtStrs protein are involved in specific stress conditions with the process of leaf senescence (Bordo and Bork 2002). An increasing number of the report suggests that Strs or Strs like protein are involved in heavy metal stress, for example, a cadmium-induced AtStr9 homolog was identified in *Datura innoxia* (Louie et al. 2003), while AtStr5 and recently claimed AtStr17a has been proposed as an ARs (Chao et al. 2014). Recent investigation has shown that Strs are involved in maintaining the cellular redox homeostasis by interacting with specific thioredoxin in the particular cellular compartment (Henne et al. 2015). The single-domain and cytoplasmic localized, human TS sulfurtransferase like domain-containing 1 (TSTD1) protein, was also postulated to play a role in sulfide-based signaling upon interaction with thioredoxin (Libiad et al. 2018). The frequently observed association of catalytically inactive Rhd modules with other protein domains suggests a distinct role of these inactive domains, possibly in regulation and signaling (Bordo and Bork 2002).

The high abundance and coexistence of putative Str proteins in *Arabidopsis* indicates each Str protein has a specific metabolic role. The functional specificity was further emphasized by their localization in different compartments of the cell (Bauer et al. 2004; Hatzfeld and Saito 2000; Nakamura et al. 2000; Papenbrock and Schmidt 2000a).

The substrate recognition and catalytic activity of Strs are mostly depended on the variance in the amino acid composition of the active-site loop (Bordo and Bork 2002; Forlani et al. 2003), which may further refer an involvement of the 20 putative AtStr proteins in distinct biological functions.

### **1.8.3 The structural relationship among rhodanases, CDC25 phosphatases, and arsenate reductases**

The structural relationship among rhodanese domains and catalytic domains of CDC25 phosphatases was confirmed by the analysis of the 3D structures of rhodanese from *Azotobacter vinelandii* RhdA and *E. coli* GlpE (Bordo et al. 2000; Spallarossa et al. 2001). Sensitive profile analysis has shown that two enzyme families share a common ancestor (Hofmann et al. 1998). Active site loop of rhodanese coincides with tyrosine phosphatase signature motif [His-Cys-(X)<sub>5</sub>-Arg], with the catalytic Cys at an identical position in short loop. In this motif, histidine (His) is a highly conserved residue that stabilizes the active site thiolate anion, but it is not essential. The catalytic Cys residue directly attacks the phosphate atom of the phosphorylated CDKs. The arginine residue is highly conserved and is required for binding and transition state stabilization of the phosphate (Forlani et al. 2003).

The primary structural difference between rhodanese and three closely related huCDC25 phosphatase isoforms (huCDC25A, huCDC25B, and huCDC25C) is that in CDC25 phosphatases the active site loop is one residue longer than in RhdA [His-Cys-(X)<sub>4</sub>-Arg]. Besides this, the engineered elongation catalytic loop of the *A. vinelandii* compromise the ability to catalyze sulfur transfer reaction and gain phosphatase ability to catalyze the artificial substrate 3-O-methyl fluorescein phosphate (Forlani et al. 2003). This typical elongated seven amino acids long active site loop is also conserved in the AtStr5 enzyme, but the regulatory N-terminal domain is absent unlike huCDC25s (Landrieu et al. 2004a). The AtStr5 can catalyze phosphate-rich substrate *in vitro*. However, its physiological role as CDC25 was argued in many functional studies (Dissmeyer et al. 2009; Spadafora et al. 2010). Conversely, the AtStr5 protein has been suggested for AR function in several *in vitro* and *in vivo* studies as discussed in the review paper, chapter II.

Not only AtStr5/AtACR2 but also OsACR2 from *O. sativa* and LmACR2 from the parasitic protozoan *Leishmania major* showed both AR and phosphatase activities (Bleeker et al. 2006; Duan et al. 2005; Zhou et al. 2006). By contrast, AR from *S. cerevisiae*

(*ScACR2p*) and *P. vittata* (*PvACR2*) do not exhibit significant phosphatase activity, (Ellis et al. 2006; Mukhopadhyay and Rosen 2001; Mukhopadhyay et al. 2000; Mukhopadhyay et al. 2003) despite sharing the 3D structure related to members of rhodanese/CDC25 superfamily and share CDC25 active site motif [His-Cys-(X)<sub>5</sub>-Arg].

By all appearance, it is evident that Rhd-like domains are associated with arsenate reduction. However, the mechanism needs to be clarified. The substrate for three types of enzymes, Strs, ARs, and phosphatases are anions which suggest their evolutionary relatedness and a common ancestor, an oxyanion-binding protein (Mukhopadhyay and Rosen 2002). Thus, Rhd domain with seven amino acid loop can bind to substrates containing phosphorous or similar As, whereas the Rhd-like domains with six amino acid loop interact with substrates containing reactive sulfur or in some cases selenium (Ogasawara et al. 2001).

#### **1.8.4 *Arabidopsis thaliana* sulfurtransferase 17a (AtStr17a or At2g21045 or AtARQ1 or HAC1)**

In addition to the *AtStr5* (*AtACR2*), recently, Chao et al. (2014) have been identified a new AR gene *At2g21045* or *HAC1* (*High Arsenic Content 1*) to be playing a crucial role to reduce the [As (V)] into [As (III)] in the outer cell layer of *Arabidopsis* roots. It was shown that *HAC1* is expressed in the root and root expression increases when *Arabidopsis* plants exposed to [As (V)]. *Arabidopsis* plant that lacks functional *HAC1*, it shows reduce root and plant growth under As exposure. The role of *HAC1* as an AR also supported by the contemporary studies of Sánchez-Bermejo et al. 2014 and they designated the same gene as *AtARQ1*, which is responsible for As tolerance. In 3D structural modeling, the HAC1 or ATQ1 protein retains overall rhodanese fold characteristic of [As (V)] reductases and containing the [C(X)<sub>4</sub>R] motif which is similar to [C(X)<sub>3</sub>R] or [HC(X)<sub>5</sub>R] (Sánchez-Bermejo et al. 2014), characteristic of the [As(V)] reductase catalytic active site (Martin et al. 2001; Mukhopadhyay and Rosen 2002). However, in phylogenetic analysis, that *HAC1* or *ATQ1* or *AT2G21045* is remarkably different from the *ACR2* rhodanese clade (Sánchez-Bermejo et al. 2014). Indeed, there is no orthologous gene of *HAC1* or *ATQ1* was identified in most plant species other than *Arabidopsis*. The same study has shown that T-DNA mutant of *HAC1* or *ATQ1* was highly sensitive to [As (V)] but not to [As (III)] compared with Col-0 plants. The HAC1 or ATQ1 was previously identified as a Str protein called *AtStr17a*. By active site loop length, the *AtStr17a* (*HAC1* or *ATQ1*) is not similar to

the other *ACR2* gene that found in several plant species. Therefore, it has been tempting to investigate the biological function of Strs, because they are deemed to be a multifunctional enzyme.

### **1.8.5 Overexpression of *Arabidopsis* AR (*AtStr5* and *AtStr17a*) in *Nicotiana tabacum***

*Nicotiana tabacum* is a long established model system for plant transformation, and therefore benefits for gene transfer, regeneration procedure and optimized vector system (Stoger et al. 2005). Tobacco is not a hyper-accumulator of semimetals/metals though it can extract and accumulate them at considerable level (Zvobgo et al. 2015). Furthermore, tobacco produces a substantial's amount of biomass and an immense number of seeds in each generation (Sarret et al. 2006). All these natural attributes make tobacco an excellent candidate for the production of a transgenic plant in the field of phytoremediation. It has been manifested that heterologous overexpression of *AtPCS1* in *N. tabacum* lead increase As tolerance and accumulation (Pomponi et al. 2006; Zanella et al. 2016). It has also been reported, that overexpression of *AtACR2* gene in *N. tabacum* can increase 1.2-fold accumulation of As in the root of a transgenic plant in comparison to the wild-type (Nahar et al. 2017). Hence, it might be an excellent approach to manipulate the AR and PCS genes in *N. tabacum* to obtain the maximum benefit from As phytoremediation.

Therefore, in the present study, we made an effort to overexpress the *Arabidopsis AtStr5/AtACR2* and *AtStr17a/HAC1/ATQ1* genes in transgenic *N. tabacum* that is overexpressing *AtPCS1* and *rolB* genes (Pomponi et al. 2006; Zanella et al. 2016). The *rolB* oncogene is derived from *Agrobacterium rhizogenes* and induces hairy root formation in the plant. The roots of *rolB* overexpressing plants multiply rapidly in culture (Capone et al. 1989) and may provide a convenient biological system to assay heavy metal tolerance experimentally (Pomponi et al. 2006).

All this approach and knowledge might provide the basis to develop genetically engineered plants that can be used for phytoremediation of As from heavily contaminated area, thus contributing to protecting human health and the environment from severe contamination.

With an aim to investigate more on the arsenate reduction aspects of AtStr5 and to improve the As phytoremediation process the following objectives have been designed for this project.

### **1.9 Aims of the project**

1. Heterologous expression of AtStr5 (At5g03455) protein in *E. coli*, purification and characterization of the *in vitro* enzyme activities of the recombinant protein.
2. Intracellular localization study of AtStr5 protein by transient transformation of *Arabidopsis* protoplasts with Green Fluorescent Protein (GFP) fusion constructs.
3. Simultaneous overexpression of *AtStr5/AtACR2-AtPCS1* and *AtStr17a/HAC1/ATQ-AtPCS1* in *Arabidopsis* and characterization of these transgenic lines under different As and sulfur concentration.
4. Heterologous expression of *AtStr5/AtACR2* and *AtStr17a/HAC1/ATQ1* gene in transgenic *N. tabacum* plants that carries *rolB-AtPCS1* genes and characterization of these lines under different As and sulfur regime.

## **CHAPTER II**

### **Review paper**

Review

## Possible Roles of Plant Sulfurtransferases in Detoxification of Cyanide, Reactive Oxygen Species, Selected Heavy Metals and Arsenate

Parvin Most<sup>1,2</sup> and Jutta Papenbrock<sup>1,\*</sup>

<sup>1</sup> Institute of Botany, Leibniz University Hannover, Herrenhäuserstr. 2, Hannover D-30419, Germany; E-Mail: shanaj777@gmail.com

<sup>2</sup> Plant Breeding Division, Bangladesh Agricultural Research Institute, Joydebpur, Gazipur 1701, Bangladesh

\* Author to whom correspondence should be addressed; E-Mail: Jutta.Papenbrock@botanik.uni-hannover.de; Tel.: +49-511-762-3788; Fax: +49-511-762-19262.

Academic Editors: Noriyuki Nagahara and Maria Wrobel

*Received: 10 November 2014 / Accepted: 9 January 2015 / Published: 14 January 2015*

**Abstract:** Plants and animals have evolved various potential mechanisms to surmount the adverse effects of heavy metal toxicity. Plants possess low molecular weight compounds containing sulfhydryl groups (-SH) that actively react with toxic metals. For instance, glutathione ( $\gamma$ -Glu-Cys-Gly) is a sulfur-containing tripeptide thiol and a substrate of cysteine-rich phytochelatins ( $\gamma$ -Glu-Cys)<sub>2–11</sub>-Gly (PCs). Phytochelatins react with heavy metal ions by glutathione S-transferase in the cytosol and afterwards they are sequestered into the vacuole for degradation. Furthermore, heavy metals induce reactive oxygen species (ROS), which directly or indirectly influence metabolic processes. Reduced glutathione (GSH) attributes as an antioxidant and participates to control ROS during stress. Maintenance of the GSH/GSSG ratio is important for cellular redox balance, which is crucial for the survival of the plants. In this context, sulfurtransferases (Str), also called rhodanases, comprise a group of enzymes widely distributed in all phyla, paving the way for the transfer of a sulfur atom from suitable sulfur donors to nucleophilic sulfur acceptors, at least *in vitro*. The best characterized *in vitro* reaction is the transfer of a sulfane sulfur atom from thiosulfate to cyanide, leading to the formation of sulfite and thiocyanate. Plants as well as other organisms have multi-protein families (MPF) of Str. Despite the presence of Str activities in many living organisms, their physiological role has not been clarified

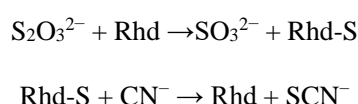
*Molecules* **2015**, *20***1411**

unambiguously. In mammals, these proteins are involved in the elimination of cyanide released from cyanogenic compounds. However, their ubiquity suggests additional physiological functions. Furthermore, it is speculated that a member of the Str family acts as arsenate reductase (AR) and is involved in arsenate detoxification. In summary, the role of Str in detoxification processes is still not well understood but seems to be a major function in the organism.

**Keywords:** arsenate; arsenate reductase; cyanide; rhodanese; sulfurtransferase

## 1. Introduction

Sulfurtransferases (Str), also called rhodanases, catalyzes the transfer of a sulfur atom from suitable sulfur donors to nucleophilic sulfur acceptors [1]. The most studied and best characterized Str is bovine liver rhodanese that catalyzes *in vitro* the transfer of a sulfane sulfur atom from thiosulfate (TS) to cyanide, leading to the formation of sulfite and thiocyanate by forming a Rhod-S intermediate, which is characterized by a persulfide bond at the sulfhydryl group of the essential cysteine residue 247 (Scheme 1) [2]:



**Scheme 1.** A sulfurtransferase reaction catalyzed by rhodanese.

Rhodanese activity has been detected in all major phyla [3]. Str/rhodanese domains can be found as tandem repeats hosting the active cysteine residue in the C-terminus, as single domain proteins, and in combination with distinct proteins domains. The prototype for a single domain Str protein is found in *Escherichia coli* (GlpE) that often interacts with thioredoxins [4,5]. It has been reported that single rhodanese domain proteins are involved in reactions to stress defense, such as the *Drosophila melanogaster* heat shock protein 67B2, the *E. coli* phage shock protein PspE [6] or the *Vibrio cholerae* shock protein q9KN65 [7]. In plants, proteins with single rhodanese domains are associated with the process of leaf senescence, for example in *Arabidopsis thaliana*, *Nicotiana tabacum* and *Raphanus sativus* (Sen1, Ntdin and Din1, respectively) [8,9]. However, the mode of action in response to stress or senescence processes is not yet known. The proteins, composed of two rhodanese domains with the catalytic cysteine in the C-terminal rhodanese domain, are represented by the bovine mitochondrial rhodanese [10] and the *Azotobacter vinelandii* rhodanese (RhdA) [11]. The amino acid composition of the active site loop containing the active cysteine residue affects the substrate recognition and specificity [12]. Notably, changing of the active site loop by one additional amino acid influences the substrate specificity of *A. vinelandii* RhdA from sulfate- to phosphate-containing compounds [13,14]. In the N-terminal domain, the cysteine residue is often replaced by aspartic acid or glycine and found to be associated with other protein domains such as MAPK phosphatases [15]. Certain stress response proteins and several ubiquitinating enzymes are also proposed to share the non-catalytic rhodanese



homology [14,16]. Therefore, it has been suggested that the inactive rhodanese domain could be involved in signaling [12] but more experimental evidence is needed.

Sulfurtransferases or Str-like proteins have been identified in different subcellular compartments. In rats, 3-mercaptopyruvate Str was identified in the cytoplasm and in mitochondria. It has been suggested to be involved in cyanide detoxification in the cytoplasm and to protect cytochrome c oxidase in mitochondria [17]. There are 20 different Strs or Str-like proteins in *A. thaliana* [18,19]. These have been classified into six groups based on their amino acid sequence similarities [20]. In wheat, Str was found to be involved in the resistance against the fungal pathogen *Erysiphe graminis* [21]. In another study, a cadmium-induced *A. thaliana* Str9 (AtStr9) homologue was identified in *Datura innoxia*, indicating a role of this Str in heavy metal stress [22]. Str/rhodanese domains are structurally similar to the catalytic subunit of arsenate reductase and Cdc25 phosphatase [14]. The high abundance of Str proteins in *A. thaliana* and other plant species [1] in different cellular compartments is speculated to pave the way for several specific biological functions, especially in abiotic and biotic stress defense.

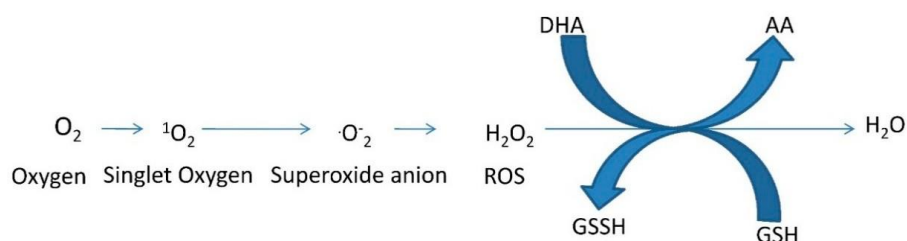
## 2. Detoxification of Cyanide

Plants are exposed to cyanide from different exogenous and endogenous sources. The largest source of cyanide in the environment comes from anthropogenic activities, like soil contaminated by various industrial wastes containing up to 11,000 mg cyanide kg<sup>-1</sup> DW soil [23]. Some natural exogenous sources including bacteria, fungi, algae, and neighboring plants are also responsible for cyanogenesis in significant amounts. The endogenous source of cyanide in plants is mainly the conversion of 1-amino-cyclopropane-1-carboxylic acid to ethylene that produces cyanide in equimolar amounts as ethylene and is drastically increased during fruit ripening and senescence [24]. Cyanide is also a potent inhibitor of respiration by inhibiting cytochrome c oxidase. Plants can readily take up cyanide and metalocyanides when present in the root zone [25]. Cyanide induces the formation of reactive oxygen species (ROS) and also triggers the production of hydrogen peroxide (H<sub>2</sub>O<sub>2</sub>) in embryonic axes of sunflower (*Helianthus annuus* L.) by stimulating NADPH oxidase and inhibiting antioxidant enzymes for instance catalase [26]. In higher plants, two metabolic pathways are involved in the detoxification and assimilation of excess cyanide. The first one is the Str pathway, also observed in bacteria and mammals. In mammals, Strs play the crucial role in catalysis of cyanide and in the formation of the less toxic thiocyanate that is primarily excreted in the urine [27]. In *Pseudomonas aeruginosa*, mitochondrial rhodanese has been proved to be involved in the protection of aerobic respiration from cyanide poisoning by transferring sulfane sulfur from thiosulfate to cyanide and yielding less toxic thiocyanate [28]. In plants, the contribution of Str to cyanide detoxification may be negligible or incidental [29]. Most recently, it was observed that the  $\beta$ -cyano-L-alanine ( $\beta$ -CAS) pathway is the principal mechanism for maintaining cyanide homeostasis in higher plants [30]. Previously, it was already suggested that  $\beta$ -cyano-L-alanine synthase (CAS) plays a more important role in cyanide detoxification than Str activity in *A. thaliana* [29]. At first, cyanide is substituted for the sulfhydryl group of cysteine to form  $\beta$ -CAS with the release of hydrogen sulfide [31]. Subsequently, the  $\beta$ -CAS is hydrolyzed by the gene product of NIT4, a dual enzyme with nitrilase and nitrile hydratase activity, yielding asparagine, aspartate and ammonia, respectively [30,32]. However, this study also explained, that the minor contribution of Str in cyanide detoxification could be based on methodological problems in the determination of

volatile hydrogen cyanide and cyanogenic compounds in plant tissue. Future work is needed to finally clarify the role of Str in cyanide detoxification in different environmental and developmental conditions.

### 3. Detoxification of Reactive Oxygen Species

Different cellular compartments such as chloroplasts (photosystems I and II), mitochondria (complex I, ubiquinone, and complex III of the electron transport chain), and peroxisomes are the major sites of formation of ROS [33]. Despite of those compartments, heavy metal ions mediate reactions (e.g., Fenton reaction) that exert an effect on the production of ROS leading to a decreased level of available antioxidant reserves [23]. Reactions with ROS damage proteins, lipids, carbohydrates, and DNA, ultimately yield in oxidative stress. Against this backdrop, plants possess an antioxidant defensive machinery to protect against stress damage. The tripeptide glutathione is an important antioxidant in many organisms preventing damage to important cellular components caused by ROS such as free radicals and peroxides (Scheme 2) [34]. Glutathione in its reduced and oxidized forms, GSH and GSSG, plays a significant role within the cellular redox state by maintaining sulfhydryl (-SH) groups. Sulfurtransferases, for example thiosulfate-thiol Str, are enzymes that participate in GSH metabolism and homeostasis [34].



**Scheme 2.** A flow chart of ROS formation and its detoxification. GSH (glutathione), GSSH (oxidized glutathione), AA (ascorbic acid) and DHA (dehydroascorbate) [35].

Various enzymes, such as superoxide dismutase, catalase, glutathione reductase, and glutathione S-transferase (GST) work in concert to control the oxidative damage by scavenging ROS [36]. Glutathione reductase found in prokaryotes and eukaryotes plays a pivotal role in the defense system against ROS, and it is localized predominantly in chloroplasts, but small amounts were found in mitochondria and the cytosol. Glutathione reductase is involved in the maintenance of the ascorbate-GSH cycle and NADPH-dependent reaction of disulphide bond recovery of GSSH by sustaining the reduced status of GSH [37]. Glutathione peroxidase provides an alternative means of detoxifying activated oxygen by using GSH to reduce hydrogen peroxide, which then yields GSSG [35]. It has been observed that glutathione reductase activities increase in the presence of cadmium in *A. thaliana*, *Vigna mungo*, *Triticum aestivum*, and *Brassica juncea*. In another study, transgenic *Nicotiana tabacum* with 30%–70% less glutathione reductase activity showed enhanced sensitivity to oxidative stress. Likewise, GSH concentrations were also elevated with heavy metal induced oxidative stress [38,39]. Plant GSTs have a crucial role to remove cytotoxic or genotoxic compounds. They have been found in maize, soybean, and *A. thaliana*. GSTs have been noticed to reduce peroxides by the assistance of GSH and yield scavengers of cytotoxic and genotoxic compounds [40].

Str might play a role in the control of redox homeostasis in the different subcellular compartments in a protein-protein interaction with thioredoxin. In this process, Str might act as a thioredoxin peroxidase with the intermediate formation of a sulfenate at the active-site cysteine as summarized in [1].

#### 4. Detoxification of Heavy Metals

Lead, cadmium, and mercury are profoundly toxic to tissue, cells and cellular components. It is known that the sulfur-containing endogenous compounds play a pivotal role in various physiological processes in organisms, such as the stabilization of protein structure and regulation of enzymatic activity, in addition to their role in redox reactions as described above. Notably, Str (rhodanese, 3-mercaptopyruvate Str and  $\gamma$ -cystathionase) plays an important role in the metabolism of L-cysteine [41]. The catalytic activity of these enzymes are decreased via heavy metals binding with -SH groups of cysteine residues [42]. Consequently, changes in the level of sulfane sulfur-containing compounds, products of L-cysteine desulfuration and glutathione, are observed. An alteration in the activity of Str after exposure to lead, cadmium, and mercury was noticed in kidneys, liver, heart, brain, and skeletal muscle of Marsh frog [42].

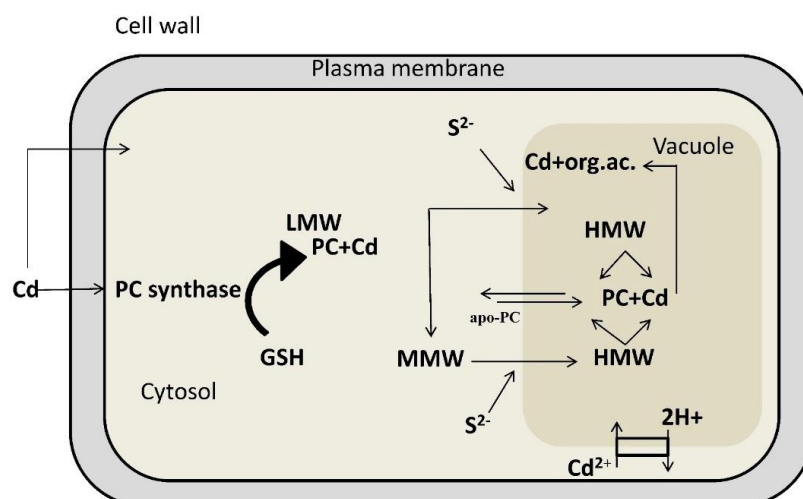


**Figure 1.** Diagram illustrating the mechanisms involved in cadmium chelation and compartmentalization in the vacuole (modified from ref. [43]). Phytochelatins are synthesized from GSH by the enzyme phytochelatin synthase. Exposure to cadmium stimulates synthesis of phytochelatins, which rapidly form a “low molecular weight” (LMW) complex with cadmium and a “medium molecular weight” (MMW) complex characterized by cadmium prevalently bound to phytochelatin with a higher polymerization level. At the tonoplast level, these complexes acquire acid-labile sulfur ( $S^{2-}$ ) and form a “high molecular weight” (HMW) complex with a higher affinity towards cadmium ions. Thus, particularly the HMW complex, highly stabilized by  $S^{2-}$  groups, seems to be decisive in cadmium detoxification. “LMW”, low molecular weight; “MMW”, medium molecular weight; “HMW”, high molecular weight; GSH, glutathione; PC, phytochelatin; apo-PC, apo-phytochelatin;  $S^{2-}$ , acid-labile sulfur; org. ac., organic acids.

Abiotic stress factors, such as exposition to heavy metals, induce the expression of sulfate assimilation and sulfate transporter genes [44]. In plants, cysteine and GSH can be synthesized in all tissues but higher biosynthetic activities of enzymes involved in cysteine and GSH production were observed in *A. thaliana* trichomes, where presumably also phytochelatins are produced for heavy metal detoxification (Figure 1) [45].

To alleviate oxidative stress, GSH functions as a direct antioxidant and also as a reducing agent for other antioxidants such as ascorbic acid [35]. Cysteine is essential for GSH synthesis. Sulfur assimilation is also regulated by the cellular oxidative state. For example, an isoform of 5-adenylyl-sulfate (APS) reductase is activated by oxidation of two SH-groups of cysteine residues in the enzyme into a disulfide bond by oxidized glutathione [46]. It has been suggested that enzymes of sulfur metabolism and GSH synthesis are post-translationally modified and activated after consumption of reduced GSH by oxidative stress mitigation [47].

#### 4.1. Sulfurtransferases with Arsenate Reductase Activity

Several plants species have been identified to accumulate arsenic in their plant tissues, for example the ferns *Pteris vittata* and *Pityrogramma calomelanos* [48]. The actual mechanisms of arsenic uptake and the manner in which plants detoxify these pollutants are not well known. Arsenate reductases (AR) are enzymes that catalyse the essential reduction reaction in the process of arsenic phytoremediation. Their active site contains a pair of cysteine residues that are essential for its catalytic action. One residue is part of the highly conserved sequence: Cys-(X)<sub>5</sub>-Arg. The mechanism of enzymatic reduction by AR involves formation of a thioester bond between the cysteine and As (V). The arginine residue assists in the stabilization of the intermediate [49].

Arsenate reductase activity was determined in an arsenate-hyperaccumulating fern. The reaction mechanism was very similar to the previously reported activity of Acr2p from yeast, using GSH as the electron donor. A T-DNA knockout mutant of *A. thaliana* with disruption in the homologous *Acr2* gene showed no AR activity [50]. Recently, it has been suggested that one member of the Str family also acts as AR in *A. thaliana*. According to the nomenclature by Bartels *et al.* [18], the orthologous protein in *A. thaliana* corresponds to AtStr5 (At5g03455), one of the 20 existing proteins containing a rhodanese domain grouped along with three other Str into “Group III”. It is predicted to be localized in the nucleus and contains a cysteine residue in the active centre [1]. The active site loop of AtStr5 has also a His-Cys-(X)<sub>5</sub>-Arg motif. Interestingly, the same protein was shown to act as Cdc25 dual-specificity tyrosine-phosphatase that is involved in the progression of the cell cycle by the removal of inhibitory phosphate residues from target cyclin-dependent kinases (CDKs) [20,51]. Notably, the His-Cys-(X)<sub>5</sub>-Arg motif coincides with the protein tyrosine phosphatase signature motif, but the regulatory N-terminal domain is absent in AtStr5 unlike human Cdc25 [52]. Thus, the rhodanese domain with seven amino acid loop is able to bind to substrates containing phosphorous or in a similar way to arsenic, whereas the rhodanese-like domains with the six amino acid loop interact with substrates containing reactive sulfur or in some cases selenium [53].

Arsenate reductase from *Saccharomyces cerevisiae* Acr2p (or ScAcr2p) and *Pteris vittata* (PvACR2) has been predicted to have three-dimensional structure related to members of rhodaneses/Cdc25 superfamily and share the Cdc25 active site motif His-Cys-(X)<sub>5</sub>-Arg. They do not exhibit significant

phosphatase activity, although *ScAcr2p* can be converted from reductase to a phosphatase by a small number of mutations [54–56]. In contrast, AtStr5 (also named as AtACR2), *OsACR2* from rice *Oryza sativa*, and *LmACR2* from the parasitic protozoan *Leishmania major* showed both arsenate reductase and phosphatase activities [50,57,58]. In another study, AtStr5 over-expressing *A. thaliana* lines were found to resemble wild-type plants without any indication of over-proliferation or increased cell cycle rates [59]. In the same study, the *AtStr5* T-DNA insertion knockout mutants and AtStr5 over-expressing lines were tested for altered behavior after auxin and cytokinin treatment, but no altered hormone response was observed. This contradicted the role of the *A. thaliana* Cdc25 homolog, the AtStr5 protein, as a regulator of the cell cycle progression.

#### 4.2. *AtStr5* as Arsenate Reductase: Possible Role in Arsenic Phytoremediation

Arsenic occurs in the environment mainly in its inorganic form, as arsenite [As (III)] and arsenate [As (V)]. Figure 2 gives the structures of the main inorganic forms of arsenic, arsenate and arsenite.

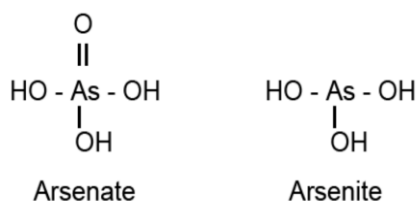


**Figure 2.** Inorganic forms of arsenic.

Both these forms of arsenic are toxic to organisms. However, As (III) is considered to be more toxic than the As (V) form. Both forms interrupt biological functions in a different manner. Arsenite binds to proteins with sulfhydryl groups interfering with their functions. It inhibits respiration by binding to vicinal thiols in pyruvate dehydrogenase and 2-oxo-glutarate dehydrogenase [60]. Arsenite does not act directly as a mutagen but induces intra-chromosomal homologous recombination [61] and generates ROS [62], whereas As (V) interferes with oxidative phosphorylation and ATP synthesis [63].

The arsenic hyperaccumulator plants are potential candidates for arsenic phytoremediation. The process by which the plant accumulates arsenic is illustrated in Figure 3. The As (V) uptake occurs via phosphate transporters, whereas As (III) influx takes place in its neutral As(OH)<sub>3</sub> form through aquaglyceroporins. The majority of arsenic found in the soil is in the arsenate form bound to different elements with different solubility, also dependent on the pH of the soil. The As (V) taken up is then reduced to As (III) by the enzyme AR. The next process is arsenite complexation with free thiol groups in order to detoxify the compound. This is followed by the vacuolar compartmentalization and storage of the arsenite-thiolate complex, thus completing the arsenic phytoremediation process [64].

The mechanism of enzymatic reduction by AR involves the formation of a thioester bond between the cysteine and As (V), and the arginine residue assists in the stabilization of the intermediate. The reduced form of AR is its active form, and the reducing agent involved in the generation of the active form of AR is either a thioredoxin or a glutaredoxin [65]. For example, AR encoded by *ArsC* gene from *Staphylococcus aureus* utilizes thioredoxin as its reducing agent, while the AR from *E. coli* R773

(encoded by *ArsC* gene) and *S. cerevisiae* (encoded by *Acr2p* gene) utilize glutathione and glutaredoxin as reducing agents [66].

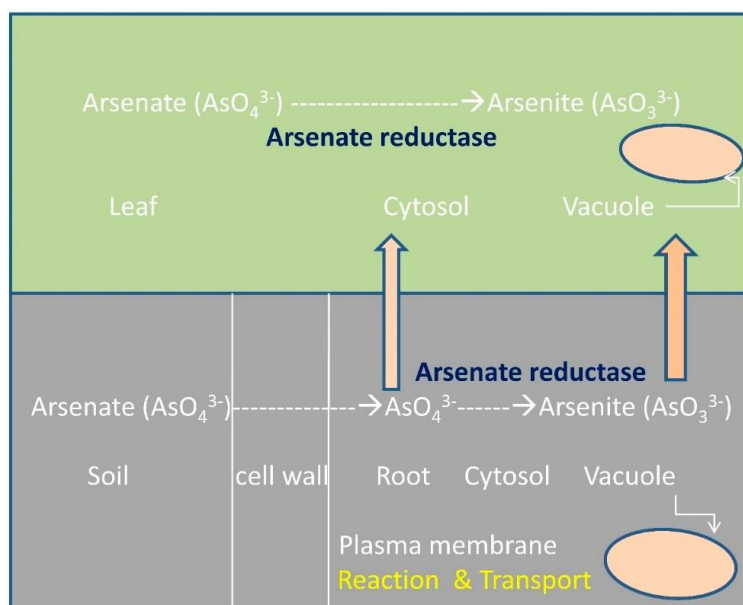


**Figure 3.** Mechanism of arsenic phytoremediation (modified from [25]).

So far the AR activity could not be confirmed for the recombinant AtStr5 *A. thaliana* protein. However, the comparison of growth of *A. thaliana* AtStr5-expressing *E. coli* cells and negative control cells cultured on media containing varying levels of arsenate (125 to 1000  $\mu\text{M}$ ) showed that AtStr5 positive *E. coli* transformants were resistant to arsenate (Papenbrock and co-workers, unpublished results). These observations further pointed towards the role of AtStr5 as an AR, maybe in an interaction process with thioredoxins.

In another study, the AR activity was observed in root extracts of T-DNA knockout *AtStr5* mutant plants unexposed to arsenate. Furthermore, it was confirmed that the AR activity of AtStr5 represents 36% of the total activity and is inducible by arsenate in *A. thaliana* roots [57]. In a similar study on plants grown under low arsenate exposure levels, the *AtStr5* mRNA was silenced using an RNAi construct. This increased the shoot arsenic accumulation 10–16 fold more than the roots of wild-type plants grown under identical conditions [59]. In contrast, the T-DNA insertion mutants of *AtStr5* accumulated less arsenic in shoots than wild-type plants over a range of arsenate concentrations [57]. Despite all these studies, the actual functional significance of AtStr5 is still a mystery. Discrepancy of these studies and broad physiological functions make AtStr5 a protein of further research interest.

A distance phylogenetic tree (ClustalW tool from EBI based on Neighbor Joining) of rhodanese/Cdc25 superfamily members demonstrates the relationships among putative AR proteins (Figure 4). AtStr5 shows 55% identity and 79% similarity with *Oryza sativa* Cdc25 (OsCdc25), and 42% identity and 61% similarity with *Pteris vittata* AR. Although AtStr5 shares the same active site region as the human Cdc25 isoforms (A, B and C), it was seen that they have less overall identity. This may be considered as another indication for the possibility that AtStr5 may not act as a phosphatase but may

have an important role in arsenate reduction. AtStr6 is similar to the human Cdc25 isoform A (huCdc25A) and since huCdc25A has no AR activity, the same can be expected of AtStr6. AtStr7 and AtStr8 form an entirely different clade in the phylogenetic tree, suggesting that they are not functionally related to AtStr5. Therefore, the other Str from group III, except AtStr5, may not show AR activity.

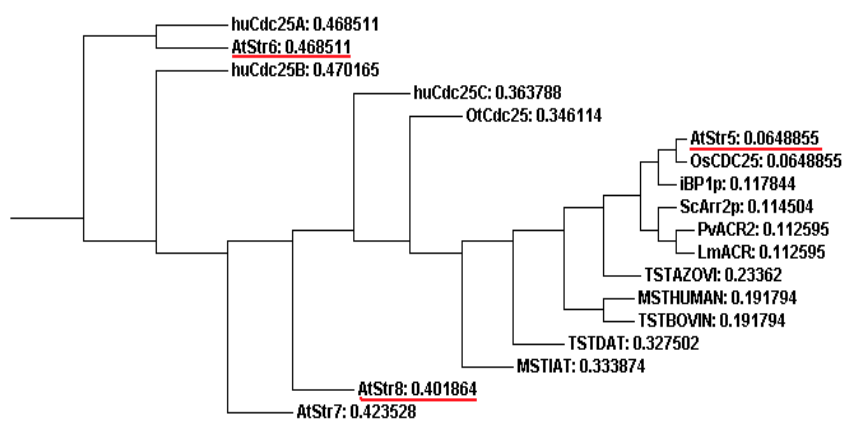


**Figure 4.** Phylogenetic tree obtained by using the Neighbor Joining method. The sequences selected for phylogenetic analysis are: Human Cdc25A (huCdc25A; NP\_001780.2), Human Cdc25B (huCdc25B; NP\_068658.1), Human Cdc25C (huCdc25C; NP\_073720.1), *Ostreococcus tauri* Cdc25 (OtCdc25; AAQ16122.1), *Oryza sativa* Cdc25 (OsCdc5; AAX54896.1), Itsy bitsy phosphatase 1 (iBP1p; Q8WZK3.1), *Saccharomyces cerevisiae* arsenate reductase (ScArr2p; NP\_015526.1), *Pteris vittata* arsenate reductase (PvACR2; ABC26900.1), *Leishmania major* arsenate reductase (LmACR; AAS73185.1), *Arabidopsis thaliana* Group III sulfurtransferases (AtStr5; AAO39886.1, AtStr6; ABO38777.1, AtStr7; ABF57279.1, AtStr8; NP\_564039.6), *Arabidopsis thaliana* 3-MP sulfurtransferase (MSTIAT; CAB64716.1), *Datisca glomerata* TS sulfurtransferase (TSTDAT; AAD19957.1), *Homo sapiens* 3-MP sulfurtransferase (MSTHUMAN; P25325.3), *Bovine taurus* TS sulfurtransferase (TSTBOVIN; P00586.3), *Azotobacter vinelandii* TS sulfurtransferase (TSTAZOVI; P52197.1). 3-MP, 3-mercaptopyruvate; TS, thiosulfate.

#### 4.3. Phytoremediation

Phytoremediation is virtually considered as a potential solution to mitigate arsenic pollution. Certain plants known as hyperaccumulators or metallophytes have the ability to reduce heavy metal contamination by accumulating higher than normal levels of toxic heavy metals in their above-ground parts [64]. The over-expression of two bacterial proteins, AR encoded by the *arsC* gene and the  $\gamma$ -glutamylcysteine synthase, has been studied in *A. thaliana* in an attempt to yield a transgenic arsenic hyperaccumulator. Notably, AR catalyzes the reduction of arsenate to arsenite ( $\text{AsO}_3^{3-}$ ) in the stem and leaves. The  $\gamma$ -ECS is involved in the first step of the phytochelatin synthesis pathway.  $\gamma$ -Glutamylcysteine complexes are formed with As (III) via its thiol groups, consequently detoxifying and preparing them for being stored away in vacuole, supporting the idea that the transgenic plants were

able to accumulate 2–3 times more arsenic than wild-type plants [59]. However, the means by which arsenite-thiolate compounds are transported into the vacuole is still unknown.

## 5. Conclusions

Various heavy metal ions trigger the overproduction of ROS or free radicals in plants which are toxic and highly sensitive to proteins, lipids, carbohydrates and DNA, and ultimately results in oxidative stress. Against this backdrop, cells are evolved with sophisticated antioxidant defense mechanisms to detoxify the deleterious consequences of ROS. These antioxidant defenses could be non-enzymatic (e.g., glutathione, proline, carotenoids and flavonoids) or enzymatic (e.g., superoxide dismutase, GR and GSTs). There is profound evidence that cyanide leads to the yield of ROS and to escalate hydrogen peroxide (H<sub>2</sub>O<sub>2</sub>) by stimulating NADPH oxidase. In this context,  $\beta$ -CAS pathway has been profoundly accepted for maintaining cyanide homeostasis in higher plants. On the other hand, Str in animals has been well described as means of detoxifying cyanide. Nevertheless, Str activities are present in many living organisms, but their physiological role here still ambiguously. Their ubiquity suggests additional physiological functions. Furthermore, it was suggested that one member of Str mimic as AR which is involved in arsenic phytoremediation and might be a promising candidate for successful removal of arsenic from soil. Henceforth, development of abiotic stress-tolerant crop via over-expression of ROS-scavenging enzymes and enzymes containing reactive sulfur groups, such as Str, may be useful.

## Acknowledgments

We would like to thank the DAAD for financial support of P.M.

## Author Contributions

The basic ideas and the structure were thought by J.P. Both authors, P.M. and J.P., contributed equally to the single paragraphs.

## Conflicts of Interest

The authors declare no conflict of interest.

## References

1. Papenbrock, J.; Guretzki, S.; Henne, M. Latest news about the sulfurtransferases of higher plants. *Amino Acids* **2010**, *41*, 53–57.
2. Gliubich, F.; Gazerro, M.; Zanotti, G.; Delbono, S.; Bombieri, G.; Berni, R. Active site structural features for chemically modified forms of rhodanase. *J. Biol. Chem.* **1996**, *27*, 21054–21061.
3. Westley, J. Rhodanase. *Adv. Enzymol. Relat. Areas Mol. Biol.* **1973**, *39*, 327–368.
4. Ray, W.K.; Zeng, G.; Potters, M.B.; Mansuri, A.M.; Larson, T.J. Characterization of a 12-kilodalton rhodanase encoded by glpE of *Escherichia coli* and its interaction with thioredoxin. *J. Bacteriol.* **2000**, *182*, 2277–2284.



5. Spallarossa, A.; Donahue, J.L.; Larson, T.J.; Bolognesi, M.; and Bordo, D. *Escherichia coli* GlpE is a prototype sulfurtransferase for the single-domain rhodanese homology superfamily. *Structure* **2001**, *9*, 1117–1125.
6. Adams, H.; Teertstra, W.; Koster, M.; Tommassen, J. PspE (phage shock protein E) of *Escherichia coli* is a rhodanese. *FEBS Lett.* **2002**, *518*, 173–176.
7. Heidelberg, J.F.; Eisen, J.A.; Nelson, W.C.; Clayton, R.A.; Gwinn, M.L.; Dodson, R.J.; Haft, D.H.; Hickey, E.K.; Peterson, J.D.; Umayam, L.A., *et al.* DNA sequence of both chromosomes of the cholera pathogen *Vibrio cholerae*. *Nature* **2000**, *406*, 477–483.
8. Azumi, Y.; Watanabe, A. Evidence for a senescence-associated gene induced by darkness. *Plant Physiol.* **1991**, *95*, 577–583.
9. Oh, S.A.; Lee, S.Y.; Chung, I.K.; Lee, C.H.; Nam, H.G. A senescence-associated gene of *Arabidopsis thaliana* is distinctively regulated during natural and artificially induced leaf senescence. *Plant Mol. Biol.* **1996**, *30*, 739–754.
10. Ploegman, J.H.; Drent, G.; Kalk, K.H.; Hol, W.G. Structure of bovine liver rhodanese. I. Structure determination at 2.5 Å resolution and a comparison of the conformation and sequence of its two domains. *J. Mol. Biol.* **1978**, *123*, 557–594.
11. Bordo, D.; Deriu, D.; Colnaghi, R.; Carpen, A.; Pagani, S.; Bolognesi, M. The crystal structure of a sulfurtransferase from *Azotobacter vinelandii* highlights the evolutionary relationship between the rhodanese and phosphatase enzyme families. *J. Mol. Biol.* **2000**, *298*, 691–704.
12. Bordo, D.; Bork, P. The rhodanese/Cdc25 phosphatase super family: Sequence structure and functions relations. *EMBO Rep.* **2002**, *3*, 741–746.
13. Forlani, F.; Carpen, A.; Pagani, S. Evidence that elongation of the catalytic loop of the *Azotobacter vinelandii* rhodanese changed selectivity from sulfur-to phosphate-containing substrates. *Protein Eng.* **2003**, *16*, 515–519.
14. Hofmann, K.; Bucher, P.; Kajava A.V. A model of Cdc25 phosphatase activity catalytic domain and Cdk-interaction surface based on the presence of a rhodanese homology domain. *J. Mol. Biol.* **1998**, *282*, 195–208.
15. Farooq, A.; Chaturvedi, G.; Mujtaba, S.; Plotnikova, O.; Zeng, L.; Dhalluin, C.; Ashton, R.; Zhou, M.M. Solution structure of ERK2 binding domain of MAPK phosphatase MKP-3: Structural insights into MKP-3 activation by ERK2. *Mol. Cell* **2001**, *7*, 387–399.
16. Fauman, E.B.; Cogswell, J.P.; Lovejoy, B.; Rocque, W.J.; Holmes, W.; Montana, V.G.; Rink, M.J.; Piwnicka-Worms, H.; Saper, M.A. Crystal structure of the catalytic domain of the human cell cycle control phosphatase, Cdc25A. *Cell* **1998**, *93*, 617–625.
17. Nagahara, N.; Ito, T.; Minami, M. Mercaptopyruvate sulfurtransferase as a defense against cyanide toxification: Molecular properties and mode of detoxification. *Histol. Hispathol.* **1999**, *14*, 1277–1286.
18. Bartels, A.; Mock, H.P.; Papenbrock, J. Differential expression of *Arabidopsis* sulfurtransferases under various growth conditions. *Plant Physiol. Biochem.* **2007**, *45*, 178–187.
19. Bauer, M.; Papenbrock, J. Identification and characterization of single-domain thiosulfate sulfurtransferases from *Arabidopsis thaliana*. *FEBS Lett.* **2002**, *532*, 427–431.
20. Landrieu, I.; da Costa, M.; de Veylder, L.; Dewitte, F.; Vandepoele, K.; Hassan, S.; Wieruszkeski, J.M.; Corellou, F.; Faure, J.D.; van Montagu, M.; *et al.* A small CDC25 dual-specificity tyrosine-phosphatase isoform in *Arabidopsis thaliana*. *Proc. Natl. Acad. Sci. USA* **2004**, *101*, 13380–13385.

21. Niu, J.S.; Yu, L.; Ma, Z.-Q.; Chen, P.-D.; Liu, D.-J. Molecular cloning, characterization and mapping of a rhodanese like gene in wheat. *Acta Genet. Sin.* **2002**, *29*, 266–272.
22. Louie, M.; Kondor, N.; Dewitt, J.G. Gene expression in cadmium-tolerant *Datura innoxia*: Detection and characterization of cDNAs induced in response to Cd<sup>2+</sup>. *Plant Mol. Biol.* **2003**, *52*, 81–89.
23. Henny, C.J.; Hallock, R.J.; Hill, E.F. Cyanide and migratory birds at gold-mines in Nevada, USA. *Ecotoxicology* **1994**, *3*, 45–58.
24. Yip, W.-K.; Yang, S.F. Cyanide metabolism in relation to ethylene production in plant tissues. *Plant Physiol.* **1988**, *88*, 473–476.
25. Doucleff, M.; Terry, N. Pumping out the arsenic. *Nat. Biotechnol.* **2002**, *20*, 1094–1096.
26. Oracz, K.; El-Maarouf-Bouteau, H.; Kranner, I.; Bogatek, R.; Corbineau, F.; Bailly, C. The mechanisms involved in seed dormancy alleviation by hydrogen cyanide unravel the role of reactive oxygen species as key factors of cellular signaling during germination. *Plant Physiol.* **2009**, *150*, 494–505.
27. Ressler, C.; Tataka, J.G. Vicianin, prunasin, and β-cyanoalanine in common vetch seed as sources of urinary thiocyanate in the rat. *J. Agric. Food Chem.* **2001**, *49*, 5075–5080.
28. Cipollone, R.P.; Ascenzi, P.; Tomao, F.; Imperi, P.; Visca, P. Enzymatic detoxification of cyanide: Clues from *Pseudomonas aeruginosa* Rhodanese. *J. Mol. Microbiol. Biotechnol.* **2008**, *15*, 199–211.
29. Meyer, T.; Burow, M.; Bauer, M.; Papenbrock, J. Arabidopsis sulfurtransferases: Investigation of their function during senescence and in cyanide detoxification. *Planta* **2003**, *217*, 1–10.
30. Machingura, M.; Ebbs, S.D. Functional redundancies in cyanide tolerance provided by β-cyanoalanine pathway genes in *Arabidopsis thaliana*. *Int. J. Plant Sci.* **2014**, *175*, 346–358.
31. Hatzfeld, Y.; Maruyama, A.; Schmidt, A.; Noji, M.; Ishizawa, K.; Saito, K. β-cyanoalanine synthase is a mitochondrial cysteine synthase-like protein in spinach and *Arabidopsis*. *Plant Physiol.* **2000**, *123*, 1163–1172.
32. Piotrowski, M.; Schonfelder, S.; Weiler, E.W. The *Arabidopsis thaliana* isogene NIT4 and its orthologs in tobacco encode β-cyano-L-alanine hydratase/nitrilase. *J. Biol. Chem.* **2001**, *276*, 2616–2621.
33. Moller, I.M. Plant mitochondria and oxidative stress: Electron transport, NADPH turnover, and metabolism of reactive oxygen species. *Annu. Rev. Plant Physiol. Mol. Biol.* **2001**, *52*, 561–591.
34. Uhteg, L.C.; Westley, J. Purification and steady-state kinetic analysis of yeast thiosulfate reductase. *Arch. Biochem. Biophys.* **1979**, *195*, 211–222.
35. Slater, A.; Scott, N.W.; Fowler, M.R. *Plant Biotechnology: The Genetic Manipulation of Plants*, 2nd ed.; Oxford University Press: Oxford, UK, 2008; p. 231.
36. Mittler, R.; Vanderauwera, S.; Gollery, M.; van Breusegem, F. Reactive oxygen gene network of plants. *Trends Plant Sci.* **2004**, *9*, 490–498.
37. Chalapathi Rao, A.S.V.; Reddy, A.R. *Glutathione Reductase: A Putative Redox Regulatory System in Plant Cells. Sulfur Assimilation and Abiotic Stresses in Plants*; Khan, N.A., Singh, S., Umar S., Eds.; Springer: Heidelberg, Berlin, 2008; pp. 111–147.
38. Ding, S.; Lu, Q.; Zhang, Y.; Yang, Z.; Wen, X.; Zhang, L.; Lu, C. Enhanced sensitivity to oxidative stress in transgenic tobacco plants with decreased glutathione reductase activity leads to a decrease in ascorbate pool and ascorbate redox state. *Plant Mol. Biol.* **2009**, *69*, 577–592.

39. Foyer, C.H.; Noctor, G. Redox homeostasis and antioxidant signaling: A metabolic interface between stress perception and physiological responses. *Plant Cell* **2005**, *17*, 1866–1875.
40. Dixon, D.P.; Davis, B.G.; Edwards, E. Functional divergence in the glutathione transferase super-family in plants: Identification of two classes with putative functions in redox homeostasis in *Arabidopsis thaliana*. *J. Biol. Chem.* **2002**, *277*, 30859–30869.
41. Toohey, T.I. Sulphane sulfur in biological systems: A possible regulatory role. *Biochemistry* **1989**, *264*, 625–632.
42. Kaczor-Kamińska, M.; Sura, P.; Wróbel, M. Changes in activity of three sulfurtransferases in response to exposure to cadmium, lead and mercury ions. *J. Environ. Prot.* **2013**, *4*, 19–28.
43. Tomsett, A.B.; Thurman, D.A. Molecular biology of metal tolerances of plants. *Plant Cell Environ.* **1988**, *11*, 383–394.
44. Nocito, F.F.; Pirovano, L.; Cocucci, M.; Sacchi, G.A. Cadmium-induced sulfate uptake in maize roots. *Plant Physiol.* **2002**, *129*, 1872–1879.
45. Gutiérrez-Alcalá, G.; Gotor, C.; Meyer, A.J.; Fricker, M.; Vega, J.M.; Romeo, L.C. Glutathione biosynthesis in *Arabidopsis trichome* cells. *Proc. Natl. Acad. Sci. USA* **2000**, *97*, 11108–11113.
46. Bick, J.A.; Setterdahl, A.T.; Knaff, D.B.; Chen, Y.; Pitcher, L.H.; Zilinskas, B.A.; Leustek, T. Regulation of the plant-type 5-adenylsulfate reductase by oxidative stress. *Biochemistry* **2001**, *40*, 9040–9048.
47. Kazuki, S. Sulfur assimilatory metabolism: The long and smelling road. *Plant Physiol.* **2004**, *136*, 2443–2450.
48. Peer, W.A.; Baxter, I.R.; Richards, E.L.; Freeman, J.L.; Murphy, A.S. Phytoremediation and hyperaccumulator plants. In *Molecular Biology of Metal Homeostasis and Detoxification*; Tamás, M.J., Martinoia, E., Eds.; Springer: Heidelberg, Berlin, Germany, 2005; Volume 14, pp. 299–330.
49. Fernandes, A.P.; Holmgren, A. Glutaredoxin: Glutathione-dependent redox enzymes with functions far beyond a simple thioredoxin backup system. *Antioxid. Redox Signal.* **2004**, *6*, 63–74.
50. Duan, G.L.; Zhu, Y.G.; Tong, Y.P.; Cai, C.; Kneer, R. Characterization of arsenate reductase in the extract of roots and fronds of Chinese brake fern, an arsenic hyperaccumulator. *Plant Physiol.* **2005**, *138*, 461–469.
51. Sorrell, D.A.; Chrimes, D.; Dickinson, J.R.; Rogers, H.J.; Francis, D. The *Arabidopsis* CDC25 induces a short cell length when overexpressed in fission yeast: Evidence for cell cycle functions. *New Phytol.* **2005**, *165*, 425–428.
52. Landrieu, I.; Hassan, S.; Sauty, M.; Dewitte, F.; Wieruszkeski, J.M.; Inzé, D.; de Veylder, L.; Lippens, G. Characterization of the *Arabidopsis thaliana* Arath; CDC25 dual-specificity tyrosine phosphatase. *Biochem. Biophys. Res. Commun.* **2004**, *322*, 734–739.
53. Ogasawara, Y.; Lacourciere, G.; Stadtman, T.C. Formation of a selenium-substituted rhodanese by reaction with selenite and glutathione: Possible role of a protein perselenide in a selenium delivery system. *Proc. Natl. Acad. Sci. USA* **2001**, *98*, 9494–9498.
54. Mukhopadhyay, R.; Shi, J.; Rosen, B.P. Purification and characterization of ACR2p, the *Saccharomyces cerevisiae* arsenate reductase. *J. Biol. Chem.* **2000**, *275*, 21149–21157.
55. Mukhopadhyay, R.; Rosen, B.P. The phosphatase C(X)<sub>5</sub>R motif is required for catalytic activity of the *Saccharomyces cerevisiae* Acr2p arsenate reductase. *J. Biol. Chem.* **2001**, *276*, 34738–34742.

56. Mukhopadhyay, R.; Zhou, Y.; Rosen, B.P. Directed evolution of a yeast arsenate reductase into a protein-tyrosine phosphatase. *J. Biol. Chem.* **2003**, *278*, 24476–24480.
57. Bleeker, P.M.; Hakvoort, H.W.; Blik, M.; Souer, E.; Schat, H. Enhanced arsenate reduction by a Cdc25-like tyrosine phosphatase explains increased phytochelatin accumulation in arsenate-tolerant *Holcus lanatus*. *Plant J.* **2006**, *45*, 917–929.
58. Zhou, Y.; Bhattacharjee, H.; Mukhopadhyay, R. Bifunctional role of the leishmanial antimonate reductase LmACR2 as a protein tyrosine phosphatase. *Mol. Biochem. Parasitol.* **2006**, *148*, 161–168.
59. Dhankher, O.P.; Rosen, B.P.; McKinney, E.C.; Meagher, R.B. Hyper-accumulation of arsenic in the shoots of Arabidopsis silenced for arsenate reductase, ACR2. *Proc. Natl. Acad. Sci. USA* **2006**, *103*, 5413–5418.
60. Leonard, A.; Lauwerys, R. Carcinogenicity, teratogenicity, and mutagenicity of arsenic. *Mutat. Res.* **1980**, *75*, 49–62.
61. Helleday, T.; Nilsson, R.; Jenssen D. Arsenic (III) and heavy metal ions induce intrachromosomal homologous recombination in the *hprt* gene of V79 Chinese hamster cells. *Environ. Mol. Mutagen.* **2000**, *35*, 114–122.
62. Chou, W.C.; Jie, C.; Kenedy, A.A.; Jones, R.J.; Trush, M.A.; Dang, C.V. Role of NADPH oxidase in arsenic-induced reactive oxygen species formation and cytotoxicity in myeloid leukemia cells. *Proc. Natl. Acad. Sci. USA* **2004**, *101*, 4578–4583.
63. Carbonell, A.A.; Aarabi, M.A.; Delaune, R.D.; Grambrell, R.P.; Patrick, W.H. Arsenic in wetland vegetation: Availability, phytotoxicity, uptake and effects on plants growth and nutrition. *Sci. Total Environ.* **1998**, *217*, 189–199.
64. Shah, K.; Nongkynrih, J.M. Metal hyperaccumulation and bioremediation. *Biol. Plant.* **2007**, *51*, 618–634.
65. Li, R.; Haile, J.D.; Kennelly, P.J. An arsenate reductase from *Synechocystis* sp. strain PCC 6803 exhibits a novel combination of catalytic characteristics. *J. Bacteriol.* **2003**, *185*, 6780–6789.
66. Shipley, S.; Nordin, A.B.; Tang, C.G.; Kim, S.K. Phytoremediation for arsenic contamination: Arsenate reductase. *The Pulse* **2008**, *6*, 1–12.

© 2015 by the authors; licensee MDPI, Basel, Switzerland. This article is an open access article distributed under the terms and conditions of the Creative Commons Attribution license (<http://creativecommons.org/licenses/by/4.0/>).

## CHAPTER III

### Characterization of group III *Arabidopsis* sulfurtransferase 5 proteins

#### Abstract

In *Arabidopsis thaliana*, 20 proteins containing one or more rhodanese domain and Str-patterns were identified, and they are classified into six groups according to their amino acid sequence homology. The present work focuses on the characterization of the AtStr5 protein, which has been ambiguously identified as both phosphatase (Arath; CDC25) and arsenate reductase (AtACR2). The AtStr5 protein was expressed heterologously in *Escherichia coli*, however, upon expression, the majority of the proteins were found in forming inclusion bodies and form protein aggregation during the purification process. Trial to optimize all bottleneck concerning the expression and purification leads to achieve the protein in a soluble state which is essential for enzymatic-assay. In an enzymatic determination, the AtStr5 showed phosphatase activity over Str, and phosphatase activity was abolished when catalytic cysteine 72 was replaced by the alanine 72, which indicates cysteine is the critical residue for substrate recognition. The AtStr5 enzyme showed ~3000-fold enhancement of  $k_{cat}/K_m$  for 3-OMFP over pNPP resembles the other known DS-PTPases. However, the substrate affinity and other kinetic parameters of AtStr5 were remarkably lower than the human CDC25B. The AtStr5 showed ~1.5-fold lower  $K_m$  value, ~11-fold lower  $k_{cat}$  and ~17-fold lower  $k_{cat}/K_m$  values than the huCDC25B, which raises the question about the mitotic accelerator role of this protein. The Str activity was very negligible with the substrate 3-MP and estimated  $K_m$  value was ~29 mM, which is significantly higher than other characterized AtStrs. In a GFP mediated subcellular localization study of AtStr5, the truncated GFP fusion constructs (132 aa and 117 aa) were found in the cell cytoplasm. However, the localization of the full-length (146 aa) fusion protein remained unclear; occasionally it appeared to be in the nucleus. It might be possible that the protein has a dual localization (nucleus and cytoplasm) similar to the huCDC25B, having both phosphatase and arsenate reductase activities *in vitro*. The knowledge of substrate preference *in vitro* and the subcellular localization of AtStr5 protein will provide an essential clue for the elucidation of its specific functions in the multicellular organism.

## 1 Introduction

Sulfurtransferases (Strs) enzymes comprise a superfamily that catalyzes the transfer of sulfur from suitable sulfur donors to nucleophilic sulfur acceptors, and they are ubiquitously distributed in all organisms. Despite their prevalence across species, the distinct physiological roles of most Strs are not fully understood. The structurally well define rhodanese (Rhd) homology domain is the typical feature of Strs protein family that unifying all members of this multiprotein family.

In *Arabidopsis thaliana*, 20 proteins containing one or more Rhd-domains and Str-patterns were identified (Bartels et al. 2007; Bauer and Papenbrock 2002). They are classified into six groups according to their amino acid sequence homology (see Table 1 Chapter I). Members of groups I and VI have been characterized in more detail in previous studies (Bauer and Papenbrock 2002; Papenbrock and Schmidt 2000a, b). Group I consists of two two-domain Str proteins, and they prefer 3-mercaptopyruvate (3-MP) over thiosulfate (TS) as a sulfur donor *in vitro* (Papenbrock and Schmidt 2000a, b). While group VI includes five proteins that contain only the C-terminal Str-pattern and thus possess similarity to the single-domain Str from bacteria, among them two of the single-domain proteins have been shown to prefer TS over 3-MP as a sulfur donor *in vitro* (Bauer and Papenbrock 2002). Group IV comprises three single domain protein; one has to lack the catalytic Cysteine (Cys) residues (Bartels et al. 2007). Group III includes four proteins, except for the AtStr5, other three remain uncharacterized. However, the AtStr5 protein has been ambiguously identified as both Arath; CDC25 (Landrieu et al. 2004a; Landrieu et al. 2004b) and arsenate reductase (AtACR2) (Bleeker et al. 2006; Dhankher et al. 2006; Duan et al. 2005). Although *in vitro* assays show Str or phosphatase activity associated with Rhd or rhodanese-like domains (RLDs), particular biological roles for most members of this multiprotein family have not been well understood (Spallarossa et al. 2001). Different specific function for Strs has been proposed. An increasing number of report suggests that Strs or Strs like protein are involved in heavy metal stress, for example, a cadmium-induced AtStr9 homolog was identified in *Datura innoxia* (Louie et al. 2003), while AtStr5 (Bleeker et al. 2006; Dhankher et al. 2006) and AtStrs17a/HAC1/ATQ1 have been proposed as potential arsenate reductases (ARs) (Chao et al. 2014) and involved in the As detoxification process.

The AtStr5 protein is catalytically and structurally similar to the CDC25 phosphatase enzyme. These two enzyme families share a common evolutionary origin (Hofmann et al. 1998). The active site loop of the AtStr5 protein contains [His-Cys-(X)5-R] motif and is also shared by another enzyme family of AR that involve in As detoxification process, for instance, yeast (ScACR2p) (Mukhopadhyay et al. 2003). Both yeast AR (ScACR2p) and AtStr5 (potential AtACR2) protein share the seven amino acid longer catalytic motif of CDC25. However, unlike the CDC25 protein, the N-terminal regulatory region is absent in both AtStr5 and ScACR2 proteins (Landrieu et al. 2004b; Mukhopadhyay et al. 2003). The yeast ScACR2p protein did not show phosphatase activity, even though it shares the CDC25 catalytic motif (Ellis et al. 2006; Mukhopadhyay et al. 2003). By contrast, the AtStr5 protein shows dual functionality as phosphatase (Landrieu et al. 2004a; Landrieu et al. 2004b) and AR *in vitro* (Dhankher et al. 2006; Duan et al. 2005; Redekar and Papenbrock 2010, unpublished). However, the *in vivo* function of the AtStr5 protein remains controversial, and this is the concern of this current project.

The intracellular localization has been studied for understanding the *in vivo* physiological function of Strs. In every organism analyzed, the gene products of Strs were localized to different subcellular compartments (Bauer et al. 2004; Libiad et al. 2018; Nagahara et al. 1995; Ray et al. 2000a). *Arabidopsis* Str (AtStrs) proteins of groups I, II and VI have been located in the chloroplast, the mitochondrion and the cytoplasm by different methods (Bauer et al. 2004; Hatzfeld and Saito 2000; Nakamura et al. 2000; Papenbrock and Schmidt 2000a). In GFP mediated intracellular localization studies, proteins are labeled with the green fluorescent protein (GFP) from *Aequoria victoria*, which is an *in vivo* marker for protein localization studies, these constructs are used to transform *Arabidopsis* protoplasts and subsequently analyzed under a fluorescence microscope. To investigate the *in vivo* function of AtStr5 and to obtain more information about its putative substrate localization in the metabolic network, the correct subcellular localization of AtStr5 might be one more step forwards the elucidation of its function.

## 2 Material & methods

### 2.1 *In vitro* biological function elucidation for recombinant AtStr5 (At5g03455) protein

#### 2.1.1 DNA cloning techniques

##### 2.1.1.1 Cloning into a pGEM®-T cloning vector

For the amplification of a complementary DNA (cDNA) sequence encoding AtStr5 (At5g03455), the full-length EST clone RAFL19-08-B21 was obtained from RIKEN BIORESOURCE CENTER, Japan. For bacterial expression, a 396 bp sequence of *AtStr5* and its mutant form *AtStr5: Ala72* (where catalytic cysteine 72 was replaced by alanine 72) were used to produce the expression clones with the pQE-30 vector (Qiagen). Likewise, 510 bp and 423 bp of *AtStr17a* (*HAC1/ATQ1*) sequences were amplified from the cDNA of *Arabidopsis* Col-0 plant. The primer pairs used for the production of the expression clones are listed in **Table 1**.

**Table 1. Overview of the expression clones produced.** The name of the protein, the length of the PCR amplified product, the primer pairs designed with the respective restriction sites and the respective vectors used are listed.

Protein name	Base No.	Primer pairs	Restriction sites	Vector
AtStr5	396	P158 5'- ggatccgcatggcgagaagcat-3'	<i>Bam</i> HI	pQE-30
		P159 5'- ctgcagggcgcaatcgcccttgca-3'	<i>Pst</i> I	
Mutant of AtStr5:Ala72	396	P1: P158 5'- ggatccgcatggcgagaagcat-3'	<i>Bam</i> HI	pQE-30
		P2: P159 5'- ctgcagggcgcaatcgcccttgca-3'	<i>Pst</i> I	
		P3: P1007 5'- gtc ttc cat gct gcc ttga-3'		
		P4: P1008 5'-tcaa ggc agc atg gaa gac-3'		
AtStr17a	510	P1159 5'- ggatccatacatattctctcctcaacctttct - 3'	<i>Bam</i> HI	pQE-30
		P312 5'- aagctgttttcctttggcct -3'	<i>Hind</i> III	
	423	P311 5'- ggatccgaggaacaaaacca -3'	<i>Bam</i> HI	pQE-30
		P312 5'- aagctgttttcctttggcct -3'	<i>Hind</i> III	



The PCR reaction carried 0.2 mM dNTPs (Roth, Karlsruhe, Germany), 0.4  $\mu$ M of each primer (MWG, Ebersberg, Germany), 1 mM MgCl<sub>2</sub> (final concentration, respectively), 1  $\mu$ l Green Taq DNA-Polymerase (Thermofisher, Germany), 5  $\mu$ l 10x PCR Green buffer and about 1  $\mu$ l template DNA in a final volume of 50  $\mu$ l. The amplification was performed in a programmable PCR cycler using 28 reaction cycles consisting of a 1 min initial denaturation step at 94°C, and about 1  $\mu$ l template DNA in a final volume of 50  $\mu$ l. The amplification was performed in a programmable PCR cycler using 28 reaction cycles consisting of a 1 min initial denaturation step at 94°C, a 1 min primer annealing step at 55°C a 1 min elongation step at 72°C. The final elongation step was performed for 600 s at 72°C. The amplified PCR product was analyzed on 1% agarose gels. For DNA extraction from agarose gels, the Gen Elute™ Agarose Spin Column was placed in a collection tube. The spin column was pre-washed by adding 100  $\mu$ l of 1x TE buffer to the 'spin column, followed by centrifugation at 16,060 g for 10 s. The spin column was transferred to a fresh collection tube. The band of interest was excised from the agarose gels and loaded in the pre-washed spin column. The spin column was then centrifuged at 16,060 g for 10 min. The eluted DNA of each target gene was collected in the collection tube and stored at 2-8°C.

The *AtStr5*, catalytic Cys72 mutant of *AtStr5*, *AtStr5: Ala72* and *AtStr17a* were then ligated to pGEM®-T vector. The ligation mix of 20  $\mu$ l contained 10  $\mu$ l 10x ligation buffer, 1  $\mu$ l pGEM®-T vector, 8  $\mu$ l of the template cDNA insert and 1  $\mu$ l T4 DNA ligase were mixed and stored overnight at RT. The ligated sample was then used to transform the competent XL1-Blue *E. coli* cells and BL-21 DE3 strain. The *E. coli* competent cells were prepared for transformation, and its competency was checked with known plasmid before beginning to the final transformation. The competent cells were thawed on ice for 20 min or more till its de-frozen. About 200  $\mu$ l of competent cells were added to the 1.5 ml-reaction tube with a ligation reaction mixture and incubated on ice for 30 min. The 1.5 ml-reaction tube was then placed in a water bath for 90 s at 42°C. The 1.5 ml-reaction tube was then immediately placed on ice for 2 min. About 500  $\mu$ l of antibiotic-free LB medium was added to the 1.5 ml-reaction tubes and is 'then incubated in a shaker incubator at 37°C, 800 rpm for 1 h. After 1 hour of incubation, 100  $\mu$ l mix was plated onto an LB plate containing ampicillin (final concentration 100  $\mu$ g ml<sup>-1</sup>), IPTG (final concentration 0.4 mM) and X-Gal (final concentration 40  $\mu$ g ml<sup>-1</sup>). The plate was incubated at 37°C overnight. For plasmid

mini preparation, the transformed colonies were inoculated in a 3 ml LB broth with ampicillin (final concentration 100  $\mu\text{g ml}^{-1}$ ).

The media were incubated in an incubator shaker at 37°C, 180 rpm overnight. About 1.5 ml of the overnight grown culture was centrifuged at 1500 g for 10 min. The cell pellet was suspended in 300  $\mu\text{l}$  of the P1 buffer by vortexing. About 300  $\mu\text{l}$  of P2 buffer was added, mixed gently and incubated for 5 min at room temperature (RT), followed by the addition of 300  $\mu\text{l}$  of P3 buffer, vortexing and incubation on ice for 15 min. The mixture was centrifuged at 15,700 g for 15 min at 4°C. The supernatant was added to 0.7 volume of isopropanol in a fresh 1.5 ml reaction tube, followed by centrifugation at 15,700 g for 15 min at 4°C. About 100  $\mu\text{l}$  of 70% ethanol was added to the pellet and centrifuged at 15,700 g for 10 min. The ethanol was discarded, followed by short centrifugation for 10 s and the rest of the ethanol was pipetted out. The 1.5 ml reaction tube was allowed to dry for 5 min, and the plasmid pellet was resuspended in 50  $\mu\text{l}$  of autoclaved water. The plasmid was stored at 4°C.

These plasmids were digested with *Bam*HI and *Pst*I to confirm the correct recombination. The digestion mix of 20  $\mu\text{l}$  contained (0.5-1)  $\mu\text{g}$  plasmid DNA, 2  $\mu\text{l}$  10x Tango buffer, and 0.5  $\mu\text{l}$  each of the restriction enzymes. The reaction mixture was incubated in a water bath at 37°C for 1h. The results were analyzed by agarose gel electrophoresis. The correct digestion pattern bearing recombinant pGEM®-T plasmid DNA was sent for sequencing to Eurofins MWG Operon, Ebersberg, Germany. This nucleotide sequence was verified by aligning with similar sequences using the BLAST program ([www.blast.ncbi.nlm.nih](http://www.blast.ncbi.nlm.nih)).

#### 2.1.1.2 Cloning into a pQE-30 expression vector

The recombinant pGEM®-T vectors (contain either *AtStr5* or *AtStr17a*) and expression vector (pQE-30) was digested with *Bam*HI and *Pst*I, as described above. The results were analyzed by agarose gel electrophoresis. The *AtStr5* and pQE-30 DNA were extracted from the respective bands in agarose gel, using Gen Elute™ Agarose Spin Column. The ligation mix of 20  $\mu\text{l}$  contained 2  $\mu\text{l}$  10 x ligation buffers, 10  $\mu\text{l}$  pQE-30 vector, 8  $\mu\text{l}$  *AtStr5* insert and 1  $\mu\text{l}$  T4 DNA ligase were mixed and stored overnight at RT.

This ligation sample was used to transform competent XL1-Blue/BL21-(DE3) of *E. coli* cells as described above. About 100  $\mu\text{l}$  of the transformation mix was plated onto an LB plate containing ampicillin (final concentration 100  $\mu\text{g ml}^{-1}$ ), for BL-21 (DE3) strain additional antibiotic chloramphenicol (50  $\mu\text{g ml}^{-1}$ ) was added to the same LB plate.

The plate was incubated at 37°C overnight. The plasmids were isolated from transformed colonies, followed by restriction digestion with *Bam*HI and *Pst*I. The results were analyzed by agarose gel electrophoresis.

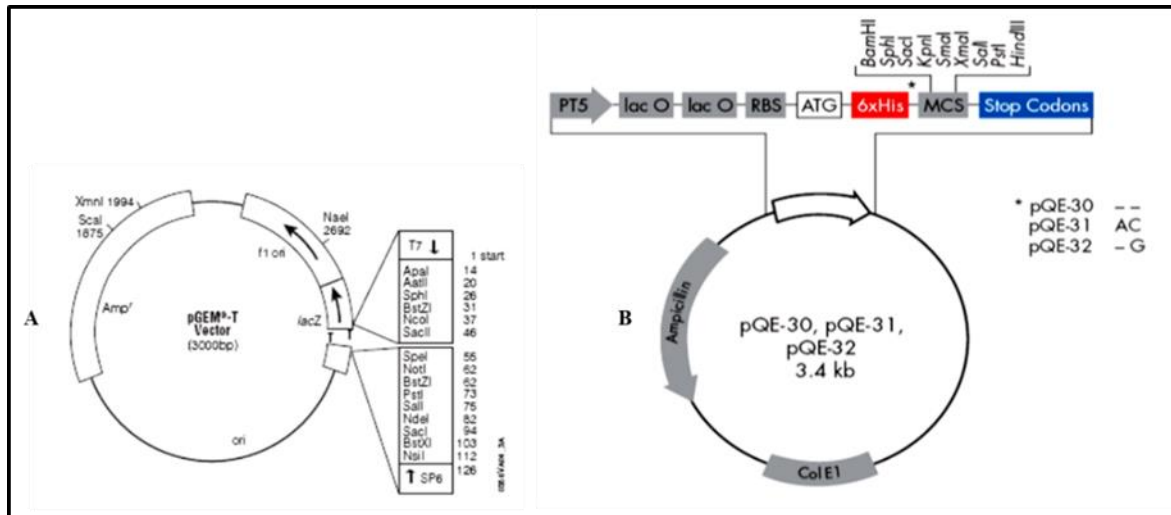


**Figure 1.** Vector map of (A) pGEM®-T cloning vector (Promega) (B) pQE-30 protein expression vector (Qiagen)

### 2.1.2 Expression, extraction, and purification of AtStr5 proteins from transformed *E. coli*

For the heterologous expression of AtStr5, the pQE-30 expression vectors were transformed into the *E. coli* strains XL1-Blue and BL-21 (DE3), as described above. The recombinant protein was expressed under different conditions: after growth of the *E. coli* cultures at 37°C to an OD<sub>600</sub> of 0.6-0.8 in Luria Bertani (LB) medium (10 g L<sup>-1</sup> tryptone, 5 g L<sup>-1</sup> yeast extract, 10 g L<sup>-1</sup> NaCl, pH 7.0) and rich LB medium (35 g L<sup>-1</sup> tryptone, 20 g L<sup>-1</sup> yeast extract, 10 g L<sup>-1</sup> NaCl, pH 7.0) containing ampicillin (100 µg ml<sup>-1</sup>) for BL-21 (DE3) chloramphenicol (50 µg ml<sup>-1</sup>), expression was carried out for 1 to 3 h at 37°C at 180 rpm after induction with 0.5 mM and 1 mM final concentration of isopropyl-β-D-galactoside (IPTG; AppliChem). To avoid the formation of the inclusion bodies the expression of the proteins was alternatively carried out at 25°C at 200 rpm for 3 h. About 1 ml sample was collected from each of the cultures separately in a 1.5 ml-reaction tube at hourly intervals. The remaining culture in the flasks was kept on ice for 10 min to stop the growth and centrifuged at 1500 g, 4°C for 10 min. The supernatant was discarded, and the pellet was frozen at -20°C for protein purification. The hourly samples, including the control, were centrifuged at 1500 g, 4°C for 10 min and the supernatant was discarded.

The pellets were suspended in 100  $\mu$ l of protein gel loading buffer. The samples were then heated at 95°C for 30 min. The expression of the samples was analyzed by sodium dodecyl sulfate (SDS) -polyacrylamide gel electrophoresis (PAGE) and Western blotting. Cell lysis was acquired by adding lysozyme (final concentration 1 mg ml<sup>-1</sup>, Roth) and vigorous homogenizing and sonification. The recombinant protein was purified under non-denaturing condition by Ni-NTA affinity chromatography according to the instruction provided by the Äkta protein purification system. The Äkta lysis and elution buffer composition were (20 mM NaH<sub>2</sub>PO<sub>4</sub>, 0.5 M NaCl, 20 mM imidazole) and (20 mM Na-phosphate, 0.5 M NaCl, 0.5 M imidazole) respectively. Additionally, 5 mM Dichlorodiphenyltrichloroethane (DDT) and 10% glycerol was added in lysis, elution and dialysis buffer (20 mM Tris HCl, pH 8.0) to overcome precipitation problem. The protein concentration was determined according to the Bradford (Bradford 1976) using bovine serum albumin (Roth) as a protein standard. Expression and purification of proteins were checked by SDS-PAGE and Western blot analysis.

### **2.1.3 SDS-PAGE and Western blot analysis**

The expressed protein was separated on SDS-PAGE, according to (Laemmli 1970). Samples were heated at 95°C in a sample buffer (56 mM Na<sub>2</sub>CO<sub>3</sub>, 56 mM dithiothreitol, 2% [w/v] SDS, 12% [w/v] sucrose, 2 mM EDTA) for 15 min to denature the protein. Cell debris was removed by centrifugation and supernatants were directly loaded onto the SDS gel. The resulting gels were either stained with Coomassie Brilliant Blue to visualize the proteins or blotted onto nitrocellulose membranes (Sambrook et al. 1989). For immunodetection, RGS anti-His antibody (Qiagen), anti-mouse Ig (Sigma) and anti-rabbit antibody conjugated with alkaline phosphatase (Sigma) were used successively. Colorimetric detection was done using nitroblue tetrazolium (NBT) and 5-Bromo-4-chloro-3-indolyl-phosphate (BCIP) as substrates for alkaline phosphatase.

### **2.1.4 Enzyme activity measurement**

#### **2.1.4.1 Phosphatase assay with para-nitrophenyl phosphate (pNPP)**

The phosphatase assay was performed as per the method described by Li et al. 2003. The phosphatase activity was initially assayed using pNPP as substrate. Purified protein (5  $\mu$ g) was incubated for 30 min at 37°C in 200  $\mu$ l of 100 mM Tris-HCl (pH 7.5) containing 5

mM DTT. Assay was performed with different concentrations of *p*NPP (0.5, 1.5, 3.5, 5, 10, 15, 20, 35, 45, and 50 mM).

The reaction was terminated by the addition of 800  $\mu$ l of 1N NaOH, and the absorbance of the resulting solution was determined at a wavelength of 410 nm. Each value was corrected for non-enzymatic *p*NPP hydrolysis. The quantity of *p*-nitrophenol (PNP) produced was calculated using an extinction coefficient of 17800 M<sup>-1</sup>cm<sup>-1</sup>. Kinetic constant was obtained by nonlinear regression of Michaelis-Menten equation using Sigma plot version 13.0.

#### 2.1.4.2 Phosphatase assay with 3-O-methylfluorescein-phosphate (3-OMFP)

One mM 3-O-methylfluorescein-phosphate (OMFP) was freshly prepared in DMSO. The OMFP substrate solution was diluted in different concentrations (as 0, 10, 20, 30, 40, 50, 100, 200, 300 and 400  $\mu$ M) with assay buffer (100 mM Tris-HCl, pH 8.2, 40 mM NaCl, 1 mM DTT and 20% glycerol) to total 1 ml volume. The 5  $\mu$ g of the purified enzyme was added to all the dilutions and samples were incubated at 20°C for 10 min. The enzyme concentration was determined from the linear part of the graph. Absorbance was recorded at 477 nm. The quantity of OMF produced was calculated using an extinction coefficient of 27,200 M<sup>-1</sup> cm<sup>-1</sup>) and followed the instruction described by (Forlani et al. 2003). Kinetic constant was obtained by nonlinear regression of Michaelis-Menten equation using Sigma plot version 13.0.

$$\text{Specific activity} \left( \frac{\text{nmol}}{\text{min}} \right) = \frac{\text{adjusted Vmax(O.D./min)} * \text{reaction volume (L)} * (10^6 \mu\text{M/mol})}{\text{OMF extinction coeff.} * \text{path correction} * \text{amount of protein (mg)}}$$

### 2.1.4.3 Sulfurtransferase assay

The sulfurtransferase assay was established by (Papenbrock and Schmidt 2000a). In general, the reaction mixture of 1 ml contains 0.1 M Tris / HCl, pH 9.0 for 3-MP as a starting substrate and pH 8.0 for TS as a starting substrate, 10 mM KCN, 5 mM mercaptoethanol and 1-10  $\mu\text{g}$  purified enzyme. For standard calibrations, sodium thiocyanate was added in different concentrations as 0, 50, 100, 200, 400, 600, 800  $\mu\text{M}$ . The total volume was made to 950  $\mu\text{l}$  with distilled water. Finally, the reaction was started by adding 5 mM 3-MP/TS as the starting material. After incubation for 20 min at 37°C, the reaction was stopped by addition of 200  $\mu\text{l}$  of the acidic  $\text{FeCl}_3$  solution. Following centrifugation at 13,000 g for 3 min, the absorbance was measured at 452 nm.

For determination of enzyme activity of the purified protein, the sodium thiocyanate in the assay mixture was replaced by 1-10  $\mu\text{g}$  of purified enzyme and treated as described above. For control, AtStr1 as a positive and BSA as negative control were used for this assay. Each experiment was done three times with a respective control for each treatment. The enzyme kinetic was determined with nine different substrate concentrations (1, 3, 5, 10, 20, 30, 50, 60 and 70 mM) with 3  $\mu\text{g}$  of purified enzyme.

## 2.2 Determination of the intracellular localization of AtStr5

### 2.2.1 Plant material and growth conditions

Seeds of *Arabidopsis thaliana* (L.) Heynh. ecotype C24, were initially obtained from the Arabidopsis Biological Resource Center, ABRC. The seeds were germinated in soil medium in a greenhouse. The soil was a mixture of VM70L clay and 45L sand provided by Einheitserdewerke Werkverband e.V. Germany. The 2-week-old seedlings were transferred into a larger tray where 24 seedlings were evenly distributed in developing rosette leaves. The seedling tray was placed in a climate chamber at 20-21°C under a 16 h light / 8 h dark cycle at a light intensity 120  $\mu\text{mol m}^{-2} \text{s}^{-1}$  (fluorescent lamps, OSRAM -L58W/77 FLUORA, Germany). The younger rosette leaves from the 3 to 4-week-old plants were used for protoplast isolation.

### 2.2.2 Cloning into a pGEM®-T cloning vector

For subcellular localization studies of AtStr5, its nucleotide sequence (438 bp) was analyzed by online available computer-based prediction programs. Based on this

information and previous literature search, three different lengths 438, 396 and 351 bp of *AtStr5* were amplified from the cDNA of *Arabidopsis* Col-0 plant. The primer pairs used for the construction of fusion clones with the GFP are listed in **Table 2**. Subsequently, they were cloned into a pGEM®-T vector as discussed above for cloning into the pQE-30 expression vector. The recombinant pGEM®-T clones were confirmed by sequencing (Eurofins MWG Operon, Ebersberg, Germany).

**Table 2. Overview of the GFP fusion clones produced.** The name of the protein, the length of the PCR amplified DNA fragment, the primer pairs designed with the respective restriction sites and the respective vectors used are listed.

Protein name	Base No.	Primer pairs	Restriction sites	Vector
AtStr5 (full-length)	438	P872 5'-cca tgg ca <u>ggg</u> aga agc ata ttt tcc ttt ttc-3'	<i>Nco</i> I	pGFP-N
		P236 5'-gga tcc ggc gca atc gcc ctt-3'	<i>Bam</i> HI	pGFP-C
AtStr5 :42 bp deleted	396	P235 5'- catggcgatggcgagaagca 3'	<i>Nco</i> I	pGFP-N
		P236 5'-gga tcc ggc gca atc gcc ctt-3'	<i>Bam</i> HI	pGFP-C
AtStr5 :87 bp deleted	351	P873 5'- cca tgg ca ctc cct ctt cat cgt cgt cc-3'	<i>Nco</i> I	pGFP-N
		P236 5'-gga tcc ggc gca atc gcc ctt-3'	<i>Bam</i> HI	pGFP-C

### 2.2.3 Cloning into pBSK based GFP-C/-N vectors for localization study

After sequence confirmation, each version of *AtStr5* cDNA sequence was ligated into pBSK-based enhanced GFP containing vectors to obtain either GFP fusions with the 5' end of the GFP coding sequence (pGFP-N) or with the 3' end (pGFP-C). The gene-cassettes were driven by the CaMV-35S promoter with a double enhancer and the polyA-tail from CaMV-35S.

The pGEM®-T plasmid with the *AtStr5* cDNA sequence was digested with *Bam*HI and *Nco*I restriction enzymes. The pBSK-based pGFP-C and pGFP-N vectors were digested with *Nco*I and *Bgl*III restriction enzymes. The digestion mix of 20 µl contained 5 µl plasmid DNA, 4 µl 10 x Tango™ buffers, and 0.5 µl each of the restriction enzymes and 10 µl H<sub>2</sub>O

for both pGEM ®-T harboring *AtStr5* and pGFP-N /-C vectors. The reaction mixture was incubated in a water bath at 37°C for an hour. The digestion pattern was analyzed on 1% agarose gels following agarose gel electrophoresis. The Gen Elute™ Agarose Spin Column placed in a collection tube was used to extract DNA from the agarose gel as previously described. The extracted *AtStr5*-DNA was ligated to each of the pGFP-C and pGFP-N vectors. The ligation mix of 20 µl contained 2 µl 10 x ligation buffer, 8 µl pGFP-C or pGFP-N vector, 8 µl *AtStr5* insert and 2 µl T4 DNA ligase were mixed and stored overnight at RT.

Transformation of competent XL1-Blue competent *E. coli* cells with the ligation samples was performed as previously described. About 100 µl of the transformation mix was plated onto an LB plate containing ampicillin (final concentration 100 µg ml<sup>-1</sup>). The plate was incubated at 37°C overnight. The success of cloning was confirmed by performing colony PCR.

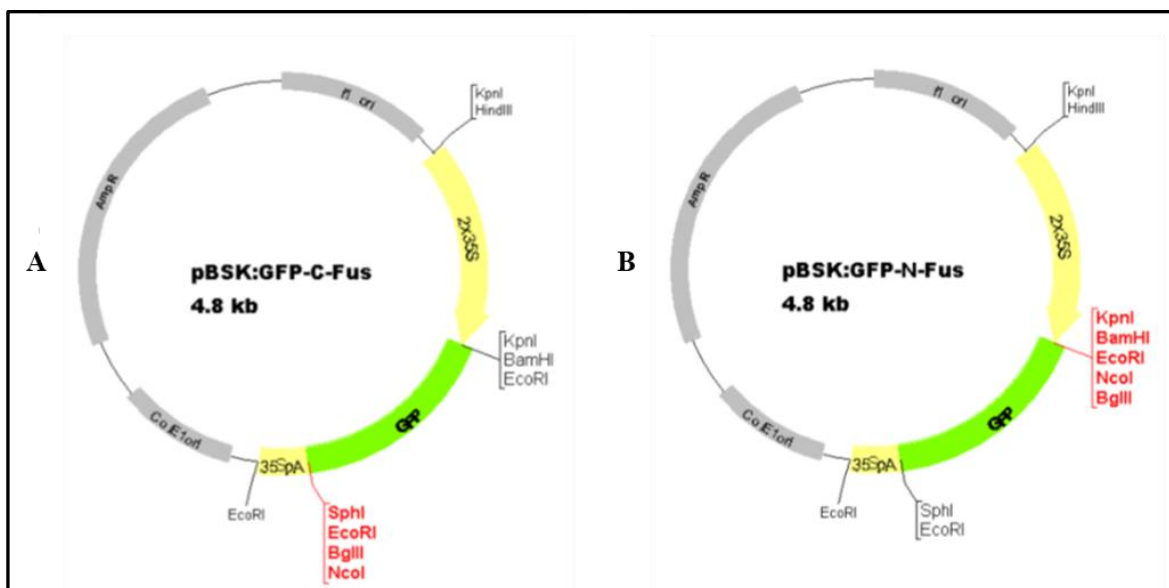


**Figure 2.** Vector map of pBSK based (A) pGFP-C and (B) pGFP-N vectors (Nowak et al. 2004).

#### 2.2.4 Transient transformation of GFP fusion construct into *Arabidopsis* protoplasts

The young rosette leaves of 3 to 4-weeks-old *Arabidopsis* plant were used for the preparation of protoplast according to them (Yoo et al. 2007). About 30-40 leaves were sliced with a sharp scalpel and transferred into small Petri dish (3.5 x 3.5 cm) with 3 ml enzyme solution (1 % [w/v] cellulase Onozuka R-10, 0.25 % [w/v] macerozyme R-10, 0.4 M mannitol, 20 mM KCl, 20 mM MES-KOH pH 5.7, 10 mM CaCl<sub>2</sub> x H<sub>2</sub>O, 0.1% [w/v]



bovine serum albumin. The leaves-enzyme solution was shaken for 60 min at RT on a rotary shaker at 40 rpm, followed by 1 min at 80 rpm. The suspension was filtered through Nylon gaze with 75-micron mesh sieve and distributed evenly in 2 ml round bottom vials. It was centrifuged for 2 min at 100 g, 4°C, subsequently, the pellet was gently resuspended in 500 µl W5 medium (154 mM NaCl, 125 mM CaCl<sub>2</sub> x 2H<sub>2</sub>O, 5 mM KCl, 5 mM glucose and 5 mM MES-KOH, pH 5.7) by tapping. Centrifugation step was repeated as earlier, and the pellet was again re-suspended in 500 µl W5 medium and incubated on ice for 30 min. This suspension was centrifuged, and the pellet was then resuspended in 150 µl MMG solution (0.4 M mannitol, 15 mM MgCl<sub>2</sub> x 6H<sub>2</sub>O and 4 mM MES-KOH, and pH 5.7) by gentle tapping.

About 10 µl of plasmid sample (final concentration 10 to 20 ng) and 110 µl PEG (4 g polyethylene glycol 4000, 6.5 ml H<sub>2</sub>O, 0.8 M mannitol and 1 M CaCl<sub>2</sub> x 2H<sub>2</sub>O) solution was added to and mixed gently with protoplast suspension. This suspension was incubated at 30°C at RT. About 1000 µl of the W5 medium was added to the suspension and was centrifuged for 2 min at 100 g and 4°C. Finally, the pellet was mixed gently with 50 µl of W5 medium and incubated overnight at RT.

### **2.2.5 Microscopic analysis**

The transiently transformed cells and protoplast were analysed with Nikon Eclipse Ti-S fluorescence microscope (Nikon, Germany). The image was captured through a Nikon Plan Apo, 40x/0.95 objective. The fluorescence of GFP was analyzed by excitation at 480/20 nm, and emission was detected between 510/20 nm. Chlorophyll autofluorescence was analyzed by excitation of 550/75 nm, and emission was detected between 590/675 nm. The transformations were performed with each clone at least 3 times always resulting in the same subcellular localization.

### **2.2.6 Miscellaneous**

Protein estimation was carried out according to (Bradford 1976) using bovine serum albumin as a protein standard. The analyses of DNA and amino acid sequences were performed with the programs EditSeq and clone manager professional-9. For the computer-based prediction of the protein localization different programs were applied (mainly PSORT, iPSORT TargetP, Predator, and Mitroprot, Softberry NucPLoc, Plant PLoc, Chloro-P, LocTree and Predict protein).

## 3 Results

### 3.1 Expression, extraction, and purification of AtStr5 proteins from transformed *E. coli*

For the heterologous expression of the *Arabidopsis* AtStr5 proteins in *E. coli*, the 396 bp coding sequence of AtStr5 was cloned into the pQE-30 expression vector behind an N-terminal 6xHis-tag coding sequence and transformed into the *E. coli* strain XL1-Blue and BL21-(DE3). Induction with IPTG allowed for the expression of a protein sized approximately 16 kDa after 3 h of induction in LB medium. Presence of the desired 6xHis-tag protein was confirmed by Western blotting using RGS antibodies specifically designed to recognize the 6xHis-tag. It was observed that very lower level of expression and less yield of protein after purification. The major part of this protein was found in the insoluble fraction (in the pellet) after extraction from the bacterial cells (**Figure 3C**). The majority of the protein in the pellet part was also confirmed by Western blot analysis (**Figure 3D**). Trials to optimize the expression conditions with regard to a higher expression level and/or higher solubility of AtStr5 proteins included: changing the bacterial strain, double-baffled flask to ensure aeration, improving the culture media, increasing the culture volume and incubation time, keeping the lower temperature and higher speed after induction with IPTG, reduction of the concentration of IPTG for induction of the T5-promoter. However, the best result for AtStr5 expression was obtained for the strain BL21-(DE3) in 50 ml rich LB medium induced with 1 mM IPTG and expression at a temperature of 25°C at 200 rpm for 3 h (**Figure 3A**). Whereas in the same conditions, expression of AtStr5 in *E. coli* strain XL1-Blue remains unchanged (**Figure 3B**). A larger volume of the culture of at least 1 L rich LB medium was made for protein expression to increase the yield of AtStr5 protein. Cultures were divided into 5 x 200 ml during culture and expression was followed at 25°C and 200 rpm after addition of IPTG for the strain BL21-(DE3). The protein was purified by Äkta protein purification system. Sufficient protein yield was obtained (1400 mg L<sup>-1</sup>) after purification by observing a very thick band for the eluted fraction (**Figure 3E**). However, another problem has arisen concerning protein stability; the AtStr5 protein was found to form white precipitation during the purification process, indicating that the protein cannot be used for enzyme activity assays (**Figure 3F**). Trials were performed to prevent the protein precipitation by adding BSA, DDT, and glycerol to the protein purification buffer. By combining these ingredients, the formation of aggregation of the protein was prevented.

Subsequently, each component was excluded from the buffer to observe which one has a contribution to control the precipitation problem. The best result was obtained by adding 5 mM DDT and 10% glycerol both in the purification and storage buffer to reduce the formation of precipitates of AtStr5 protein.

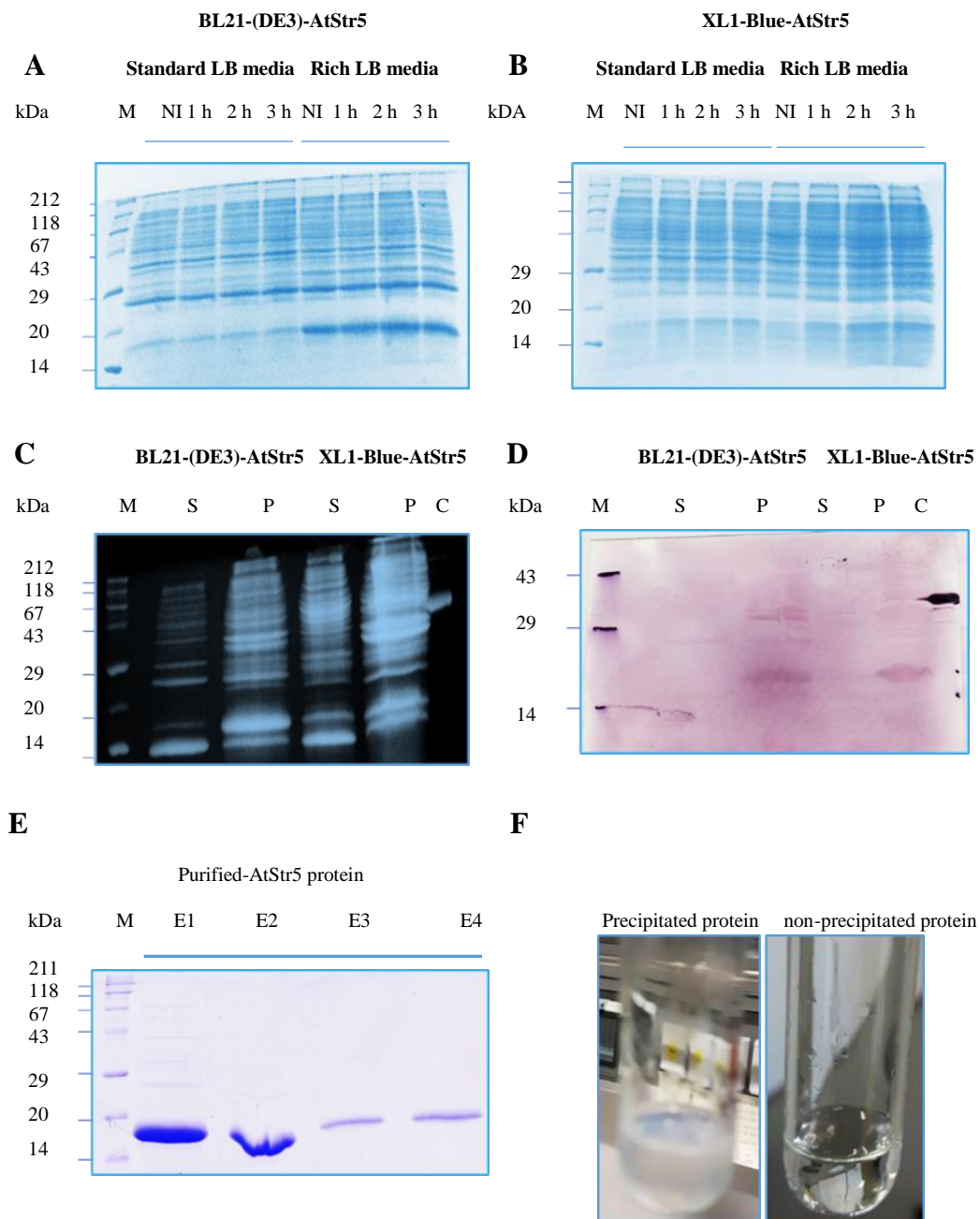
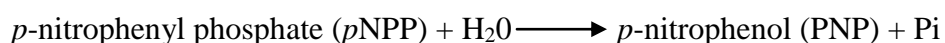
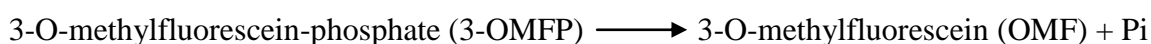


**Figure 3.** Expression and purification of AtStr5 in *E. coli*. **(A&B)** SDS-PAGE expression of AtStr5 protein in *E. coli* strains BL21-(DE3) & XL1-Blue for culturing both standard and rich LB media; lanes described from left to right: M, protein standard; NI, Non induced, before the induction of the culture with isopropyl- $\beta$ -D-galactoside; protein extract 1 h, 2 h & 3 h after induction. **(C&D)** SDS-PAGE & Western blot of proteins that were extracted from both recombinant strains [BL21-(DE3) and XL1-Blue] by adding lysis buffer followed the ultra-signification. After cell lysis and centrifugation, both supernatant (S), pellet (P) and control (C) were loaded for Western blot analysis; the Western blot was performed using RGS anti-His antibody produced in rabbit and alkaline phosphatase coupled anti-rabbit antibody as secondary antibody. **(E)** SDS-PAGE of purified AtStr5 protein with different elution fraction; E1, E2, E3 and E4 eluate fractions from purification. **(F)** Protein precipitation formation and overcoming by adding DDT & glycerol during purification.

### 3.2 Results of the phosphatase assays

The purified AtStr5 protein demonstrated phosphatase activity in the presence of substrates 3-OMFP and *p*NPP. The dephosphorylation of 3-OMFP and *p*NPP in the presence of enzyme proceeds significantly faster than in control without the enzyme, proving that catalysis occurs. The phosphatase reaction is proceeded by the following mechanism:



Although *p*NPP has been widely used to measure the phosphatase activity of protein-tyrosine phosphatase (PTPases), 3-OMFP was found the more reactive substrate for the protein DS-PTPases (Eckstein et al. 1996), which are members of a subclass of the PTPases family (Pot and Dixon 1992). The CDC25-DS-PTPases can catalyze *p*NPP, but very poorly (Dunphy and Kumagai 1991; Millar et al. 1991). The phosphatase activity of AtStr5 was determined with the substrate *p*NPP where estimated  $K_m$  value was 50 mM (Landrieu et al. 2004a). In this experiment, we measured the phosphatase activity of AtStr5 using both of these substrates. The amount of product OMF and PNP formed by the action of AtStr5 was estimated from the extinction coefficient value of OMF, as  $27,200 \text{ M}^{-1} \text{ cm}^{-1}$  at a wavelength of 477 nm and for PNP as  $17,800 \text{ M}^{-1} \text{ cm}^{-1}$  at a wavelength of 410 nm. The rate of product formation at different concentrations of the substrate was graphed to obtain  $K_m$  and  $V_{max}$  value. Kinetics parameter of AtStr5 at different *p*NPP concentration showed a  $K_m$  value of 16.1 mM and  $V_{max}$  of  $41.2 \text{ [nmol (min x mg protein)}^{-1}]$  ( $r = 0.98$ ) and with 3-OMFP the  $K_m$  value of 53.2  $\mu\text{M}$  and  $V_{max}$  of  $416.4 \text{ [nmol (min x mg protein)}^{-1}]$  ( $r=95$ ) (**Figure 4, A & B**). The  $k_{cat}$  value describes the velocity of product formation, and high  $k_{cat}$  indicates a good substrate for the particular enzyme. The  $k_{cat}$  value for *p*NPP and 3-OMFP were  $0.01014 \text{ s}^{-1}$  and  $0.1025 \text{ s}^{-1}$ . The  $k_{cat}/K_m$  for *p*NPP and 3-OMFP were  $0.00062 \text{ s}^{-1} \text{ mM}^{-1}$  and  $1.92 \text{ s}^{-1} \text{ mM}^{-1}$ . This value represents a  $\sim 3000$  fold enhancement of  $k_{cat}/K_m$  value for 3-OMFP over *p*NPP which indicates 3-OMFP is an ideal substrate for determining *in vitro* phosphatase activity of AtStr5 as like to the other DS-PTPases. The mutated AtStr5: A72

protein was unable to hydrolyze 3-OMFP substrate, in the same reaction condition, the AtStr1 and AtStr17a/HAC1/ATQ1 did not show any phosphatase activities (**Figure 5C**).

**Table 3.** The comparison of the phosphatase activity of AtStr5 with phosphatases of another organism.

Enzyme	Organism	Substrate	$K_m$ (mM)	$k_{cat}$ (s <sup>-1</sup> )	$k_{cat}/K_m$ (s <sup>-1</sup> mM <sup>-1</sup> )	Fold increase ( $k_{cat}/K_m$ )	
AtStr5	<i>Arabidopsis thaliana</i>	3-OMFP	0.053	0.1025	1.92	3096	This study
		pNPP	16.1	0.01014	0.0006		
<b>Dual specificity phosphatase</b>							
CDC25B (cat)	<i>Homo sapiens</i> , the catalytic domain of Human Cell Division Cycle 25B protein	3-OMFP	0.037	1.2	34	810	(Gottlin et al. 1996)
		pNPP	8.4	0.35	0.042	556	
VHR (native)	<i>Homo sapiens</i> , <i>Vaccinia virus</i> H1-related phosphatase	3-OMFP	0.10	1.5	15	138	
		pNPP	13	0.35	0.027		
rVH6 (GST-cat)	<i>Rattus rattus</i> , <i>Vaccinia virus</i> H1-related phosphatase	3-OMFP	0.13	0.014	0.11	0.0008	
		pNPP	10	0.008	0.0008		
<b>Phosphatase</b>							
PTP1 (native)	<i>Rattus rattus</i> , rat PTP1	3-OMFP	0.20	2.6	13	none	
		pNPP	0.87	18	21		
YOP (cat)	<i>Yersinia pestis</i> , Yersinia Outer Protein	3-OMFP	0.92	3.4	3.7	3.4	
		pNPP	1.3	1.4	1.1		

Cat, catalytic domain; GST-cat, GST- catalytic domain fusion protein

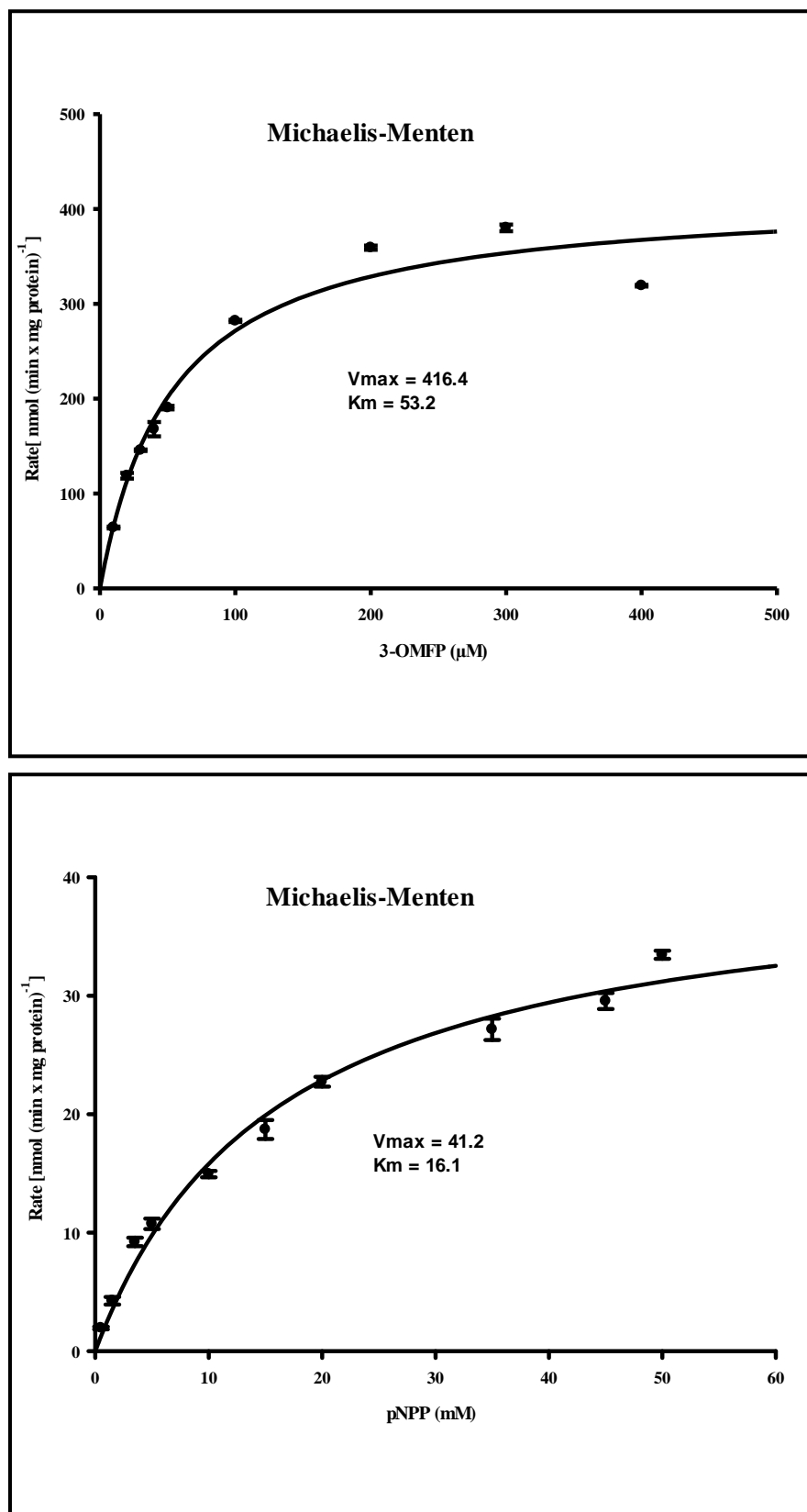


**Figure 4.** Kinetic study of AtStr5 with the substrates 3-OMFP and pNPP.

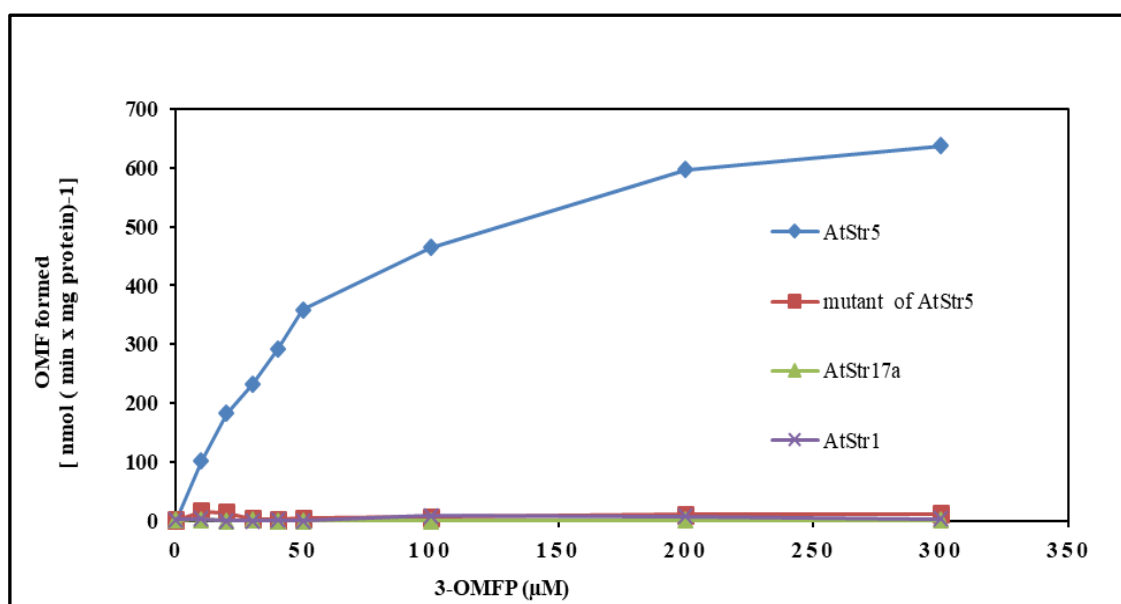
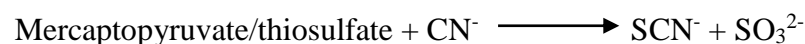


**Figure 5.** Phosphatase activity test of recombinant AtStr5, mutant AtStr5: A72, AtStr17a/HAC1/ATQ1 and AtStr1 proteins with different concentration of 3-OMFP.

### 3.3 Results of the sulfurtransferase assays

The Str reaction is catalyzed by transferring the sulfur atom from 3-MP/TS to cyanide ( $\text{CN}^-$ ) and produce less toxic thiocyanate ( $\text{SCN}^-$ ). The reaction is proceeded by the following mechanism.



The specific activity of AtStr5 with 3-MP and TS was determined. The protein-specific activity with 3-MP was  $\sim 300$  [ $\text{nmol} (\text{min} \times \text{mg protein})^{-1}$ ], which was significantly lower (6-fold lower) than the AtStr1;  $\sim 1900$  [ $\text{nmol} (\text{min} \times \text{mg protein})^{-1}$ ] (**Figure 6A**). On the other hand, the protein-specific activity with TS was undetectable. The specific activity of AtStr17a (HAC1/ATQ1) protein was also determined with the same substrates and identical condition. The protein-specific activity with both the substrates was almost undetectable. Nevertheless, the TS-specific activity was found a little bit higher [ $\sim 54$  [ $\text{nmol} (\text{min} \times \text{mg protein})^{-1}$ ]] than the 3-MP.



The kinetic parameters of AtStr5 were determined with 3-MP, from 50  $\mu\text{M}$  to 100 mM. Nine different concentrations of 3-MP (1 mM to 80 mM) and 3  $\mu\text{g}$  of the purified enzyme was used for kinetic determination. Data were fitted by nonlinear regression of Michaelis-Menten equation using Sigmaplot software version 13.0, to determine the kinetic parameters. The  $K_m$  and  $V_{max}$  value for this reaction was  $\sim 28.2$  mM and  $\sim 3389.2$  [nmol (min x mg protein) $^{-1}$ ] ( $r=0.79$ ) respectively (**Figure 6B**). The  $k_{cat}$  (turnover number), and  $k_{cat}/K_m$  (catalytic efficiency) values were at  $0.83$  s $^{-1}$  and  $0.029$  s $^{-1}$  mM $^{-1}$ , which were much lower than other characterized AtStrs (Bauer and Papenbrock 2002). The  $K_m$  value of AtStr5 is unphysiologically high because the physiological  $K_m$  for 3-MP in the cell is very low, at least lower than the calculated  $K_m$  value as discussed previously (Papenbrock and Schmidt 2000b). The  $K_m$  value describes the enzyme affinity to the substrates which is much higher for AtStr5 than described for other AtStrs (Bauer and Papenbrock 2002; Papenbrock and Schmidt 2000a, b).

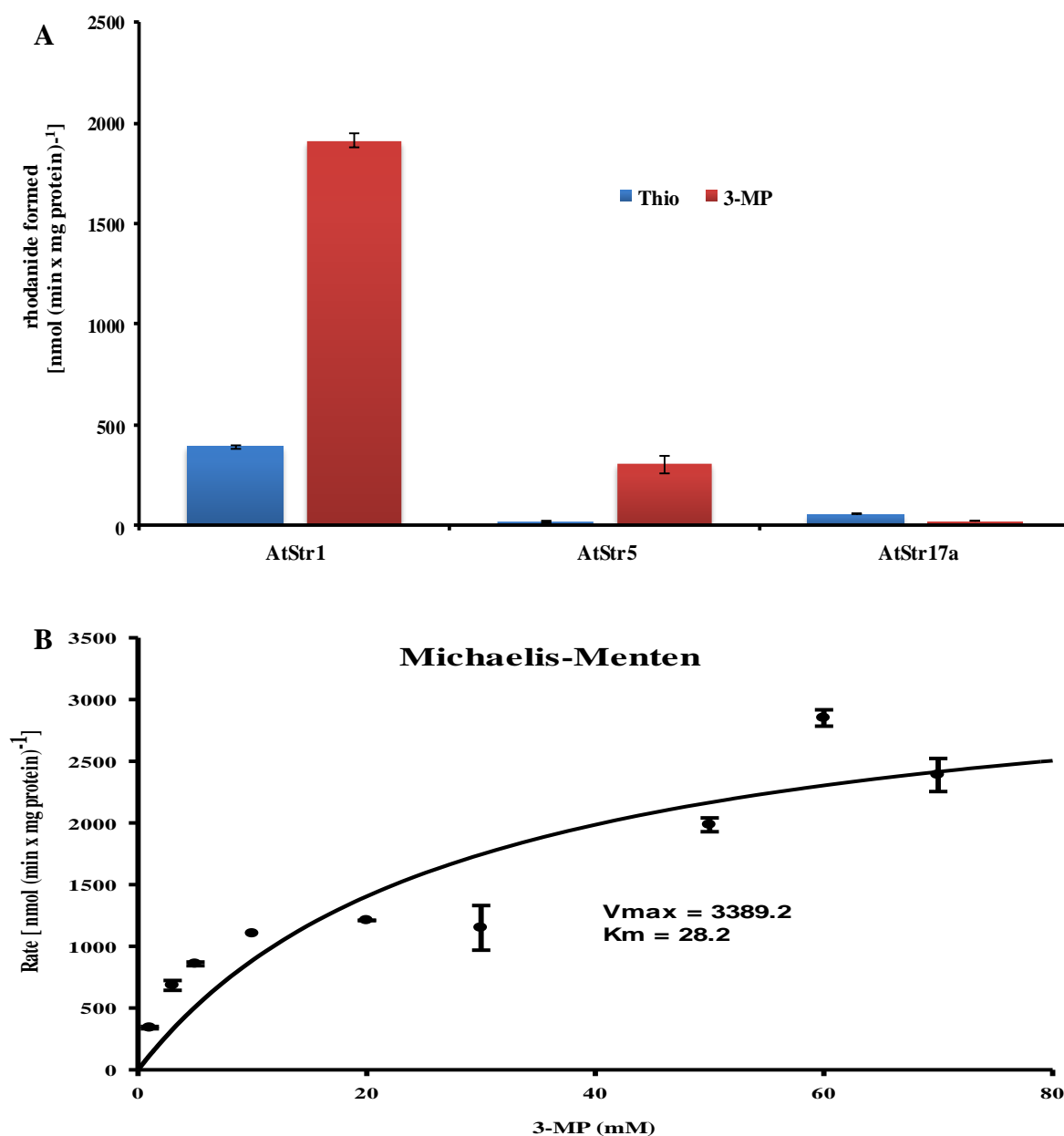


**Figure 6.** (A) Mercaptopyruvate and thiosulfate sulfurtransferase activity measurement of recombinant AtStr5 & AtStr17a/HAC1/ATQ1 protein. The mercaptopyruvate sulfurtransferase activity of AtStr5 was around  $\sim 300$  [nmol (min x mg protein)<sup>-1</sup>] which was  $\sim 6$  times less than the positive control AtStr1  $\sim 1900$  [nmol (min x mg protein)<sup>-1</sup>] and AtStr17a/HAC1/ATQ1 was undetectable. The thiosulfate sulfurtransferase activity of AtStr5 was negligible while for AtStr17a/HAC1/ATQ1 was  $\sim 54$  [normal (min x mg protein)<sup>-1</sup>]. (B) The Michaelis-Menten graph showed the  $K_m$  and  $V_{max}$  value of AtStr5 with 3-MP was  $\sim 28.2$  mM and  $\sim 3389.3$  [nmol (min x mg protein)<sup>-1</sup>].

### 3.4 Subcellular localization of AtStr5

The AtStr5 protein sequence was analyzed by computer-based available prediction methods. The different web-based tools have shown different subcellular localization of the protein: mainly mitochondria, chloroplast, and nucleus (**Table 4**). The programs PSORT, iPOSRT, TargetP, Mitoprot, Predator, and ESL-pred, have predicted the localization of a full-length AtStr5 protein is in the mitochondria, with an average probability above 50 percent. The probability for mitochondrial localization has been decreased by the program Mitoprot and Predator when 14 aa was deleted from the N-terminal part of the protein. The probability for mitochondrial localization has been wholly abolished when 29 aa was eliminated from the N-terminal region of the protein. From the above analysis, it can be predicted that if AtStr5 is a mitochondrial protein, then its mitochondrial target peptides are present within the first 29 aa of the protein. The programs NucPred, NuPLoc, eSLDB, Plant mPLoc, and Softberry, have predicted the localization of full-length AtStr5 is in the cell nucleus, among all the programs, only NucPred and Softberry have given the probability percentage are 0.26 and 0.73. The nucleus localization of the AtStr5 has not been altered even after deleting the 14 aa and 29 aa from the N-terminal part, except the program eSLDB which has shown that the truncated versions remain in the cell cytoplasm. According to the programs NucPred, NuPLoc, Plant mPLoc, and Softberry, the nucleus localization of AtStr5 is not controlled by a nucleus localization signal (NLS). It is possible a diffusion system may control the protein nucleus importing. The program cNLS which has predicted the dual localization of AtStr5, nucleus and cell cytoplasm. The programs Plant PLoc, LOCTREE and Predict Protein have predicted the localization of AtStr5 is in the chloroplast, which has not been altered for the truncated versions where 14 aa and 29 aa was deleted from the N-terminus. However, the program ChloroP cannot detect chloroplast transit peptides in the AtStr5, though this program is specifically created to recognize the chloroplast transit peptides of the protein. The *in silico* inconsistency results has given the impression for determining the localization of AtStr5 by functional approach.

**Table 4. Computer-based localization prediction analysis for AtStr5 and its two truncated mutants.** The respective probabilities are given. Abbreviations: Lo, localization; TP, target peptide; RI, reliability index; EA, expected accuracy.

Prediction program	AtStr5 (146 aa)	AtStr5 (132 aa)	AtStr5 (117 aa)	Remarks
PSORT ( <a href="http://psort.hgc.jp/form.html">http://psort.hgc.jp/form.html</a> )	Lo: Mitochondria matrix space Probability: 0.703, P:26	Lo: Mitochondria matrix space Probability: 0.640, P:49	Lo: Cytoplasm Probability: 0.45	Prediction of protein sorting signals and localization sites
iPSORT ( <a href="http://ipsort.hgc.jp/index.html">http://ipsort.hgc.jp/index.html</a> )	Mitochondria	Predicted as: having a mitochondrial targeting peptide	Not having any signal of mitochondrial targeting	Detection of N-terminal sorting signals
Target P ( <a href="http://www.cbs.dtu.dk/services/TargetP/">http://www.cbs.dtu.dk/services/TargetP/</a> )	Lo: Mitochondria Probability: 0.626 (RC-3),TP:20	Lo: Mitochondria Probability: 0.626 (RC-4), TP:6	No Localization predicted	Prediction of subcellular location
MITOPROT ( <a href="http://ihg.gsf.de/ihg/mitoprot.html">http://ihg.gsf.de/ihg/mitoprot.html</a> )	Lo: Mitochondria Probability: 0.876, TP: 29 (MGRSIFSFFTKKKK MAMARSISYITSTL)	Lo: Mitochondria Probability: 0.39, TP:15 (MAMARSISYITSTQ)	Not predicted	Calculates the N-terminal protein region that can support a mitochondrial Targeting Sequence and the cleavage site
ESLpred ( <a href="http://www.imtech.res.in/raghava/eslpred/submit.html">http://www.imtech.res.in/raghava/eslpred/submit.html</a> )	Lo: Mitochondrial protein RI:1, EA:53%	Lo: Mitochondrial protein RI:1, EA:53%	Lo: cytoplasmic protein RI:1, EA:53	A tool for subcellular localization of the eukaryotic protein
Predotar ( <a href="http://urgi.versailles.inra.fr/predotar/predotar.html">http://urgi.versailles.inra.fr/predotar/predotar.html</a> )	Lo: Mitochondria Probability: 0.71 TP: Not mentioned	Lo: Mitochondria Probability: 0.26 TP: Not mentioned	Cannot determine, without N terminal sequence and Methionine	Prediction of mitochondrial, plastid and ER targeting sequences
Plant-PLoc: ( <a href="http://www.csbio.sjtu.edu.cn/bioinf/plant/">http://www.csbio.sjtu.edu.cn/bioinf/plant/</a> )	Chloroplast (By fusing PseAA composition)	Chloroplast	Chloroplast	Predicting plant protein sub cellular location
LOCTREE2 ( <a href="https://roslab.org/services/loctree3/">https://roslab.org/services/loctree3/</a> )	Chloroplast (95%)	Chloroplast (95%)	Chloroplast (94%)	Protein subcellular localization prediction
Predict Protein ( <a href="http://ppopen.informatik.tu-muenchen.de/">http://ppopen.informatik.tu-muenchen.de/</a> )	Chloroplast	Chloroplast	Chloroplast	Predict the subcellular localization of the protein
ChloroP ( <a href="http://www.cbs.dtu.dk/services/ChloroP/">http://www.cbs.dtu.dk/services/ChloroP/</a> )	Does not contain chloroplast transit peptide	Does not contain chloroplast transit peptide	Does not contain chloroplast transit peptide	Prediction of chloroplast transit peptides
NucPred ( <a href="http://www.sbc.su.se/~maccallr/nucpred/cgi-bin/single.cgi">http://www.sbc.su.se/~maccallr/nucpred/cgi-bin/single.cgi</a> )	Nucleus (.26)	Nucleus (.04)	No protein found	Predicts if a protein spends at least part of its time
Nuc-PLoc ( <a href="http://www.csbio.sjtu.edu.cn/bioinf/Nuc-PLoc/#">http://www.csbio.sjtu.edu.cn/bioinf/Nuc-PLoc/#</a> )	Nucleolus	Nucleolus	Nucleolus	Predicting protein sub nuclear localization
e SLDB ( <a href="http://gpcr.biocomp.unibo.it/esldb/search.htm">http://gpcr.biocomp.unibo.it/esldb/search.htm</a> )	Nucleus	No protein found	No protein found	Eukaryotic subcellular localization database
Plant-mPLoc ( <a href="http://www.csbio.sjtu.edu.cn/bioinf/plant-multi/">http://www.csbio.sjtu.edu.cn/bioinf/plant-multi/</a> )	Nucleus	Nucleus	Nucleus	Predicting subcellular localization of plant proteins including those with multiple sites
Softberry: ( <a href="http://www.softberry.com/berry.phtml?topic=protcomppl&amp;group=programs&amp;subgroup=proloc">http://www.softberry.com/berry.phtml?topic=protcomppl&amp;group=programs&amp;subgroup=proloc</a> )	Lo: Nucleus Probability: 0.73	Lo: Nucleus Probability: 0.73	Lo: Nucleus Probability: 0.73	Predict the subcellular localization of protein
cNLS ( <a href="http://nls-mapper.iab.keio.ac.jp/cgi-bin/NLS_Mapper_form.cgi">http://nls-mapper.iab.keio.ac.jp/cgi-bin/NLS_Mapper_form.cgi</a> )	Lo: Nucleus and cytoplasm Cut off score:3.9 (3-4 score strong probability in this two locations)	Lo: Cytoplasm Cut off score: 2.1 (1-2 score strong probability in the cytoplasm)	Lo: Cytoplasm Cut off score: 2.1 (1-2 score strong probability in the cytoplasm)	Accurately predicts nuclear localization signals specific to the importin $\alpha\beta$ pathway by calculating NLS scores (determine NLS for yeast species)

One full-length and two truncated versions of *AtStr5* were produced by PCR to determine its subcellular location. The full-length *AtStr5* consisted of 438 bp/146 aa, and the first truncated version was produced by deleting the 42 bp/14 aa sequence from the N-terminal part of *AtStr5*, this sequence has predicted as an NLS. The second truncated version was produced by excluding the 87 bp/29 aa sequence from the N-terminal part of *AtStr5*, this sequence has predicted as mitochondrial target peptides (MP) (from Mitoprot predictor tool). Each version of *AtStr5* sequences was fused both the N- and C-terminal sites of GFP and yielded a total of six GFP fusion clones of *AtStr5* (**Figure 7**).

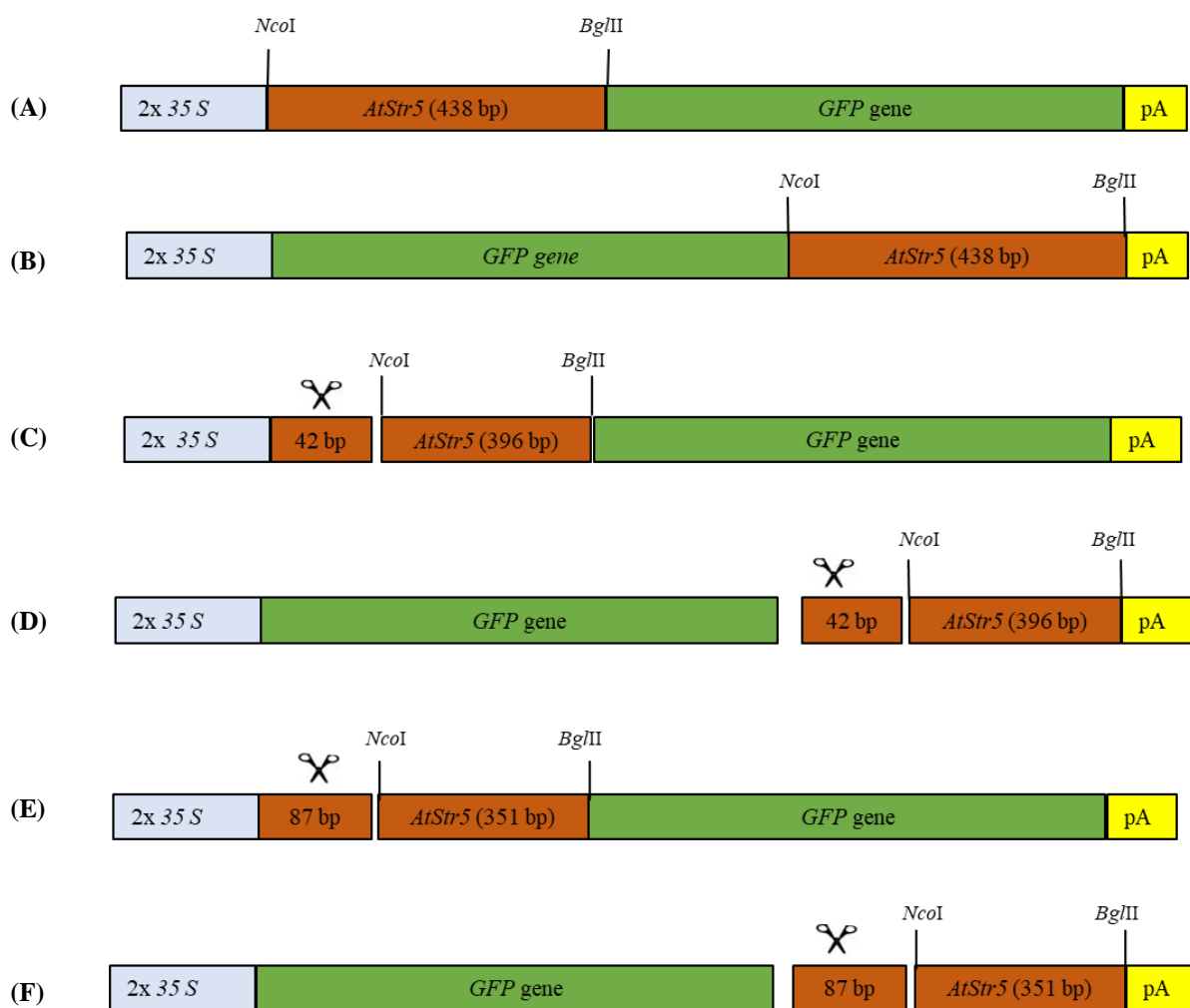


**Figure 7.** The orientation of different version of *AtStr5* into pBSK based pGFP-N/-C vectors. (**A & B**) The fusion construct of full-length *AtStr5* with 438 bp/146 aa in pGFP-N/-C vectors. (**C&D**) The fusion construct of *AtStr5* with 396 bp/132 aa in pGFP-N/-C vectors, which is devoid of putative NLS 42 bp/ 14 aa. (**E&F**) The fusion construct of *AtStr5* with 351 bp/117 aa in pGFP-N/-C vector, which is devoid of putative mitochondrial TP 87 bp/29 aa. A protein with correct localization signal in pGFP-N vector remains in the destination compartment. A protein that remains in pGFP-C vector expected to be localized into the cytoplasm, regardless of their localization signal.

After that, the *Arabidopsis* protoplasts were transformed transiently with each of that GFP fusion AtStr5 constructs. Subsequently, results were analyzed by fluorescence microscopy. Each bright field image of the corresponding transformed protoplast visualizes the intactness of the respectively transformed protoplasts. The merged image demonstrates the autofluorescence of the chloroplasts that was combined with GFP fluorescence. The fluorescence microscopy result has revealed, the 396 bp/132 aa truncated fusion constructs of AtStr5 with or without target peptide sequence were localized in the cytoplasm (**Figure 8A and 8B**). Likewise, 351 bp/117 aa truncated fusion constructs of AtStr5 with or without target peptide sequence were also found in the cytoplasm (**Figure 8C and 8D**). The full-length (438 bp/146 aa) fusion construct of AtStr5 in the pGFP-N vector was shown an unusual localization signal, in some cases, a single or double GFP spot was observed, and this result was not reproducible. Initially, it seems localization might be in the nucleolus (**Figure 9A**). However, DAPI test was unsuccessful to validate these results. The full-length fusion construct of AtStr5 in the pGFP-C vector was found in the cytoplasm (**Figure 9B**). Notwithstanding, this result suggested that this two truncated version of AtStr5 does not contain any C-terminal target peptide sequences for localization, such as peroxisomes and endoplasmic reticulum.

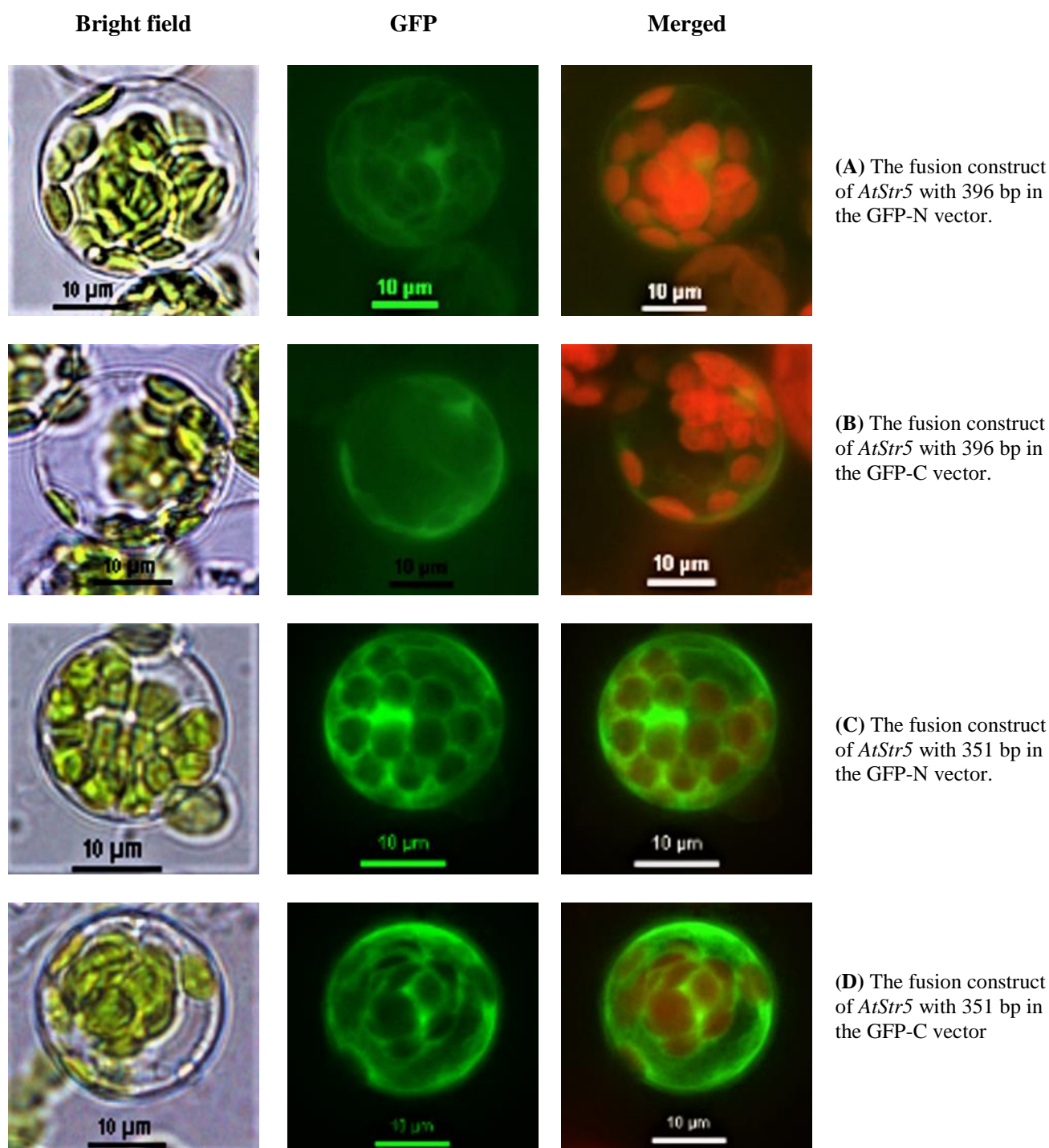


**Figure 8.** Subcellular localization of different truncated constructs of *AtStr5* in the pGFP-N/-C vector. *Arabidopsis* protoplasts were transfected with indicated (A, B, C, D) fusion construct. (A & B) Both N- and C- terminal GFP fusion construct of *AtStr5* (396 bp/132 aa) were shown cytoplasmic localization. (C&D) Both N- and C- terminal GFP fusion construct of *AtStr5* (351 bp/117 aa) were demonstrated cytoplasmic localization. All images were made by Nikon Eclipse Ti-S inverted fluorescence microscope, all fluorescence images are displayed in the GFP channel (green; excitation 488 nm/emission 509/525 nm) and chlorophyll autofluorescence (red; excitation 408 nm/emission 620/700 nm). The Brightfield (BF) images of each transformed protoplast were visualized by the intact plasma membrane, GFP fluorescence of respective protoplast was shown their localization signal. The merge images of the same protoplast were displayed autofluorescence of chloroplast that was merged with respective GFP fluorescence. All photos are representative of  $n \geq 3$  independent experiments. All scale bars = 10  $\mu\text{m}$ .



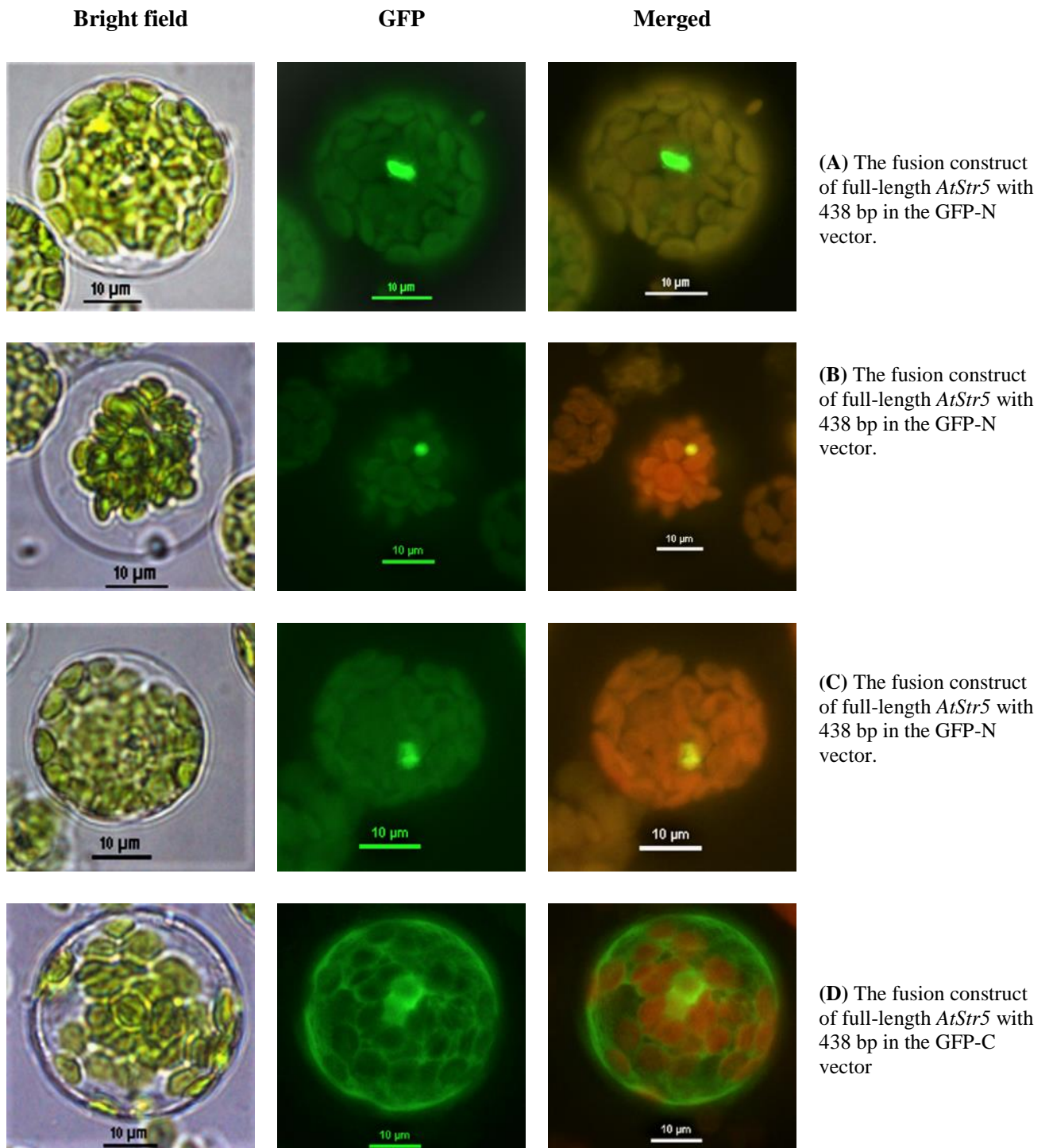


**Figure 9.** The subcellular localization of full-length *AtStr5* protein in the the pGFP-N/-C vector. *Arabidopsis* protoplasts were transfected with indicated (A, B, C, D) fusion construct. (A, B, & C) The GFP-N-terminal full-length fusion construct of *AtStr5* (438 bp/146 aa) was shown an unusual localization signal. (D) The GFP-C-terminal full-length fusion construct of *AtStr5* (438 bp/146 aa) was found in the cell cytoplasm. All images were made by Nikon Eclipse Ti-S inverted fluorescence microscope, all fluorescence images are shown in the GFP channel (green; excitation 488 nm/emission 509/525 nm) and chlorophyll auto-fluorescence (red; excitation 408 nm/emission 620/700 nm). The Bright field (BF) images of each transformed protoplast were visualized by the intact plasma membrane, GFP fluorescence of respective protoplast was shown their localization signal. The merge images of the same protoplast were displayed auto-fluorescence of chloroplast that was merged with respective GFP fluorescence. All photos are representative of  $n \geq 2-3$  independent experiments. All scale bars = 10  $\mu\text{m}$ .



## 4 Discussion

As long as the rhodanese homology domain protein AtStr5 from *A. thaliana* gene locus At5g03455 was proposed to show tyrosine phosphatase and AR activity, our objective was to determine its *in vitro* Str, phosphatase, and AR activity and widen its scope of biological functionality. The coding sequence of *AtStr5* cloned into a pQE-30 expression vector under the control of T5 promoter was transformed with two different kinds of strain, *E. coli* XL1-Blue and BL-21 (DE3) to detect which strain shows over-expression of proteins. It was observed that induction with IPTG allowed for the expression of a protein sized approximately 16 kDa after 3 h of induction in LB medium.

The yield of purified AtStr5 protein was found very low after purification. Formation of protein aggregates due to protein over-expression was considered as the bottleneck for less recovery of AtStr5 of total soluble proteins. Therefore, the induction experiment was conducted at lower temperatures (25°C) and higher speed (200 rpm), which allows the bacterial culture growth at the sub-optimal level and thus maintaining the number of protein molecules below a threshold. It avoids the formation of high molecular weight aggregates of misfolded proteins called inclusion bodies. In this context, *E. coli* strain BL-21 (DE3) has shown a higher expression level in rich-LB media. Although soluble protein expression was very less, good protein yield was found after purification by taking a larger volume of culture media (1400 mg l<sup>-1</sup>). Although sufficient protein yield was obtained by changing the growth condition of bacteria, the formation of protein precipitation was observed in the purified solution. It has been reported that if the protein molecules contain cysteine residues and they are joined together by a disulfide bond and called cystine, this oxidation could become a problem and could lead to protein aggregation. The AtStr5 protein sequence was analyzed by the ExPasy ProtParam tool, which has shown that the instability index (II) of AtStr5 is 45.84. The ProtParam tool describes a protein whose instability index is smaller than 40 is predicted as stable, a value above 40 predicts that the protein may be unstable (Gasteiger et al. 2005). Attempts were taken to riské the protein from aggregation problems such as changing the concentration of the ingredient in buffer composition, the addition of BSA, glycerol, and DTT to stabilize and creating the reducing environment for AtStr5 to keep it active. Each of the components was optimized to achieve the purified protein for suitable activity assay. In this purification process, we found that both DTT (5 mM) and glycerol (10%) are necessary to keep the protein stable and active. The reducing capacity of DDT creating a reducing environment, which prevents the protein from becoming oxidized. Additionally, glycerol precludes the protein to form an

aggregation by inhibiting protein unfolding and by stabilizing aggregation-prone intermediates through preferential interactions with hydrophobic surface regions that favor amphiphilic interface orientations of glycerol (Vagenende et al. 2009).

After successful recovery of protein through optimization, the enzyme assay for Str and phosphatase have been initiated. The *in vitro* AR activity of AtStr5 was not repeated in this work since considerable studies already showed its AR activity *in vitro* even *in vivo* (Bleeker et al. 2006; Dhankher et al. 2006; Ellis et al. 2006; Nahar et al. 2017).

The AtStr5 protein was proposed as Arath; CDC25 due to sharing the similar structural association and same catalytic motif with huCDC25 protein. The huCDC25B protein has shown a higher affinity to the substrate 3-OMFP and also higher catalytic efficiency comparing to the substrate *p*NPP *in vitro*. The similar behavior also observed in other DS-PTPases, for example, human VHR and rat rVH6 (Denu et al. 1995; Zhang 1995), though, this DS-PTPases are not involved in the cell cycle system, they are possible function is mitogenic signaling. By contrast, the Yersinia phosphatase enzyme, YOP and rat phosphatase, PTP1 (Zhang 1995; Zhang et al. 1992) did not show higher catalytic fold to the 3-OMFP over *p*NPP. In this experiment, the phosphatase activity of AtStr5 was conducted using both of these substrates and to investigate whether AtStr5 also similarly catalyze of those substrates. The AtStr5 showed ~3000-fold enhancement of  $k_{cat}/K_m$  for 3-OMFP over *p*NPP, which suggests the AtStr5 seems to be a DS-PTPases. By contrast to the huCDC25B, the enzyme shows a lower turnover rate ( $k_{cat}$ ) and lower catalytic efficiency ( $k_{cat}/K_m$ ), which raises the question about the mitotic accelerator role of AtStr5. The AtStr5 shows ~11-fold lower  $k_{cat}$  value, and ~17-fold lower catalytic efficiency ( $k_{cat}/K_m$ ), though AtStr5 and CDC25B share the same catalytic motif (**Table 3, result part**). Moreover, in many physiological studies, the phosphate role of AtStr5 (Arath; CDC25) was excluded, for instance, the Arath; CDC25 is unable to complement the temperature-sensitive CDC25-22 yeast mutant and, unlike other cell cycle regulatory genes Arath; CDC25 is not up-regulated in rapidly dividing tissues (Dissmeyer et al. 2009; Sorrell et al. 2005). Neither the overexpression nor the T-DNA insertional line of Arath; CDC25 was shown an altered growth and altered cell cycle rate in comparison to wild-type plant (Dissmeyer et al. 2009; Spadafora et al. 2010).

Furthermore, the Arath; CDC25 overexpressing plants were found insensitive to the hydroxyurea (HU), an agent induce DNA damage by interrupting DNA replication, process or DNA checkpoint pathway, However, in yeast and animals the CDC25 phosphatase activity is negatively regulated in HU induce stress (Mailand et al. 2000). Considering the

finding of the above studies and our kinetic data does not support the CDC25 role of AtStr5 protein. However, the *in vitro* phosphatase activity of AtStr5 might be explained due to similar oxyanion binding site because huCDC25B and huCDC25C can also catalyze *in vitro* another oxyanion rich substrate like arsenate (Bhattacharjee et al. 2010).

The phosphatases activity of AtStr5 was abolished when catalytic Cys was replaced by Ala residue, however, in the huCDC25B enzyme, both Cys and arginine residues are required for phosphatase activity (Bhattacharjee et al. 2010). Thus, it is proved that the catalytic Cys has an essential role in substrate binding for the protein with Rhd domain. However, the length and the composition of the amino acid are crucial for its substrate recognition and specificity (Bordo and Bork 2002). Here, we tested the phosphatase activity of AtStr1 and AtStr17a (HAC1/ATQ1) which are contained six amino acid longer an active site loop [Cys-(X)<sub>4</sub>-R]. We found they are unable to catalyze either *p*NPP or 3-OMFP.

Additionally, it has been demonstrated that the engineered elongation catalytic loop of the *A. vinelandii* compromise the ability to catalyze sulfur transfer reaction and gain phosphatase ability to catalyze the artificial substrate 3-OMFP (Forlani et al. 2003). From this work, it was further established that Rhd domain with seven amino acid loop such as AtStr5 could hydrolyze phosphorous rich substrates *in vitro*, for example, 3-OMFP and *p*NPP, whereas the Rhd-like domains with six amino acid active site loop interact with substrates containing reactive sulfur or in some cases selenium (Ogasawara et al. 2001). However the *in vitro* substrate acceptance always not reflect its original physiological substrates, because some enzymes can react with the analogous substrates, as mentioned above the huCDC25B and huCDC25C also accepted arsenate rich substrates.

The Str activity of AtStr5 was determined using the substrates 3-MP and TS, while 3-MP and TS Strs activity were noticed in many prokaryotic and eukaryotic (Westley 1973; Wood and Fiedler 1953). In *A. thaliana* 20 different Strs and Strs-like proteins have been identified, and they contain at least one Rhd domain. The two domains of Strs enzymes were found in both 3-MP and TS activities, preferring 3-MP than TS (Papenbrock and Schmidt 2000a, b).

The single domain TS preference AtStr protein has also been identified, such as AtStr16 and AtStr18 in *Arabidopsis* (Bauer and Papenbrock 2002). However, their TS specificity is not higher than the two domains AtStr protein. It is likely that both substrates (3-MP and TS) used *in vitro* assays, could also be metabolized biologically. In this work, the single Rhd domain containing AtStr5 protein showed 3-MP specific Strs activity but significantly lower when compared with AtStr1 (positive control). The TS specific Strs activity of

AtStr5 was the almost undetectable limit. Therefore, enzymes kinetics were determined with 3-MP. The AtStr5 showed a remarkably higher  $K_m$  (~ 28.2 mM) for 3-MP which is significantly higher than other characterized Strs protein, so far (Bauer and Papenbrock 2002; Papenbrock and Schmidt 2000a, b). The  $k_{cat}$  and  $k_{cat}/K_m$  were  $0.83\text{S}^{-1}$  and  $.029\text{S}^{-1}\text{mM}^{-1}$ . The higher  $K_m$  and lower catalysis rate ( $k_{cat}$ ) and catalytic efficiency  $k_{cat}/K_m$  indicate that AtStr5 is not an actual MST specific protein. It has been demonstrated that the active site loop amino acid sequences are distinct in TSTs and MSTs. In TSTs two positively charged amino acid is present [CRXGX (R/T)] to interact with the negative charges of oxygen atoms in TS. On the other hand, the uncharged serine residue in the MST motif [CG(S/T) GVT] participates in the hydrogen bonding network with two additional arginines that includes the carboxyl groups of pyruvate. However, the conserved catalytic site of AtStr5 (CALSQVR) neither represents typical TSTs nor MSTs motif, only holding Rhd conserved motif, where Cys is the first position with one charged residue (arginine) at the proximal position.

In typical MST motif composition, the charged amino acid is absent. It might be the possible reason that AtStr5 could not recognize TS substrate *in vitro*. Furthermore, the 3-MP specific activity is also negligible, and kinetic behaviors were also alike with other characterized AtStrs. Not only the active site composition but also the length of the active site of AtStr5 is also different which is seven instead of six that are common in other AtStrs. The longer active site loop of AtStr5 creates a wider catalytic pocket, therefore it can accommodate phosphorous and another analogous atom which has van der Waals radius slightly larger than a sulfur atom (1.9 versus 1.85Å). By all appearance, the AtStr5 does not represent Str protein.

The knowledge about protein subcellular localization in the cell in the organism often helps to elucidate its function. Compartmentation plays a vital role in regulation and communication of cellular processes, especially in plants (Papenbrock and Grimm 2001). The subcellular localization of AtStr5 was investigated through a GFP-fusion approach to elucidate its functional specificity. The GFP reporter has been very successfully used in many protein localization studies including AtStrs localization (Bauer et al. 2004). In this experiment, we have constructed pGFP -N/-C terminal-fusion constructs of full-length and two truncated forms of AtStr5 protein. The full-length AtStr5 protein consists of 146 aa (438 bp), and two truncated versions are 132 aa (396 bp) and 117 aa (351 bp). The first truncated version of AtStr5 consists of 132 aa after deletion of 14 aa from the N-terminal part as considered NLS (MGRSIFSSSTK) (Landrieu et al. 2004a). The second truncated version of AtStr5 is composed of 117 aa (351 bp), where 29 aa were deleted based on the prediction of the MITOPROT-program (Claros and Vincens 1996). The MITOPROT-program has shown, the highest probability for mitochondrial localization of AtStr5 is 0.8%, and the respective cleavage site is 29 aa. It has been expected that the target gene cloned in the pGFP-N vector will be localized in their destination compartment and the same gene cloned in the pGFP-C vector will remain in the cell cytoplasm regardless its localization signal. We have observed the localization of both truncated fusion constructs of AtStr5 were in the cell cytoplasm, which indicates that C-terminal part of AtStr5 protein does not contain any localization signal.

On the other hand, the localization of full-length AtStr5 protein was not precisely identified. Although occasionally it appears to be in the nucleus, the biological replicate did not produce reproducible results. The occasional signal may be the result of GFP artifact. All three fusion-constructs that were fused in the pGFP-C vector were localized in the cytoplasm as expected. The experiment was repeated 3-4 times, except for full-length protein, other truncated version was shown a similar result. We have included a sufficient control to avoid the artifact of the localization process. Our previous mitochondrial localized protein AtStr1 and empty pGFP-C were used to prevent the technical error.

The sequence analysis of AtStr5 and its two truncated versions by the different computer-based program has shown similar localization for the full length and 14 aa deleted version of the AtStr5 protein (**Table 4**). According to the prediction of a web-based application, the full-length protein must be localized in the cell cytoplasm, because, 14 aa deleted protein was found in the cell cytoplasm in experimentally.

On the other hand, none of the computer-based programs have predicted that localization of AtStr5 or its 14 aa deleted mutant in the cytoplasm instead showed in the mitochondria, nucleus or chloroplast. Nevertheless, if the protein is genuinely cytoplasmic, it could have found in the cytoplasm without any interference likewise the truncated version of AtStr5 (132 aa). Therefore, it's not plausible to depend on only the prediction method. Some studies mentioned the limitation of *in silico* approach (Reumann et al. 2009; Richly and Leister 2004); sometimes experimental evidence arises different result with the computational predictions from various algorithms. These discrepancies should not come as a surprise, as the output of the prediction programs is usually based on only partially defined targeting signals that allow a high degree of sequence variability unless targeting signals are defined more precisely.

From the mutant analysis in this experiment, it was evident that the localization signal is present in the N-terminus part of the protein and, which has been interrupted by any biological interference. It could be possible the overexpression of the fusion construct by CaMV 35S promoter lead to higher expression and subsequently could lead to mistargeting or silencing of the protein (Tanz et al. 2013). Alternatively, it could be possible the fused GFP could be the reason for a conformational modification in the target protein, and a localization signal could become active, which is generally isolated in the absence of FP or when it lacks some endogenous ligand. One of the computer-based program cNLS predicted the localization of AtStr5 might be dual, in nucleus and cytoplasm. However, there are no so many programs available that can predict the dual localization of the protein. The nucleus localization of AtStr5 also considered by analyzing its N-terminal 14 aa (MGRSIFSSSTK KKK), where basic four lysine residues present, but this kind of prediction often not supportive. Nevertheless, the possibilities of AtStr5 in dual localization cannot be ignored because its can catalyzes both phosphates and arsenate rich substrate *in vitro* as like huCDC25 enzymes, they ae also dual localized (nucleus and cytoplasmic) protein. Additionally newly identified AR enzyme HAC1 also dual localized (nucleus and cytoplasmic) protein.

## CHAPTER IV

### **Simultaneous overexpression of AtStr5, AtStr17a, and the phytochelatin synthase protein AtPCS1 in *Arabidopsis thaliana*, an approach to improve arsenic phytoremediation**

#### **Abstract**

The extensive contamination of arsenic (As) in the environment led to the evolution of arsenate reductase (ARs) enzymes in many species including plants. Reduction of As from arsenate [As (V)] to arsenite [As (III)] is thought to be the first step of As detoxification, which is accomplished by ARs. The molecular mechanisms underlying plant As detoxification are still not well understood for all species. It has been suggested that after reduction, the reduced [As (III)] can bind with the thiol-rich peptides phytochelatins (PCs) and form [As (III)]-PCs complexes. Subsequently, the [As (III)]-PCs complex can be sequestered into the vacuole. It is evident that AR and PCS genes are very crucial for the As detoxification system. Hence, manipulation of these genes might assist to improve the As phytoremediation system. In the present study, we have cloned the *Arabidopsis* potential ARs (*AtStr5* and *AtStr17a*) and PCS (*AtPCS1*) genes in the plant expression vectors (pBinAR and pBin-Hyg-TX) under the control of the CaMV 35S promoter. Following *Arabidopsis* floral dip transformation method, we have produced the homozygous single overexpressing lines of *AtStr5<sup>oe</sup>* and *AtStr17a<sup>oe</sup>*. The homozygous single overexpressing line of *AtStr5<sup>oe</sup>* and *AtStr17a<sup>oe</sup>* were re-transformed with the pBin-Hyg-TX-*AtPCS1* construct to produce the dual overexpressing line of *AtStr5-AtPCS1* and *AtStr17a-AtPCS1*. The co-overexpression of AR and PCS genes are in progress. Analysis of these mutants under different As and sulfur treatment might explain essential aspects of the As phytoremediation process.

## 1 Introduction

Arsenic (As) is the 20th most ubiquitous metallic element in the environment, with an estimated concentration ranging 1.5-3 mg kg<sup>-1</sup> in the Earth's crust (Drewniak and Sklodowska 2013; Zhao et al. 2010). The contamination of As is not only limited to the soil and groundwater, but its deposition in the food crop is also increasing tremendously. Therefore, restrict the entry of As in the food crop is one of the major challenges of the modern world. It has been reported that rice grain can accumulate up to 7.23 mg g<sup>-1</sup> of As, exceeding the Chinese maximum-allowed contaminant level of 1.50 mg g<sup>-1</sup> for inorganic As (Okkenhaug et al. 2012; Williams et al. 2009). In Bangladesh and the United States, agricultural soils are contaminated with three-fold more As than the baseline (Panda et al. 2010) which is the alarming situation of the humanity. There is an urgent need to understand the mechanisms of assimilation and metabolism of As in crop plants which can allow to develop the mitigation methods for crop plants and to eliminate the As from contaminated zones. Therefore, a detailed understanding of biochemical aspects of As regards its bioavailability, transport and uptake mechanisms and the potential mitigation approaches is vital for developing appropriate techniques to reduce As uptake and accumulation in plants. Phytoremediation is such a crucial plant-based approach that can offer to eliminate the toxic As from the polluted environment by using naturally occurring or genetically engineered plants. The principle of this technique is to exploit the ability of plants to extract the toxic element and organic pollutants from soil and water, degrade them or transport them to vegetative tissues and accumulate them in cellular compartments to protect cytosolic proteins and other cellular components. Effective phytoremediation offer three essential aspects as (1) an efficient uptake of metal or metalloids and translocation to the aerial organs; (2) the ability to accumulate and tolerate high levels of metals or metalloids, and (3) a well-developed root system, rapid shoot growth and abundant shoot biomass (Claire-Lise and Nathalie 2012). Although most of the hyperaccumulators satisfy the first two requirements, the major limitations of natural As-hyper accumulators are their slow growth rate, reduced biomass and tend to grow in the moist environment which prevents them to be deployed in phytoremediation purposes. Due to the limitations of hyperaccumulators, various approaches have been considered to make this technique fruitful. One of the critical aspects of As phytoremediation is to understand the molecular mechanism of the As detoxification process.



It has been well accepted that followed uptake the first step of As detoxification in plants is arsenate [As (V)] reduction which is catalyzed by arsenate reductase (*ACR2*). After reduction of As from [As (V)] into [As (III)], the next step of detoxification is chelation formation with phytochelatin (PCs). It seems to be a promising approach to co-overexpress both AR and PCS genes in the same transgenic plant which in turn lead to more reduction and more chelation. To verify the above hypothesis and to understand the As detoxification process in more details, we have intended to co-overexpress potential AR (*AtStr5/AtACR2* and *AtStr17a/HAC1/ATQ1*) and *AtPCS1* of *Arabidopsis*, with an objective to enhance As reduction, and increase chelation with PCs for further vacuolar sequestration. The concerted action of AR-PCS genes can ultimately facilitate to improve the As phytoremediation process. The potentiality of AR and PCS proteins in the As detoxification system was discussed in Chapter 1 of this thesis.

## 2 Material & Methods

### 2.1 DNA isolation and cloning

The total RNA was isolated from 15-day-old *Arabidopsis* seedlings (ecotype Columbia, Col-0) following the RNA Mini-prep technique developed by (Sokolovsky et al. 1990). Four  $\mu$ l (0.5-5  $\mu$ g) of total RNA were reverse transcribed using the first strand cDNA synthesis kit (Thermo Fisher). Two  $\mu$ l of complementary DNA (cDNA) was used to perform a polymerase chain reaction (PCR) reaction. For amplification of *AtStr5/AtACR2*, *AtStr17a/HAC1/ATQ1*, and *AtPCS1* genes, each primer was synthesized with the addition of restriction endonuclease site (*KpnI* and *SalI*) to allow directional cloning of the PCR product. All primer pairs, the length of the PCR product, the source material, restriction sites, annealing temperature, and vectors are included in **Table 1**.

**Table 1. Overview of the clones produced.** The PCR source material, length of the PCR product, corresponding primer pairs and annealing temperature, and their respective expression vectors are listed.

Gene ID/ Gene name and size (bp)	Source material	Primer pairs	Internal primer number & their annealing temp (°C)	Vector
<i>At5g03455/ AtStr5/AtACR2</i> (399)	cDNA	<i>KpnI</i> 5'-GGT ACC ATG GCG ATG GCG AGA AGC -3' <i>SalI</i> 5' - GTC GAC TTA GGC GCA ATC GCC CTT -3'	P968A / P969A 61.9	pBinAR
<i>At2g21045/ AtStr17a</i> (423)	cDNA	<i>KpnI</i> 5' - GGT ACC ATG GAG GAA ACA AAA CCA AA -3' <i>SalI</i> 5' -GTC GAC TTA GTT TTC CTT TGG CCT GA-3'	P970 / P971 57.4	pBinAR
<i>At2g21045/ AtStr17a/HAC1/ ATQ1</i> (510)	cDNA	<i>KpnI</i> 5' - GGTACCATGTATACATATTCTCTC CTCAACCTT-3' <i>SalI</i> 5' - GTCGACTTAGTTTTTCCTTTGGCCTG A-3'	P1011 / P971 59.5	pBinAR
<i>At5g44070/ AtPCS1</i> (1458)	cDNA	<i>KpnI</i> 5' - GGT ACC ATG GCT ATG GCG AGT TTA -3' <i>SalI</i> 5' - GTC GAC CTA ATA GGC AGG AGC AGC -3'	P972 / P1018 54.2	pBin- Hyg-TX

The PCR reaction contained 0.2 mM dNTPs (Roth, Karlsruhe, Germany), 0.4 µM of each primer (Eurofins genomics, Ebersberg, Germany) 1 µl DreamTaq DNA-Polymerase (Thermofisher, Germany), 5 µl 10x PCR Green buffer and about 1 µl template DNA (0.2-0.5 µg in a final volume of 50 µl). The amplification was performed in a programmable PCR cyler using 28 reaction cycles consisting of a 1 min initial denaturation step at 94°C, a 1 min primer annealing step (included in table 1, for each gene) and 1 min elongation step at 72°C. The final elongation step was performed for 600 s at 72°C. The amplified PCR product was analyzed on 1% agarose gels.

For DNA extraction from agarose gels, the Gen Elute™ Agarose Spin Column (Sigma Aldrich) was placed in a collection tube. The spin columns were pre-washed by adding 100 µl of 1x TE buffer to the spin column, followed by centrifugation at 16060 g for 10 s. The spin column was transferred to a fresh collection tube. The bands of interest were excised from the agarose gel and loaded into the pre-washed spin column. The spin column was then centrifuged at 16060 g for 10 min. Each collection tube with eluted DNA of *AtStr5/AtACR2*, *AtStr17a/HAC1/ATQ1*, and *AtPCSI* were stored at 4°C.

*AtStr5/AtACR2* and *AtStr17a/HAC1/ATQ1* (423 bp) genes were then ligated to the pGEM®-T vector (Promega). The ligation mixes of 10 µl contained 5 µl 2 x ligation buffers, 1 µl pGEM®-T vector, 3 µl *AtStr5/AtACR2* and *AtStr17a/HAC1/ATQ1* cDNA insert and 1 µl T4 DNA ligase were mixed and stored overnight at 4°C. The ligated sample was then used to transform competent XL1-Blue *E. coli* cells. The competent cells were thawed on ice for 30 min or more till de-frozen. About 200 µl of competent cells were added to the 1.5 ml reaction tube with the ligation reaction mixture and incubated on ice for 30 min. The 1.5 ml reaction tube was then placed in a water bath for 90 s at 42°C. The 1.5 ml reaction tube was then immediately put on ice for 2 min. About 500 µl of LB medium without antibiotic was added to the 1.5 ml reaction tube and is then incubated in a shaker incubator at 37°C, 800 rpm for 1 hour. After 1 hour of incubation, 200 µl of the mix was plated on LB plate containing ampicillin (final concentration 100 µg ml<sup>-1</sup>), IPTG (final concentration 0.4 mM) and X-Gal (final concentration 40 µg ml<sup>-1</sup>). The plate was incubated at 37°C overnight. The Pfu polymerase (Thermo Scientific) amplified *AtStr17a* (510 bp), and *AtPCSI* genes were cloned into pJET1.2/blunt cloning vector followed the instruction provided by Thermo Scientific.

For plasmid Mini-preparation, the transformed colonies were inoculated in a 3 ml LB broth with ampicillin (final concentration 100 µg ml<sup>-1</sup>). The media was incubated in an incubator shaker at 37°C, 180 rpm overnight. About 1.5 ml of the overnight grown culture was centrifuged at 1500 g for 10 min. The cell pellet was suspended in 300 µl of the P1 buffer by full vortex. About 300 µl of P2 buffer was added, mixed gently and incubated for 5 min at RT, followed by addition of 300 µl of P3 buffer, gently mixing and incubation on ice for 15 min. The mixture was centrifuged at 15,700 g for 15 min at 4°C. The supernatant was added to 0.7 volume of isopropanol to a fresh 1.5 ml reaction tube, followed by centrifugation at 15,700 g for 15 min at 4°C.

About 100 µl of 70% ethanol was added to the pellet and centrifuged at 15,700 g for 10 min. The ethanol was discarded, followed by short centrifugation for 10 s and rest of the ethanol was pipetted out. The 1.5 ml reaction tube was allowed to dry for 5 min, and the plasmid pellet was re-suspended in 50 µl of autoclaved water. The plasmid DNA for all four clones were stored at 4°C.

These plasmids were sequentially digested with *KpnI* and *SalI* restriction enzymes to confirm the correct recombination. Firstly, the digestion contained total 30 µl digestion mix; 15 µl plasmid DNA, 3 µl *KpnI* unique buffers, 3 µl of *KpnI* restriction enzymes and 9 µl Milli-Q water. The reaction mixture was incubated in a water bath at 37°C for 2 h, and the reaction was terminated at 80°C for 20 min. Subsequently, *KpnI* digested DNA product was purified and precipitated by Na-Acetate buffer (pH 5.0) and re-suspended in 20 µl of Milli-Q water. Afterward, this purified plasmid DNA was re-digested with 3 µl of *SalI* enzymes, 3 µl orange buffer O, and 4 µl of Milli-Q water. The reaction was terminated at 65°C for 20 min. The total digestion reaction was loaded on 1% agarose gels. The correct digestion pattern bearing clones were sent for sequencing to GATC Biotech Company, Germany. These nucleotide sequences were searched in the BLAST program of NCBI, to confirm the presence of the desired insert into the vector. This program compares the translated nucleotide query to all the protein sequences in the database. This BLAST program has shown that sequences have 100% identity with the existing protein sequence of NCBI reference sequences: AK117898.1, GB BT008306.1, and NP\_199220.1 for AtStr5/AtACR2, AtStr17a/HAC1/ATQ1, and AtPCS1 protein.

### 2.1.1 Cloning into plant expression vectors (pBinAR and pBin-Hyg-TX)

The recombinant pGEM®-T and pJET1.2/blunt plasmids and plant expression vectors pBinAR and pBin-Hyg-TX were digested with the *KpnI* and *SalI* restriction enzymes. The sequential digestion was performed as described earlier. The digestion pattern was analyzed on 1% agarose gels. The Gen Elute™ Agarose Spin Column was placed in a collection tube to extract DNA from the agarose gels as previously described. The extracted DNA of *AtStr5/AtACR2* and *AtStr17a/HAC1/ATQ1* genes were ligated into a pBinAR vector, and *AtPCS1* gene was ligated into a pBin-Hyg-TX vector. The ligation mixes of 30 µl contained 2 µl 10x ligation buffer, 3 µl pBinAR or pBin-Hyg-TX vector, 15 µl target insert and 2 µl T4 DNA ligase and 8 µl sterile water were mixed and left on lab table for overnight at RT.

Subsequently, the *E. coli* XL1-Blue competent cells were used for transformation as described previously. About 100 µl of the transformation mix was plated onto an LB plate containing kanamycin (final concentration 50 µg ml<sup>-1</sup>). The plate was incubated at 37°C overnight. The success of cloning was confirmed by colony PCR amplifying both *NPTII* and target genes. Subsequently, glycerol stock of each clone was prepared for future work.

### 2.1.2 Cloning into *Agrobacterium tumefaciens* (strain GV3101)

Plasmid DNA was isolated from the positive clone of each expression vectors containing the target gene, of that plasmid DNA 15 µl was used to transform the GV3101 competent *A. tumefaciens* cells for plant transformation. The competent cells were thawed on ice for 30 min or more. About 500 µl of competent cells were added to the 1.5 ml reaction tube with 500-1000 ng (~15 µl) of recombinant plasmid DNA and incubated on ice for 5 min. The 1.5 ml reaction tube was then immersed in liquid nitrogen for 5 min and subsequently in a water bath for 5 min at 37°C. About 500 µl of 2YT (5 g l<sup>-1</sup> yeast extract, 16 g l<sup>-1</sup> bacto tryptone and 5 g l<sup>-1</sup> NaCl, pH adjusted to 7.0) medium without antibiotic was added to the 1.5 ml reaction tube and incubated in a shaker incubator at 28°C, 180 rpm for 3 h. After 3 h of incubation, the bacterial mixture (200 and 400 µl) were plated onto a 2YT agar medium containing rifampicin (100 µg ml<sup>-1</sup>), and kanamycin (100 µg ml<sup>-1</sup>). The plates were incubated at 28°C for two days. The positive colonies were confirmed by colony PCR using gene-specific primers.

## 2.2 Plant preparation and transformation to generate stable transformants

Seeds of *Arabidopsis thaliana* ecotype Columbia-0 (Col-0) were obtained from the *Arabidopsis* Biological Resource Centre (ABRC). Seeds were germinated in a greenhouse for 2-3 weeks at 22-23°C, 14 h light/10 h dark photoperiod, at a light intensity 40 Klux. After 3 weeks each seedling was transferred into 7 cm diameter pots which were filled with *A. thaliana* preferable growing soil. The soil was a mixture of (VM70L clay and 45L sand) provided by Einheitserdewerke Werkverband e.V. Germany. The plants were maintained in a climate chamber at 20-21°C under a 16 h light/ 8 h dark cycle at a light intensity 120  $\mu\text{mol m}^{-2} \text{s}^{-1}$  (fluorescent lamps, OSRAM -L58W/77 FLUORA, Germany). After 7-8 weeks, the plants with sufficient floral bud were used for transformation by floral dip method (Clough and Bent 1998). The transformation method in a brief, when the primary bolts were reached 1-2 cm in height, they were clipped to instigate the emerging of many secondary bolts, thus facilitate to produce ample amount of floral buds for inoculation. Plants were not watered for the next 2-3 days to allow efficient infiltration of the bacterial suspension. Prior transformation all open flowers and silique were eliminated. Five biological replicates of plant per construct were taken for infiltration. The *Agrobacterium tumefaciens* strain GV3101 harboring the gene of interest; pBinAR-*AtStr5/AtACR2*, pBinAR-*AtStr17a/HAC1/ATQ1* and pBin-Hyg-TX (control), pBin-Hyg-TX-*AtPCS1* were grown in a 2-YT liquid medium with kanamycin (100  $\mu\text{g ml}^{-1}$ ) and rifampicin (100  $\mu\text{g ml}^{-1}$ ). The  $\text{OD}_{600}=0.8$  were adjusted with the 5% sucrose solution mixed with 0.05% Tween 80. The bacterial suspension was added to a beaker and inflorescence were immersed in a suspension for 2-5 s with gentle agitation by hand. Afterward, plants were laid down in a plastic tray and covered with a dark plastic bag for overnight in a low light condition to increase the internal humidity for sufficient infection. Subsequently, plastic bags were removed, and watering was continued for recovery of the nascent inoculated plants. After 2-3 days, the inflorescences were covered by a transparent plastic bag for seed collection. In the meantime, if any new secondary bolts are appearing on the treated plants were removed. From these treated T0 plants, T1 seeds of each construct were harvested in a pool and stored at 4°C under desiccation before proceeded to the next step.

### 2.2.1 Seeds sterilization for primary transformants

About 10 mg seeds of putative T1 transformants were taken in 1.5 ml reaction tube. The seeds were surface sterilized by submerging them with 1 ml of 70% (V/V) ethanol for 5-10 minutes thorough overhead shaking followed by 10 min washing with sodium hypochlorite solution (1:1 diluted with H<sub>2</sub>O). The removing and replacement steps were carried out under the clean bench. Traces of hypochlorite were removed by multiple washing with sterile water. After washing the seeds, they were suspended in 500 µl of sterile water. The sterilized seeds were pipetted and evenly distributed over the surface of 0.5 x MS media (Murashige and Skoog 1962) with proper antibiotic. T1 seeds obtained from the inoculation of constructs pBinAR-*AtStr5/AtACR2* and pBinAR-*AtStr17a/HAC1/ATQ1* were selected on MS media with 50 µg.ml<sup>-1</sup> kanamycin (AppliChem GmbH) while pBin-Hyg-TX (control) and pBin-Hyg-TX-*AtPCS1* inoculated plants were selected on MS media with 30 µg ml<sup>-1</sup> hygromycin (Roth). Seeds on the Petri plates were vernalized for 2 days in the dark at 4°C to break the dormancy. Afterward, seeds were transferred to a climate chamber and incubated at 4-6 hrs, at 21°C in continuous white light (light intensity 120 µE m<sup>-2</sup> sec<sup>-1</sup>) to stimulate the germination. Then wrapped with aluminum foil and incubated for 2 days at 20-21°C under 8h light/16h darkness cycle with light intensity 120 µE m<sup>-2</sup> sec<sup>-1</sup> (Harrison et al. 2006). Later, aluminum foil was removed, and seeds were continuously grown in a climate chamber with the same condition.

The T1 resistance plants were screened after 2-4 weeks of germination and transferred into the individual pots. The plant was maintained in a climate chamber in the same condition until harvesting. T2 seeds were harvested individually and grown in a subsequent generation until reached to homozygosity by the condition mentioned above.

### 2.2.2 PCR analysis of T1 primary overexpressing transformants

The molecular confirmation of T1 plants was carried out by amplifying the resistance gene that presents in the T-DNA region of the expression vector. The *NPTII* gene was amplified using the internal primer P387/P388 to confirm the overexpression of *AtStr5/AtACR2* and *AtStr17a/HAC1/ATQ1* in the T1 primary transformants. Likewise, *HPTII* gene was amplified with the internal primer P1016/P1017 for the confirmation of overexpression of *AtPCS1* and *HPTII* (empty vector) in corresponding T1 primary transformants.

The genomic DNA of T1 primary transformants were extracted according to the standard DNA isolation procedure (Sambrook et al. 1989). About 100 mg of T1 transformants fresh tissue was crushed to a fine powder using liquid nitrogen and homogenized in 250  $\mu$ l freshly made extraction mix. About 400  $\mu$ l freshly made extraction mix was added, and the samples were incubated with for 60 min at 65°C. About 700  $\mu$ l of chloroform: isoamyl alcohol (24:1) was added to samples, followed by vortexing for 30 sec. Samples were then centrifuged for 10 min at 9500 g, and the DNA in the supernatant was precipitated with 750  $\mu$ l of isopropanol and again centrifuged. The precipitate was then washed with 70% ethanol. The pellet dried and mixed with 100  $\mu$ l TE with 0.5  $\mu$ g/100  $\mu$ l RNase and dissolved by incubating at 65°C for 15-30 min. The DNA samples were quantified using a spectrophotometer.

The PCR reaction contained 0.2 mM dNTPs, 0.4  $\mu$ M of each primer, 0.5  $\mu$ l Dream Taq DNA-Polymerase, 2  $\mu$ l 10x PCR Green buffer and about 1  $\mu$ l template DNA in a final volume of 20  $\mu$ l. The amplification was performed in a programmable PCR cycler using 28 reaction cycles consisting of a 1 min initial denaturation step at 94°C, a 1 min primer annealing step at 39°C for *NPTII* and 51.6°C for *HPTII* and a 1 min elongation step at 72°C. The final elongation step was performed for 600 s at 72°C. The amplified PCR product was analyzed on 1% agarose gels.



### 2.3 Southern blotting

Southern blotting was performed to transfer restricted genomic DNA fragments onto a nylon membrane. Firstly 2 pieces of long Whatman paper (12 cm x 26 cm) with their both ends hanging in bottom tray were kept on inverted gel cast mold in a container. Two pieces of Whatman papers (12 cm X 13.5cm) with gel size dimension were layered on it. At every step, these layers were moistened with 10x SSC, and air bubbles were removed with a glass rod. The gel was kept inverted with well openings facing on the side of Whatman papers. Nylon membrane with gel size dimension, soaked in 10x SSC buffer is placed on the gel. 2 pieces of Whatman papers with gel size dimension were placed on it. The stack of dry absorbent papers was placed at the top. Weight (bottle on a glass plate) was kept on the adsorbent paper stack so to start the capillary action. The container was filled with 500 ml 10x SSC, so that the hanging ends of the Whatman paper are just dipped in the buffer and blotting was allowed overnight. DNA was fixed to the membrane by incubating the membrane for 2 min in UV crosslinker.

#### 2.3.1 Restriction enzyme selection and digestion for Southern blot analysis

The genomic DNA sequences of each insert were analyzed by Clone Manager Professional-9 program to choose the correct restriction enzymes for southern analysis. The restriction enzymes that are present in the T-DNA sequence, but not within the insert were selected for overnight digestion. About 15-20 µg of genomic DNA was digested with 2 µl of each restriction enzymes at 37°C overnight in the water bath. The name of the restriction enzymes for each overexpressing transformants was presented in **Table 2**. The digested samples were separated on 1% agarose gels by running in gel electrophoresis for 1.5 hrs at 100V in 1xTAE buffer. After completion of electrophoresis, the gel was washed in 250 Mm HCl until lower band on the gel display yellow coloration, then with distilled water. Further washing steps included shaking in denaturing solution washing for 30 min, distilled water wash followed by stirring with neutralization solution for 30 min.

**Table 2.** The name of restriction enzymes used for restriction of the T1 overexpressing transformants of different genes for Southern blot analysis.

Name of the constructs used for inoculation of <i>Arabidopsis</i> (Col-0) -T0-plant	T1- overexpressing lines	Restriction enzymes
pBinAR- <i>AtStr5/AtACR2</i> (399 bp)	T1- <i>AtStr5/AtACR2</i> overexpressing lines	<i>EcoRI</i> , <i>NcoI</i> , <i>XbaI</i> , <i>XhoI</i> and <i>BamHI</i>
pBinAR- <i>AtStr17a/HAC1/ATQ1</i> (423 bp)	T1- <i>AtStr17a/HAC1/ATQ1</i> overexpressing lines	<i>HindIII</i> , <i>EcoRI</i> and <i>BamHI</i>
pBinAR- <i>AtStr17a/HAC1/ATQ1</i> (510 bp)	T1- <i>AtStr17a/HAC1/ATQ1</i> overexpressing lines	<i>EcoRI</i> and <i>HindIII</i>
pBin-Hyg-TX- <i>AtPCS1</i> (1458 bp)	T1- <i>AtPCS1</i> ) overexpressing lines	<i>EcoRI</i> , <i>HindIII</i> and <i>XhoI</i>
pBin-Hyg-TX (1010 bp)	T1-pBin-Hyg-TX overexpressing lines	<i>EcoRI</i> and <i>HindIII</i>

### 2.3.2 DIG probe synthesis

For probe synthesis, target genes their sources, primer pairs, product length, and annealing temperature were included in **Table 3**. The amplified PCR product was then used as a template for DIG-probe synthesis using PCR-DIG probe synthesis kit. PCR mix contained PCR-DIG probe synthesis mix (200  $\mu$ M dATP, 200  $\mu$ M dCTP, 200  $\mu$ M dGTP, 130  $\mu$ M dTTP, 70  $\mu$ M DIG-dUTP, 0.4  $\mu$ M of each primer, 0.75  $\mu$ l Enzyme mix, 5 $\mu$ l 10x PCR buffer with MgCl<sub>2</sub> and about 1  $\mu$ l template DNA in a final volume of 50  $\mu$ l. The amplification was performed in same primer pairs using 28 reaction cycles consisting of a 1 min initial denaturation step at 94°C, a 1 min primer annealing step temp vary for different gene and a 1 min elongation step at 72°C. The final elongation step was performed for 600 sec at 72°C. The amplified PCR product was observed by agarose gel electrophoresis in 1% agarose gels made in 1x TAE buffer.

**Table 3.** List of DIG labeled DNA probes and their source material, corresponding primer sequence, annealing temperature, and product length are presented in the following table.

Name of the gene used for DNA probe synthesis with Digoxinin	Source sequence	PCR primer pairs	Primers & annealing temperature (°C)	Product length (bp)
<i>AtStr5/AtACR2</i> <i>/At5g03455</i>	Internal clone 1035	<i>KpnI</i> 5'-GGT ACC ATG GCG ATG GCG AGA AGC -3' <i>SalI</i> 5' - GTC GAC TTA GGC GCA ATC GCC CTT -3'	P968/P969A 61.9	399
<i>AtStr17a/HAC1</i> <i>/</i> <i>ATQ1</i> <i>/At2g21045</i>	Internal clone 1034	<i>KpnI</i> 5' - GGT ACC ATG GAG GAA ACA AAA CCA AA -3' <i>SalI</i> 5' -GTC GAC TTA GTT TTC CTT TGG CCT GA-3'	P970/P971 57.4	423
<i>AtStr17a/HAC1</i> <i>/</i> <i>ATQ1/</i> <i>At2g21045</i>	Internal clone 1045	<i>KpnI</i> 5'- GGTACCATGTATACATATTCTCTCC TCAACCTT-3' <i>SalI</i> 5' - GTCGACTTAGTTTTCCCTTTGGCCTG A-3'	P1011/P971 59.5	510
<i>AtPCS1/</i> <i>At5g44070</i>	c-DNA	<i>KpnI</i> 5' - GGT ACC ATG GCT ATG GCG AGT TTA -3' 5'-CATGGCTTCCCAAAGAAGT-3'	P972/P1018 54.2	600
<i>HPTII /</i> <i>pBinHyg-TX</i>	Internal clone 1046	5' - ATGAAAAAGCCTGAACTCACC- 3' 5' - CTATTTCTTTGCCCTCGGAC-3'	P1016/1017 51.6	1010

### 2.3.3 Hybridization with DIG-labeled probes

After fixing the DNA to the membrane, it was initially incubated in pre-hybridization solution, thereby preventing nonspecific binding of the probe to the membrane. The membrane was shaken for an hour in the pre-hybridization solution at 40°C in a water bath. For the hybridization, DIG-labeled PCR product (probe) was denatured for 10 min in boiling water. The probe was then transferred into 25 ml of freshly prepared pre-hybridization solution and given to the membrane. Once used probes can be directly applied after its denaturation for 10 min at 68°C and then given to the membrane. The hybridization took place overnight at 55°C in a shaking water bath.

### 2.3.4 Colorimetric detection with NBT/BCIP

For detection, a high-affinity anti-DIG antibody was used, which is conjugated with alkaline phosphatase. This alkaline phosphatase removes the phosphate group of BCIP (5-bromo-4-chloro-3-indolyl-phosphate) the resulting products dimerizes under oxidizing conditions to generate the blue precipitate (5, 5'-dibromo-4,4'-dichloro-indigo). While the reaction between BCIP and NBT proceeds the NBT is reduced to its colored form to give an enhanced color reaction. The unbound probe was removed by several washing steps. Therefore, the membrane was washed twice for 10 min on a shaker in 2xSSC / 0.1% SDS at RT, followed by two times washing of 10 min in 0.5 x SSC / 0.1% SDS at 55°C in a shaking water bath. To prevent nonspecific binding of the antibody to the membrane, it was incubated briefly in 1 x wash buffer (DIG wash and block set) and followed by incubation for 45 min at RT in 1x blocking solution. The anti-DIG antibody was diluted 1:5000 with the blocking solution and placed on the membrane. After 30 minutes, the unbound antibodies were removed by washing membrane twice for 15 mins with 1 x wash buffer on a shaker at RT. Then the membrane was equilibrated in detection buffer for 2 min. The color substrate solution was diluted 1:50 with detection buffer and placed on the membrane. The color reaction was carried out in the dark without swirl and lasted between 15 minutes to several hours. After coloration, the reaction was stopped with distilled water for 5 min.

### 2.4 Gene expression study by Genevestigator

Genevestigator is a useful online platform which enables to analysis the specific gene expression in several factors such as development, tissue type, disease, genetic modification or external stimulus by using a global expression profile. There are three leading toolsets in this program; Condition search tools that help to find conditions that are relevant for genes of interest, Gene search tools enables to see genes that are specifically expressed in conditions of interest similarity search tools assist in finding genes that are similar within a data space. Under each tool, there is the concept of Meta profiles, which shows how strongly a gene is expressed in different anatomy parts, and which stage of development or perturbations, which are also summarized into representative expression responses. Meta-profiles summarize expression levels, according to the biological context of the sample. In contrast to normal expression profiles where each signal value denotes the expression level of one gene in one sample, each signal value in a meta-profile

corresponds to the average expression level of one gene over a set of samples sharing the same biological context, e.g., samples from the same tissue. Genevestigator does this by querying a manually curated database combining results from tens of thousands of microarrays. Genevestigator contains data from a variety of species, including human, rat, mouse, various plants and microorganisms.

To investigate the overexpression of *AtStr5/AtACR2*, *AtStr17a/HAC1/ATQ1* and *AtPCSI* genes the absolute expression of each gene was analyzed in this Genevestigator program. The analyzed result from this program have assisted to interpret the result obtained from the overexpression experiments.

## **2.5 Northern blotting and RNA extraction**

Northern blotting was carried out to determine the gene expression of putative overexpressing mutant lines of *AtStr5/AtACR2*, *AtStr17a/HAC1/ATQ1*, *AtPCSI*, and the empty vector. The total RNA of each putative overexpressing and wild-type plant was extracted from the leaf of 20 days-old *Arabidopsis* according to the method described by Sokolovsky et al. (1990). The plant material (~100-300 mg) was finely grounded in a mortar using liquid nitrogen and incubated with 0.75 ml of lysis buffer and 0.75 ml of PCI for 15-20 min on an overhead shaker at RT. Supernatants obtained after centrifugation of these plant materials were mixed with equal volume of phenol-chloroform-isoamyl alcohol (PCI), and the samples were centrifuged again. Supernatants were mixed with 0.75 ml 8 M LiCl and allowed to precipitate overnight at 4°C. Samples were vortexed vigorously, centrifuged and the pellet was precipitated in 300 µl DEPC-H<sub>2</sub>O solution, 30 µl 3 M sodium acetate, pH 5.2 and 750 µl 98% ethanol, for 30 min at -70°C. Pellets were washed with 70% ethanol, air dried and dissolved in ~ 50 µl DEPC- H<sub>2</sub>O. RNA samples were stored at -70°C for further northern blotting analysis.

### 2.5.1 Detection by CDP-Star

The initial steps are same as for NBT/BCIP detection method. In the last step, instead of color substrate solution, a chemiluminescent substrate for alkaline phosphatase, CDP star is used. CDP star enables extremely sensitive and faster detection of biomolecules by producing visible light. The membrane is incubated with a CDP star solution (5 µl CDP star + 500 µl TMN detection buffer) for 5 min, and the membrane is sealed in plastic film. The membrane impression is developed in the X-ray film (Kodak BioMax XAR film) by putting the film over the membrane in the film developer case for 5-10 min. The X-ray film is developed in developer and fixer solutions.

### 2.6 Construction of dual genes overexpressing transgenic lines

The homozygous overexpressing lines of *AtStr5/AtACR2* and *AtStr17a/HAC1/ATQ1* were taken for further transformation with the construct of pBin-HyG-TX-*AtPCS1* for production of dual gene overexpressing lines. In this case, all experimental conditions and procedure will be followed as described above.

## 3 Results

In the present study, we attempted to simultaneous overexpress *Arabidopsis* sulfurtransferases (*AtStr5* and *AtStr17a*) that have a potential role as arsenate reductases (*AtACR2* and *HAC1/ATQ1*), and phytochelatin synthase (*AtPCS1*) genes, that enhances PCs-[As (III)] complex formation followed by As-reduction then the As detoxification process is completed.

### 3.1 DNA cloning technique

The full-length coding region of *AtStr5/AtACR2*, *AtStr17a/HAC1/ATQ1* and *AtPCS1* addition with restriction enzyme recognition sites for *KpnI* and *SalI* were amplified by RT-PCR from cDNA of *Arabidopsis* Col-0 ecotype. The quality of RNA preparation was assessed by denaturing agarose gel prior cDNA synthesis. The denaturing gel system is necessary because as most RNA forms an extensive secondary structure by intramolecular base pairing which interrupts the migration of RNA in the gel according to its size. The intact RNA was reverse transcribed into cDNA by the reverse enzyme transcriptase which was used as a template for amplification of each gene. The correct amplified fragment was analyzed on a 1% agarose gels (**Figure 1A**). On NCBI data record, for

*AtStr17a/HAC1/ATQ1* gene two-gene product were observed one encode a 140 amino acid and other 169 amino acid protein, they might be the result of alternative splicing of gene expression. To investigate whether their encoded proteins shows different functions, here we included both sequences of this gene for cloning. After amplification, the complete target gene was cloned into an intermediate vector either pGEM®-T or pJET1.2/blunt vector (**Figure 1B**). Both are linearized vectors and very efficient for cloning. The property of pGEM®-T is that it carries T7 and SP6 promoter sequences in reverse direction on opposite strands, so that insertion strand direction does not limit the cloning. Presence of universal promoter sequences helps to sequence the inserted gene using primers designed complementary to these promoters. Cloning of an insert into the pGEM®-T vector interrupts the coding sequence of  $\beta$ -galactosidase. Thus the recombinant clones could be identified by blue-white screening on indicator plates. The pJET1.2/blunt vector was used, when the insert was amplified with Pfu polymerase, which creates blunt-end PCR products.

The pJET1.2/blunt vector carries the lethal gene (*eco47IR*) which is dysfunctional by ligation of a DNA insert into the cloning site. The vector carries the T7 promoter for *in vitro* transcription of the cloned insert and  $\beta$ -lactamase [*bla* (*ApR*)] gene that conferring ampicillin resistance. Therefore, cells with recombinant plasmid able to grow in ampicillin media. The *AtStr17a/HAC1/ATQ1* (510 bp) and *AtPCS1* (1458 bp) were amplified by Pfu polymerase enzymes. On the other hand, *AtStr17a/HAC1/ATQ1* (423 bp) and *AtStr5/AtACR2* (399 bp) were amplified by Green Taq polymerase enzymes. Finally, we produced four intermediate recombinant vectors; pGEM®-T-*AtStr5/AtACR2* (399 bp), pGEM®-T-*AtStr17a/HAC1/ATQ1* (423 bp), pJET1.2/blunt-*AtStr17a/HAC1/ATQ1* (510 bp) and pJET1.2/blunt-*AtPCS1* (1458 bp). The success of cloning was analyzed by digesting each recombinant vector with *KpnI* and *SalI* enzymes (**Figure 1, C-F**).





Further sequence confirmation was carried out by GATC Biotech Company, Germany. The results of the sequencing were analyzed by the Blast program of NCBI, which confirmed the presence of target gene in the respective recombinant pGEM®-T and pJET1.2/blunt vectors. After sequence confirmation, each recombinant vector of; pGEM®-T-*AtStr5/AtACR2* (399 bp), pGEM®-T-*AtStr17a/HAC1/ATQ1* (423 bp), pJET1.2-*AtStr17a/HAC1/ATQ1* (510 bp), and pJET1.2-*AtPCS1* (1458 bp) was digested with the *KpnI* and *SalI* enzymes. Likewise, the plant expression vectors pBinAR, and pBin-Hyg-TX were also digested with the same restriction enzymes for unwinding the vector at the target sites. Each digested product from vector and insert was used for ligation. Since, the plant expression vectors; pBinAR and pBin-Hyg-TX, both contain the *NPTII* gene for bacterial selection. Therefore, kanamycin (100 µg ml<sup>-1</sup>) was used in the LB plate for colony selection. After kanamycin selection, the success of ligation was reconfirmed by amplifying the corresponding target gene by their corresponding primer pairs [Figure 2 (A-D)]. Finally, two recombinant pBinAR constructs, pBinAR-*AtStr5/AtACR2* and pBinAR-*AtStr17a/HAC1/ATQ1* and one pBin-Hyg-TX-*AtPCS1* were produced [Figure 3 (A-C)]. Subsequently, the competent cells of *A. tumefaciens* strain GV3101 were used for transformation of those recombinant expression vectors for plant transformation. Transformation with GV3101 was confirmed by colony PCR using a gene-specific primer. The empty pBin-Hyg-TX vector was transformed into GV3101 to be used as a control for the As experiment. The success of cloning of the empty vector was verified by amplification of a *NPTII* gene (Figure 2E). The strain GV3101 is widely used for plant transformation process, and it has proven more productive for *Arabidopsis* transformation (Bechtold et al. 1993; Katavic et al. 1994).

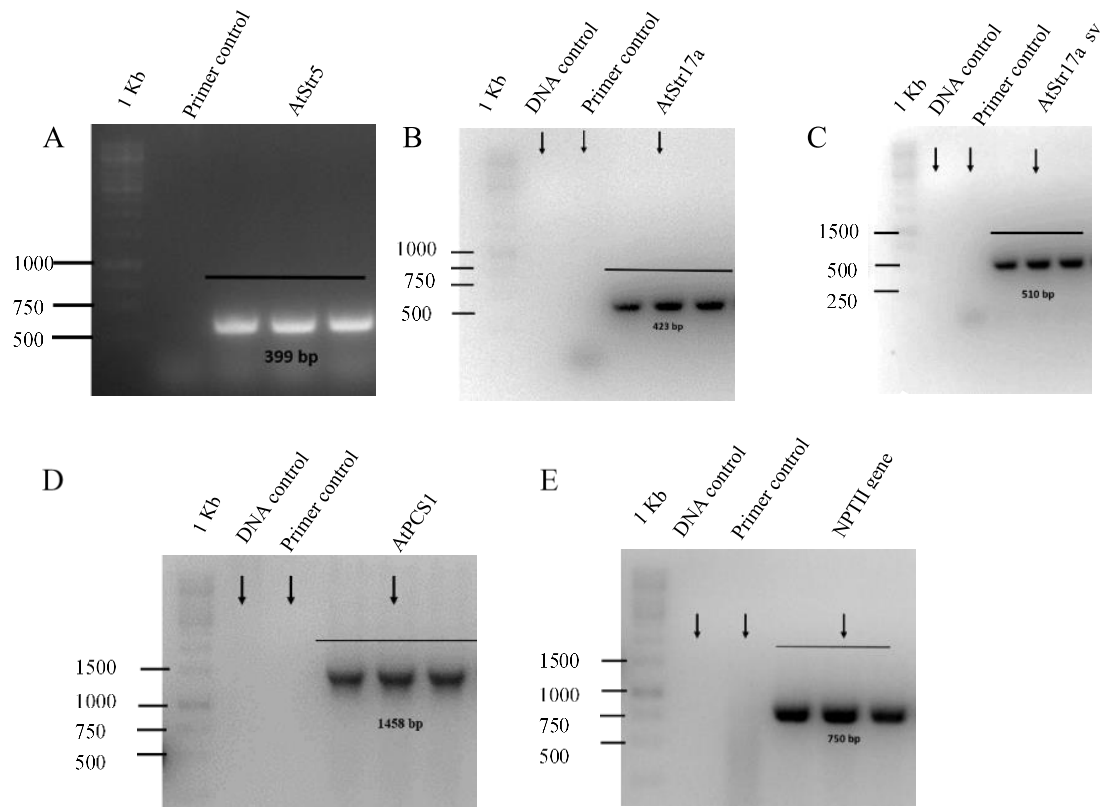


**Figure 2.** Positive clones confirmation for the constructs; pBinAR-*AtStr5*, pBinAR-*AtStr17a/HAC1/ATQ1-sv*, pBinAR-*AtStr17a/HAC1/ATQ1*, pBin-Hyg-TX-*AtPCS1* and pBin-Hyg-TX (empty vector) by colony PCR using insert-specific primers. Each amplified product was analyzed on 1% agarose gels. The result showed that each gene was correctly amplified according to their size, referring successful integration of each target gene into the plant-expression vectors; (A) ~399 bp of *AtStr5*, (P968A/P969A) (B) ~ 423 bp of *AtStr17a/HAC1/ATQ1*, (P970/P971) (C) ~ 510 bp of *AtStr17a/HAC1/ATQ1-sv*, (P91011/P971) and (D) ~1458 bp of *AtPCS1*, (P972/P973) and (E) ~750 bp of *NPTII* for empty vector (P387/P388). The first two lanes of each gel contain the control reactions; 1<sup>st</sup> lane: DNA without primer and 2<sup>nd</sup> lane: primer without DNA, to avoid the false positive results in PCR.

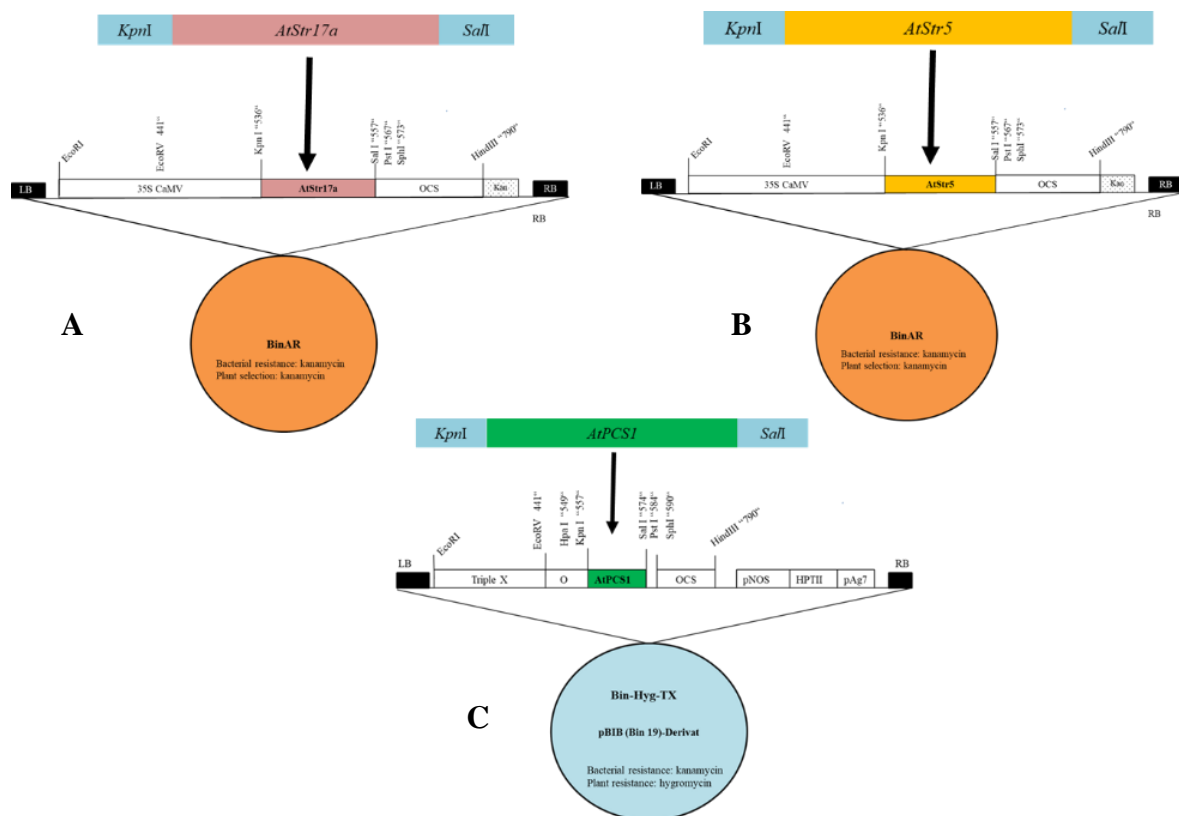


**Figure 3.** T-DNA map of the recombinant vectors pBinAR and pBin-Hyg-TX. The colored region between the restriction enzymes *KpnI* and *SalI* referring the insert integration site in the T-DNA region. (A) T-DNA integration of the *AtStr5/AtACR2* gene into the pBinAR vector (B) T-DNA integration of the *AtStr17a/HAC1/ATQ1* gene into the pBinAR vector and (C) Integration of *AtPCS1* gene into the T-DNA of pBin-Hyg-TX vectors.

### 3.2 Plant transformation and selection

The transformation method is based on the floral dip transformation of *Arabidopsis* as described by (Clough and Bent 1998). This method is simple and does not require any tissue culture technique to produce stable transformed *Arabidopsis*. In some cases, 8-12 weeks is enough to generate stable *Arabidopsis* seeds. Briefly, when the secondary inflorescence of *Arabidopsis* (Col-0) plant was about 1-10 cm, they were treated with *A. tumefaciens* GV3101 strain that carrying the gene of interest on the binary vector pBinAR and pBin-Hyg-TX. The T-DNA of these vectors contain *NPTII* and *HPTII* genes that confer resistance to kanamycin and hygromycin B respectively. After 3-5 weeks of post inoculation, when all the silique were brown and dry, then T1 seeds were harvested in bulk and subjected to screening based on kanamycin and hygromycin B resistance depending on the marker gene present in the T-DNA region of the putative T1 primary transformants. Plants inoculated with the binary construct pBinAR-*AtStr5/AtACR2* and pBinAR-

*AtStr17a/HAC1/ATQ1* were screened on MS media with 50  $\mu\text{g ml}^{-1}$  kanamycin [Figure 4 A (i)] since the T-DNA region of pBinAR contains *NPTII* gene as a selection marker. On the other hand, plants inoculated with pBin-Hyg-TX-*AtPCS1* and pBin-Hyg-TX-empty constructs were screened on MS media with 30  $\mu\text{g ml}^{-1}$  hygromycin B [Figure 4 A (ii)], since the T-DNA of pBin-Hyg-TX vector contain *HPTII* gene as a plant selection marker. The presence of the marker gene on the transgenic plants were further confirmed by PCR to avoid any pseudo-transgenic (known as an escape) plant that could arise during marker-based selection. The T1 transformed plants of pBinAR-*AtStr5/AtACR2* and pBinAR-*AtStr17a/HAC1/ATQ1* were confirmed by the presence of *NPTII* gene (Figure 4B). The T1 transformed plants of pBin-Hyg-TX-*AtPCS1* and pBin-Hyg-TX (empty vector) transformed plants were established by the presence of *HPTII* gene (Figure 4C). The total antibiotic resistance plants for each construct and from those the number of plants that showed PCR positive were listed in Table 4. We obtained 25 kanamycin resistance plants for the construct pBinAR-*AtStr5/AtACR2*, among them 13 plants were displayed in PCR positive. A large number of variation between kanamycin selection and PCR method could arise due to the use of old kanamycin stock solution because in a subsequent experiment freshly made stock solution did not shows such a variation. Similarly, 8 plants were found PCR positive out of 10 kanamycin resistant plants for the construct pBinAR-*AtStr17a/HAC1/ATQ1* (423 bp). While using pBinAR-*AtStr17a/HAC1/ATQ1* (510 bp) construct, 15 plants were shown in PCR positive out of 18 kanamycin resistance plants. On the other hand, 18 plants were found PCR positive out of 18 hygromycin B resistance for the construct pBin-Hyg-TX-*AtPCS1*. Likewise, 13 plants were found PCR positive out of 13 hygromycin B resistance for the construct pBin-Hyg-TX (empty vector).

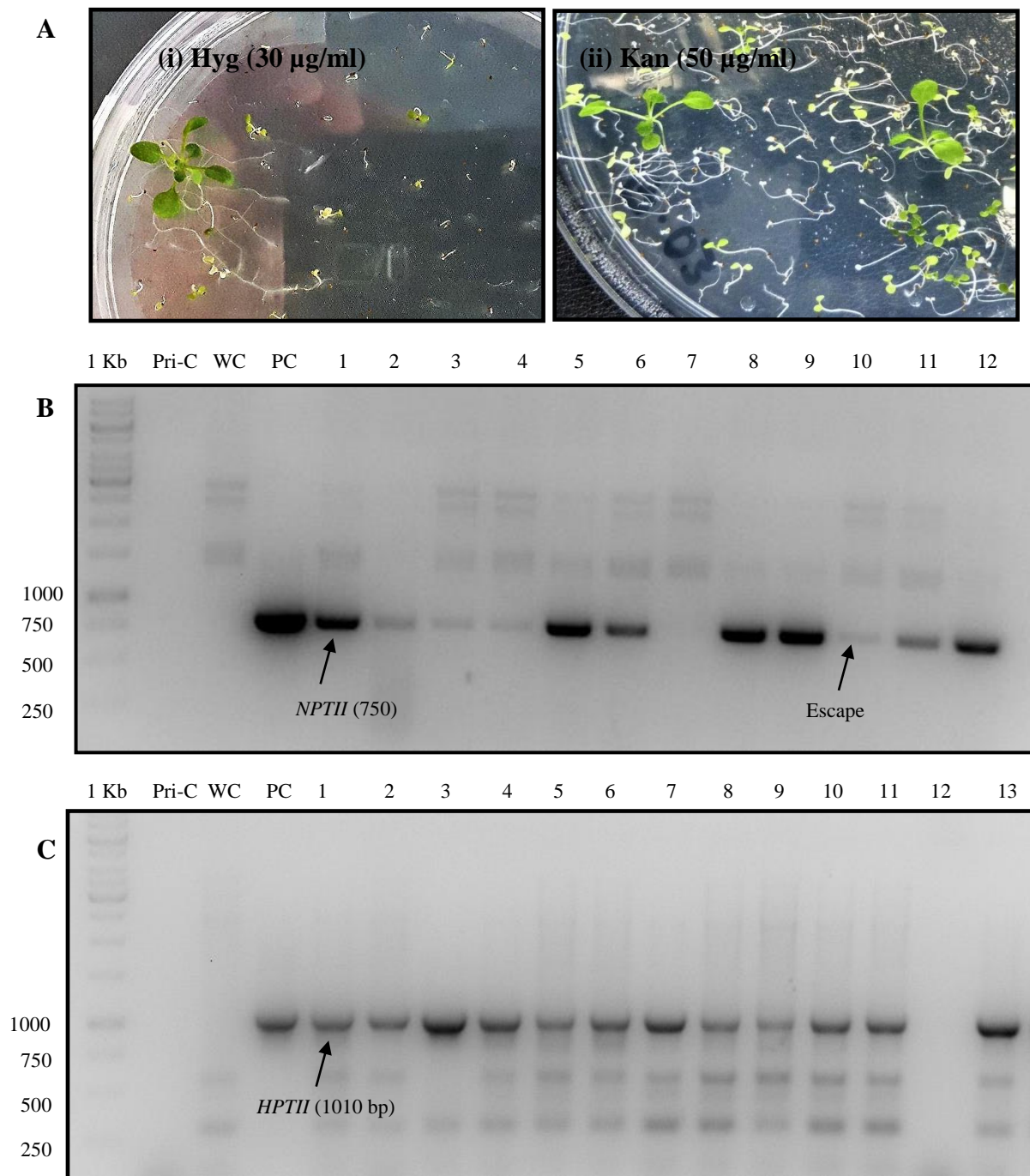


**Figure 4.** T1 seedling of *A. thaliana* Col-0, T1 seed obtains from plants subjected to floral dip transformations using the *A. tumefaciens* strain GV 3101 harboring the plasmid pBinAR-*AtStr5* and pBin-Hyg-TX-*AtPCS1*. T1 seed was distributed on the MS medium contain [A(i)] 50 µg ml<sup>-1</sup> kanamycin [A(ii)] 30 µg ml<sup>-1</sup> hygromycin-B. After stratification period (2 days at 4°C in the dark) the seedling was transferred in the climate chamber as described in the report. The [A(i)] kanamycin and [A(ii)] hygromycin resistance seedling appeared dark green, healthier while sensibly seedling appeared pale yellow, thinner and some seeds were not germinated entirely. The resistance seedling was reconfirmed by PCR; the presence of (B) *NPTII* (750 bp) and (C) *HPTII* (1010 bp) gene in the transgenic plants, confirmed the integration of a target gene. The lane Pri-con, primer control; WC, wild-type control; PC, plasmid control; P, plant.

### 3.3 Southern blot analysis

The number of T-DNA integrated into the genome of transformed plants were investigated by Southern analysis (Southern 1975). Studying the T-DNA copy number in the transgenic plant is very important because of the insertion of T- DNA occurred in randomly to the plant genome, and the transgenic loci tend to carry multiple copies. The integration of multiple copies can change their interaction with the host genome in a specific region that might arises truncation inversion, deletion, and other chromosomal rearrangements (Tinland 1996; Tzfira et al. 2004).

To investigate the T-DNA insertion pattern and copy number, genomic DNA was isolated from T1 progenies of each transformant (containing different gene) and digested with the restriction enzymes. The restriction enzymes were chosen after analysis the genomic transcript of each target gene in Clone manager professional nine program. The restriction enzyme that was not found in the target gene sequence was selected for digestion. During selection of the enzymes the emphasis was given whether they reside near the T-DNA region but apparently not within the target sequence. The list of the restriction enzymes chosen for T1 transformants of each gene, corresponding DIG label hybridization probe, their source, size, primers, and their annealing temperature is mentioned in the materials and methods section (**Table 2 & 3**). The gene-specific probe labeled with DIG was used for hybridization. Since they are overexpressing transformants, T1 transformants were screened for additional copies in comparison to wild-type plants. Four different transgenic lines were produced; each contains different target gene. The number of T1 overexpressing transformants per construct subjected to Southern analysis and their corresponding copy number was summarized in **Table 4**. Analysis of T1 transformants for each construct reveals that most of the transformants contain multiple copies of the gene and its hold the same result for all four-different construct where each contains different gene (**Figure 5 & Figure 6**). The integration of multiple inserts during transformation was found in many different studies (Glowacka et al. 2016; Jorgensen et al. 1987; Katavic et al. 1994). Though segregation analysis, is another mean to obtained homozygous line, it could not provide a reliable picture if multi-copy are inserted in the same locus or otherwise linked, more importantly, this event could lead gene silencing (Jorgensen et al. 1987). In fact, multi-copy bearing T1 plants were rejected entirely in this study. Therefore, the Southern analysis is very significant before starting homozygous line selection which can save ample amount of time.

Though the technique is laborious compared to many new technologies, it is still considered the benchmark for the precision in determining T-DNA copy number. Several southern blotting was carried out to analyzed all the T1 transformed plants obtained from each overexpressing gene; *AtStr5/AtACR2*, *AtStr17a/HAC1/ATQ1*, *AtPCSI*, and *HPTII*. However, here we have demonstrated single southern blotting picture for each overexpressing gene especially that one contains single integration of target gene. Three T1 transformants of *AtPCSI<sup>oe</sup>* (plant number 5, 8 & 9) were shown single integration out of 18 *AtPCSI<sup>oe</sup>* plants (**Figure 5A**). Analysis of 15 T1 transformants of *AtStr17a/HAC1/ATQ1<sup>oe</sup>* (510 bp) in a Southern blot, only one plant (number 16) has contained single copy insertion (**Figure 5B**). In case of T1 transformant of *AtStr17a/HAC1/ATQ1<sup>oe</sup>* (423 bp), all have carried multiple copies, and they were rejected entirely for further homozygous study (Figure not shown). Two T1 transformants (number 8 & 9) out of 13 T1 transformants of *HPTII<sup>oe</sup>* have displayed a single copy insertion (**Figure 6A**). The plant number 4, contained single insertion out of 13 T1 transformants of *AtStr5/AtACR2<sup>oe</sup>* (**Figure 6B**). Single T1 transformant (single integration) of each overexpressing gene have been selected for homozygosity study. Segregation analysis of these overexpressing line has shown inherited by Mendelian fashion 3:1 ratio (data not shown).

The single copy bearing T1 plants were considered to grow next generation for homozygosity study to produce stable overexpressed lines. Because T1 plant carrying single T-DNA locus can easily progress to a fully homozygous generation.

**Table 4.** The number of T1-overexpressing transformants per construct that were selected based on antibiotic and PCR method and the number of plants that contain single T-DNA integration sites were included in the table below.

	Recombinant construct				
	pBinAR- <i>AtStr5/AtACR2</i>	pBinAR- <i>AtStr17a/HAC1/ATQ1- sv</i> (423 bp)	pBinAR- <i>AtStr17a/HAC1/ATQ1</i> (510 bp)	pBin-Hyg-TX- <i>AtPCS1</i>	pBin-Hyg-TX
Number of plants resistant to kanamycin (50 $\mu\text{g ml}^{-1}$ )	25	10	18		
Number of plants positive in PCR among kanamycin resistance	13		15	19	
Number of plants resistant to hygromycin (30 $\mu\text{g ml}^{-1}$ )				19	13
Number of plants positive in PCR among hygromycin resistance					13
Number of plants that contain a single insertion of the target gene	1	x	1	3	2



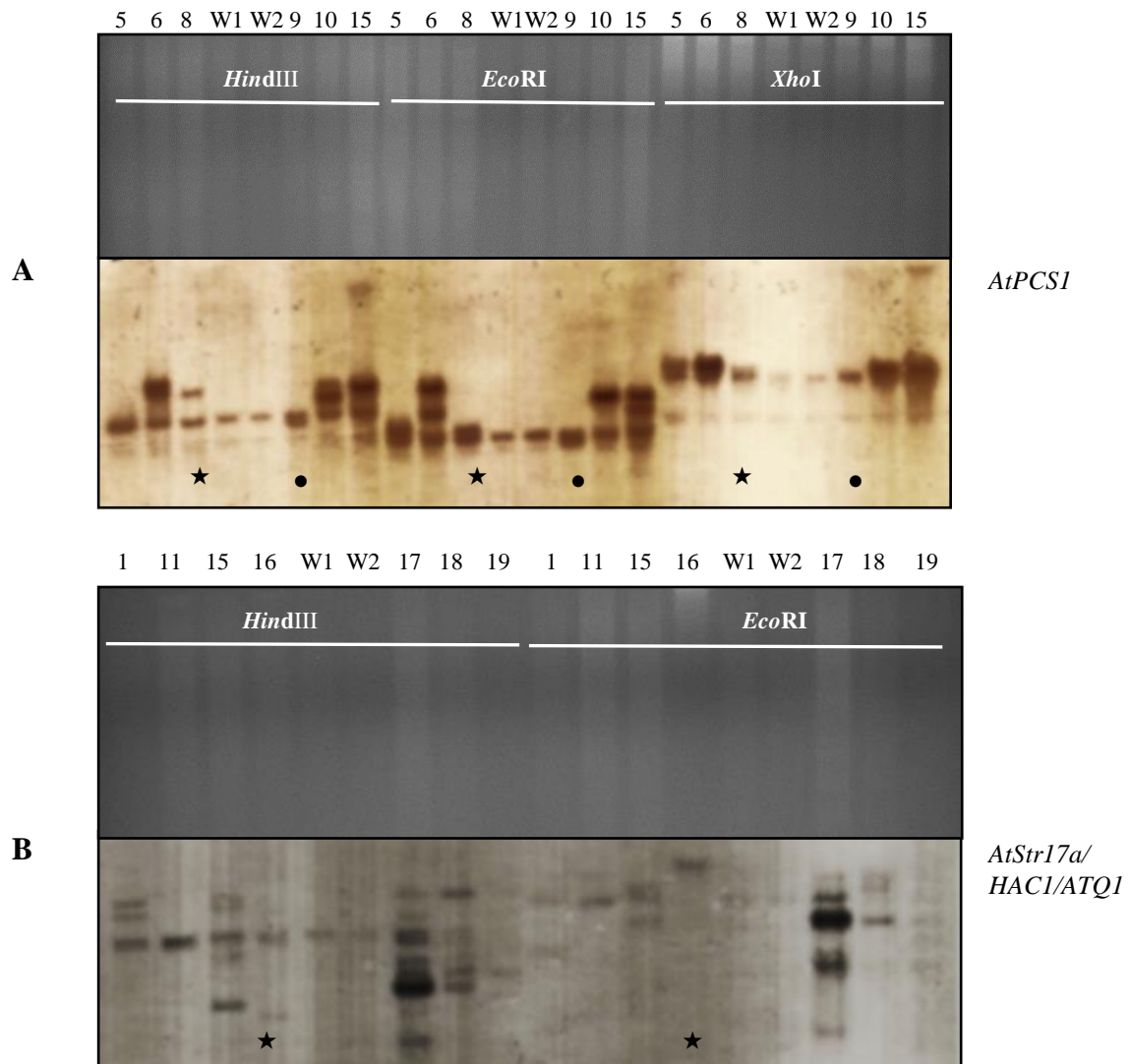


**Figure 5.** Southern blot analysis of T1 overexpressing transformants of *AtPCSI* and *AtStr17a/HAC1/ATQ1*. Genomic DNA of each overexpressing and wild-type plants was extracted, and 20  $\mu$ g was digested and subjected to Southern blot analysis using a digoxigenin-labeled probe against gene-specific sequence. **(A)** The T1 overexpressing transformant of *AtPCSI* was digested with the restriction enzymes *HindIII*, *EcoRI* & *XhoI* and two plants (number 8 & 9) out of six were contained single T-DNA integration concerning the wild-type. **(B)** Seven T1 overexpressing transformants of *AtStr17a/HAC1/ATQ1* (510 bp) were digested with *EcoRI* & *HindIII*, from them the plant number 16 has shown single insertion of a gene concerning the wild-type. The different number in each lane indicates the particular plant number and W indicates wild-type.

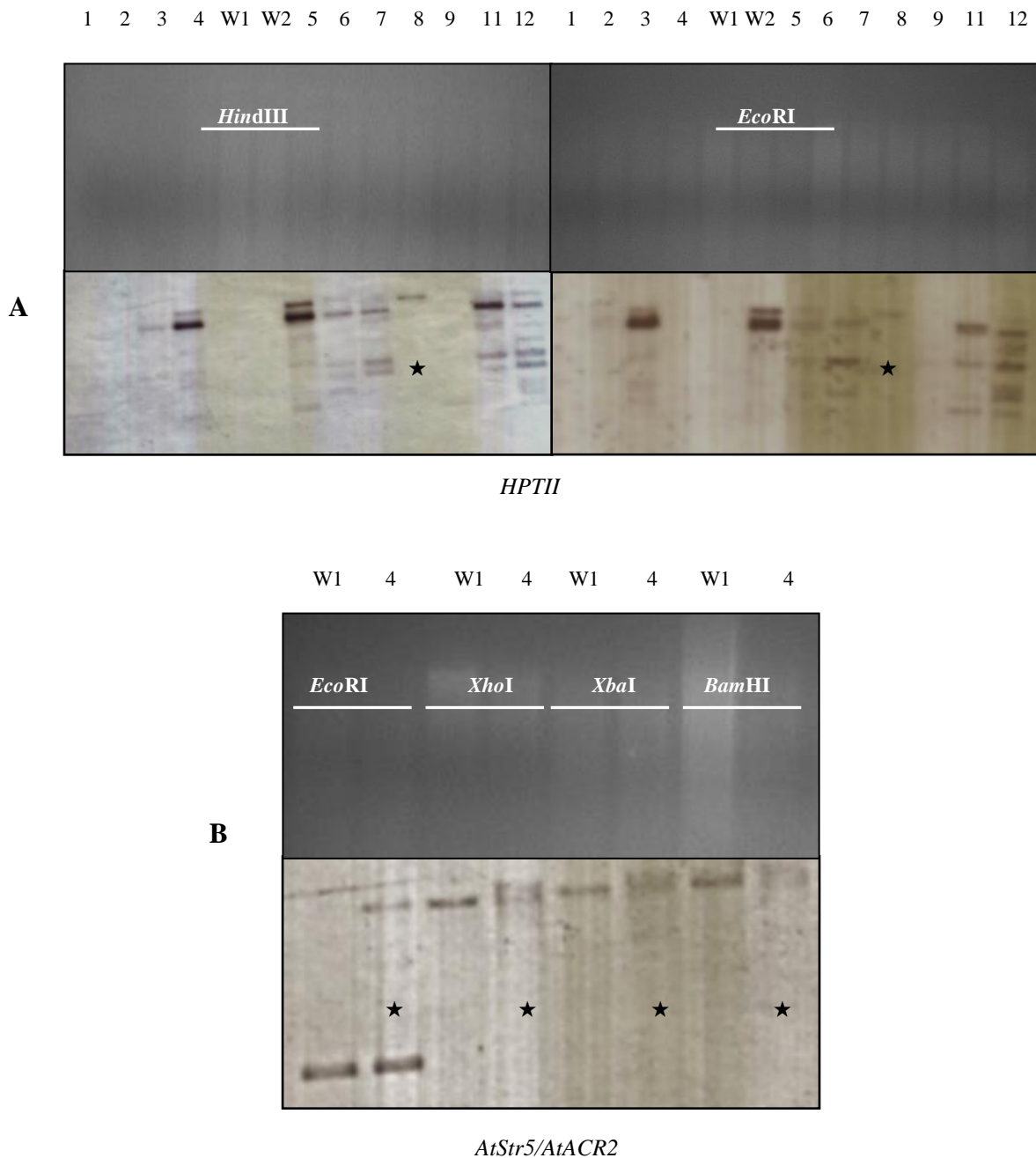


**Figure 6.** Southern analysis of T1 overexpressing transformants of the empty vectors (pBin-Hyg-TX) and *AtStr5/AtACR2*. Genomic DNA of each overexpressing and wild-type plants was isolated, and 20 µg was digested and subjected to Southern blot analysis using a digoxigenin-labeled probe against gene-specific sequence. **(A)** Twelve T1 transformants of the empty vectors (pBin-Hyg-TX) was digested with the restriction enzymes *EcoRI* & *HindIII* and hybridization with the DIG labelled-*HPTII* probe, the plant 8 and 9 were carried the single T-DNA insertion in respect to the wild-type where no *HPTII* gene was expected. **(B)** An overexpressing T1 transformant of *AtStr5/AtACR2* (plant number 4) was digested with the restriction enzymes *EcoRI*, *XbaI*, *XhoI* and *BamHI* and result of each digestion appeared one single copy insertion concerning the wild-type though the pattern of digestion was different. The different number in each lane indicate the particular plant number and W indicates wild-type.

### 3.4 Gene expression analysis by Genevestigator program

To study the gene expression of each overexpressing line, in a first attempt their wild-type expression profile was analyzed by Genevestigator program. The expression of *AtStr5/AtACR2*, *AtStr17a/HAC1/ATQ1*, and *AtPCSI* was analyzed by developmental and anatomy tool of the Genevestigator program. The developmental tool under this program considered 10 different developmental stage of the life cycle of *Arabidopsis* like the germinated seed, seedling, young rosetta, developed rosetta, bolting, young flower, developed flower, flowers, and siliques mature siliques and senescence. The Y-axis in the graph indicates the expression levels (low, medium and high) against the developmental stage in X-axis showing a positive signal of *AtStr5/AtACR2* or *AtStr17a/HAC1/ATQ1* expression in particular developmental stage. The developmental tool showed a constitutive-higher level expression of *AtStr5/AtACR2* in the different developmental stage. A further closer investigation has demonstrated that the expression was bit increase in rosetta leaves stage among all 10 developmental stage (**Figure 7**). On the other hand, *AtStr17a/HAC1/ATQ1* have exhibited higher expression in seedling stage followed by germination. After that, the expression was drastically declined in the rest of the developmental stage. The *AtPCSI* gene has shown higher expression in the vegetative to flowering stage. After flowering stage, the expression was gradually decreased and it was drastically declined in the leaf senescence stage. The expression of *AtStr5/AtACR2*, *AtStr17a/HAC1/ATQ1*, and *AtPCSI* were analyzed by the anatomy tool of Genevestigator. The anatomy tool displays how strongly a gene is expressed in different anatomical categories, including tissues and cell cultures. Investigating the expression of *AtStr5/AtACR2*, *AtStr17a/HAC1/ATQ1* and *AtPCSI* by anatomy tool revealed that *AtStr5/AtACR2* was highly expressed in phloem cell followed by abscission zone, shoot phloem companion cell and sperm cell and *AtStr17a/HAC1/ATQ1* is highly expressed in primary root cell followed by radical and lateral root. The *AtPCSI* was highly expressed lateral root cap protoplast followed by shoot phloem companion cell (**Figure 8**).

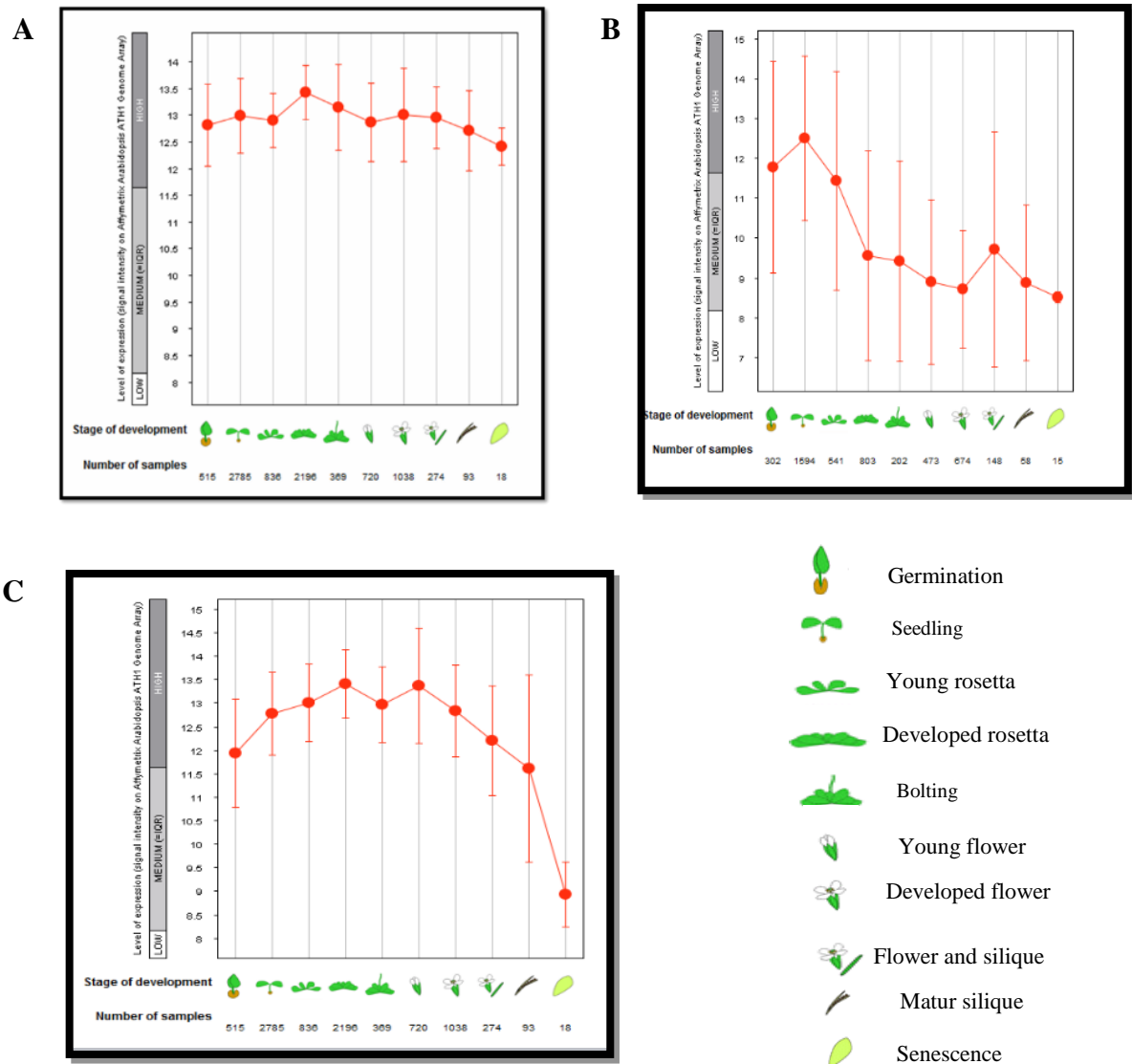


**Figure 7.** Expression profile of *AtStr5*, *AtStr17a/HAC1/ATQ1* and *AtPCS1* in different developmental stages of *Arabidopsis* (Genevestigator tool). **(A)** The *AtStr5* showed a higher level of expression in all developmental stages over the life cycle, On the other hand, **(B)** the *AtStr17a/HAC1/ATQ1* showed the highest expression in seedling stage followed by seed germination. **(C)** The *AtPCS1* showed a higher level of expression until flowering after that the expression was gradually reduced and drastically declined at the leaf senescence stage.

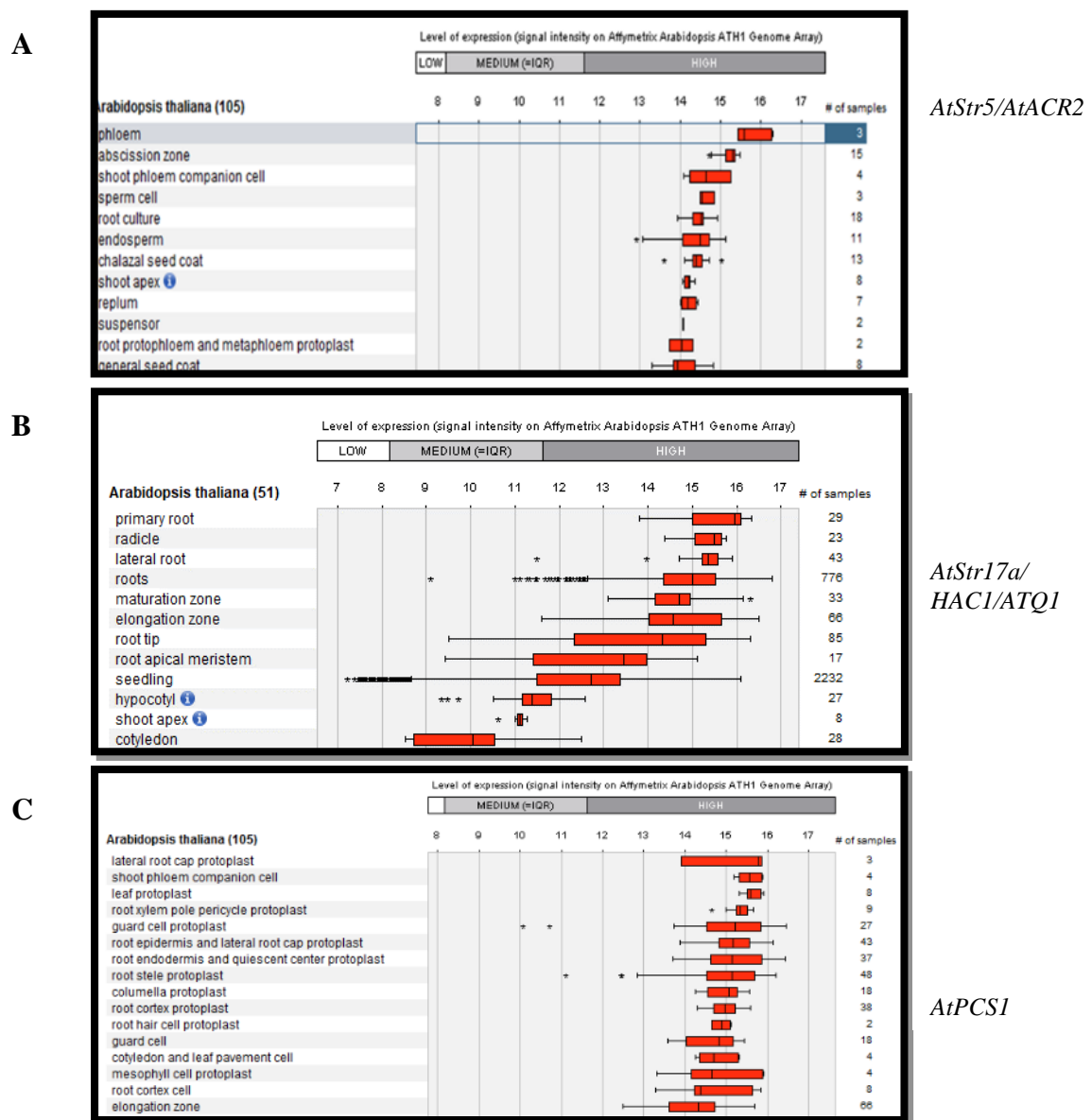


**Figure 8.** The expression profile of *AtStr5/AtACR2*, *AtStr17a/HAC1/ATQ1* and *AtPCSI* in different anatomical part of Arabidopsis (Genevestigator tool). (A) The *AtStr5* has shown highest expression in phloem tissues followed by an abscission zone (B) The *AtStr17a/HAC1/ATQ1* has displayed highest expression in root cell followed by radical and lateral root. (C) The *AtPCSI* has exhibited highest expression in lateral root cap of protoplast followed by shoot phloem companion cell.

### 3.5 Northern analysis of the T2 overexpressing lines

The putative overexpressing mutant lines of *AtStr5/AtACR2<sup>oe</sup>*, *AtStr17a/HAC1/ATQ1<sup>oe</sup>*, and *AtPCSI<sup>oe</sup>* including empty vector (pBin-Hyg<sup>oe</sup>-TX) and respective wild-type (Col-0) plant were included for Northern blot analysis. The wild-type gene expression pattern of each studied gene was investigated under the developmental and anatomical tools of the Geneinvestigator program. Based on the information where the gene is abundantly present, the plant material was collected for RNA isolation. The expression of T2 overexpressing lines of *AtStr5/AtACR2*, *AtPCSI*, and *HPTII* gene were checked by Northern blot analysis. We found overexpression of two mutant lines, *AtStr5/AtACR2<sup>oe</sup>* and pBin-Hyg<sup>oe</sup>-TX (empty vector) compared to the wild-type plants (**Figure 9**). However, *AtPCSI* gene was found to be silenced (co-suppressed with the endogenous gene) instead of overexpression. On the other hand, the expression of *AtStr17a/HAC1/ATQ1* gene in the putative *AtStr17a/HAC1/ATQ1<sup>oe</sup>* lines still need to be checked. The *AtStr17a/HAC1/ATQ1* gene is expressed in the root region (Chao et al. 2014), and currently we do not have sufficient root material for RNA isolation. The attempt to study the expression of *AtStr17a/HAC1/ATQ1* gene from leaf material was unsuccessful.

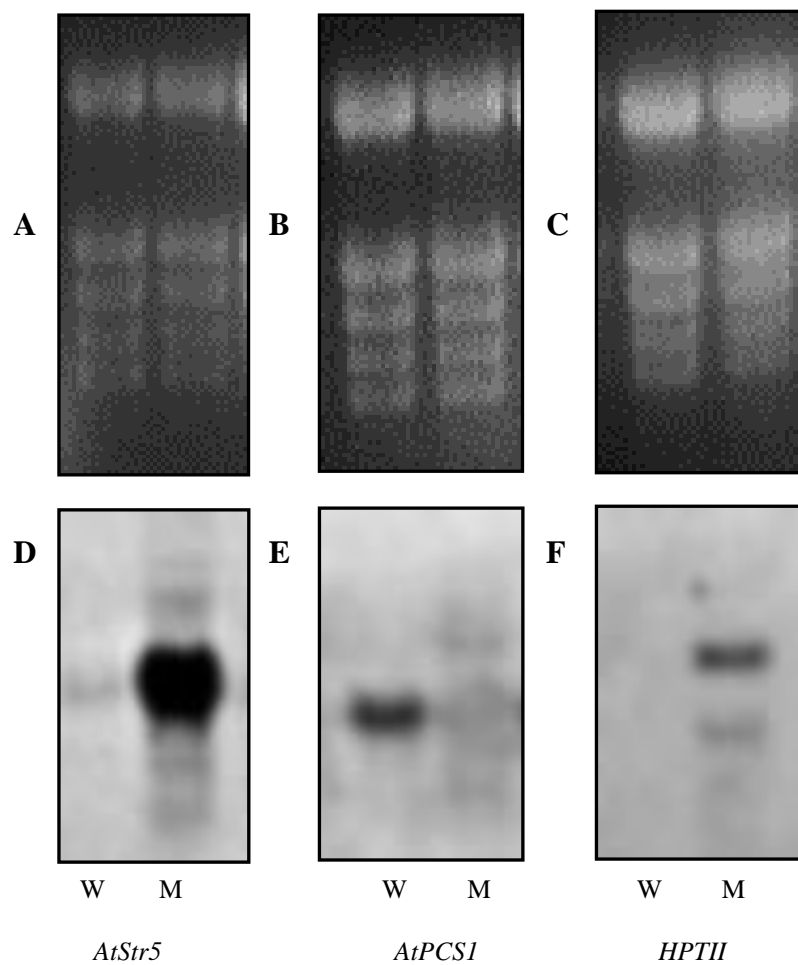


**Figure 9.** Northern blot analysis of wild-type (W) and putative overexpressing mutant (M) of *AtStr5/AtACR2*, *AtPCS1* and *HPTII* (empty vector) genes. Plants were grown in soil in the climate chamber. Total RNA was extracted from leaves, and 10  $\mu$ g RNA was loaded in each lane and blotted. To ensuring equal loading of the extracted RNA, ethidium bromide-stained gels were presented in; (A) *AtStr5/AtACR2* (B) *AtPCS1* (C) *HPTII*, and results for Northern blot hybridization with (D) *AtStr5/AtACR2* (E) *AtPCS1* and (F) *HPTII* probes were shown below of each corresponding EtBr-stained gel.

## 4 Discussion

The ultimate goal of this experiment was to improve the As phytoremediation system, and therefore, it's crucial to expand the knowledge about the mechanism of As detoxification process in plants. As a first step towards this goal, we made an effort to develop the overexpressing mutant lines of *AtStr5/AtACR2*, *AtStr17a/HAC1/ATQ1*, and *AtPCSI* genes, which are thought to be involved in the As detoxification process. We also intended to develop the co-overexpressing mutant lines of *AtStr5/AtACR2-AtPCSI* and *AtStr17a/HAC1/ATQ1-AtPCSI*.

To achieve the overexpression of each target gene, they were cloned into the plant expression vector (either pBinAR or pBin-Hyg-TX) which contains 35S promoter of cauliflower mosaic virus (CaMV) which drives the constitutive expression of chimeric genes. The AR genes *AtStr5/AtACR2* and *AtStr17a/HAC1/ATQ1* were cloned in the plant expression vector pBinAR (Höfgen and Willmitzer 1990) that contains a 35S promoter and Octopine synthase gene (*OCS*) as a terminator and neomycin phosphotransferase II (*NPTII*) gene that confers kanamycin resistance for both bacterial and plant selection. Likewise, *AtPCSI* was cloned into the pBin-Hyg-TX (Bin19 derivative: pBIB) (Becker 1990) vector which carried 35S promoter with triple time enhancer and *OCS* as a terminator. This vector contains *NPTII* gene for bacterial selection and hygromycin phosphotransferase II gene (*HPTII*) for plant selection. Both vectors were efficiently used for tobacco transformation (by the member of our previous working group), so overexpression of our target gene might not be a problem. The strain GV3101 of *A. tumefaciens* were used for transformation of recombinant expression vectors that contains target gene, and this strain is widely used for plant transformation process, and it has proven more productive for *Arabidopsis* transformation (Bechtold et al. 1993; Katavic et al. 1994).

After successful cloning, each cloned was used for floral dip transformation of *Arabidopsis*. The T1 primary transformants were selected based on an antibiotic (kanamycin and hygromycin) and PCR analysis. After that, the T1 primary transformants were taken for Southern blot analysis to establish the copy number and integration patterns of the T-DNAs inserted into the genome of the primary transgenic plants. Proper interpretation of Southern blots proved difficult due to the high copy number and complexity of the T-DNA integration patterns. We have observed that most of the T1



primary transformants contain multiple copies and complex arrangement of each target gene (in result part figure 5 and 6).

Additionally, it was noticeable that T1 transforms originated even from the same construct has shown different T-DNA integration pattern indicating that T-DNA integration occurred independently in more than one target cell in the *Agrobacterium* inoculated T0 plant. The complex T-DNA integration pattern was observed for all transformants of four different constructs in this study. The most likely explanation for this phenomenon is that multiple germline cells were independently transformed in these plants.

The integration of multiple inserts during transformation arose in many different studies (Glowacka et al. 2016; Jorgensen et al. 1987; Katavic et al. 1994). Therefore, it is important to remove those plants that contain multiple copies, before starting the homozygous line selection through segregation. Because segregation analysis could provide the information about the integration of functional insert, however number of physical insert incorporated those lines cannot be detected. The problem would be more complicated if multiple copies are inserted in the same locus or otherwise linked, more importantly, this event could lead gene silencing (Jorgensen et al. 1987). In a study where five transformants were selected as single copy insertion, based on segregation analysis, however, analysis of those transformants by Southern blot revealed only one has a functional insert (Katavic et al. 1994). In a similar case, the literature suggests numerous factors in the gene expression variation, such as the multiple inserts closely linked genetically or numerous unlinked T-DNAs most of which are inactive due to the DNA arrangement (tandem repeat or inverted repeat) or their insertion in the heterochromatic region of the chromosome.

Hence, multiple copies bearing T1 plants were rejected entirely in this study. Therefore, the Southern analysis is very significant before initiating the homozygous line selection which can save an ample amount of time. Though the technique is laborious compared to many new methods, it is still considered the benchmark for the precision in determining T-DNA copy number. We have achieved very few numbers of transformants for each construct that have single copy insertion (signed by an asterisk in the result part) and taken for subsequent study. Unfortunately, all the transformants from pBinAR-*AtStr17a/HAC1/ATQ1-sv* (423 bp) constructs have shown multiple insertions, and these plants were excluded from the homozygosity study. The single copy bearing T1 plants

were considered to grow the next generation for homozygosity study to produce stable overexpressing *Arabidopsis* lines.

Because T1 plant bearing single T-DNA locus can easily progress to a fully homozygous generation. Single copy bearing transformants were verified by genetic analysis and found they are inherited by Mendelian fashion 3:1 ratio (data not included).

The single copy bearing T2 overexpressing transformant of the gene *AtStr5/AtACR2*, *AtStr17a* and *AtPCSI* and empty vector (pBin-Hyg-TX) were taken for Northern blot analysis to visualize their gene expression pattern and the result was compared with the wild-type gene expression pattern. The excellent quality intact RNA is a prerequisite for Northern blot analysis. Additionally, the source of RNA is an essential factor that has to be considered before beginning the Northern blot analysis. The expression profile of each gene was checked under the Genevestigator program and also reviewed the related literature to isolate RNAs from appropriate plant tissue. The Genevestigator program has given the general impression about the target gene by considering the global information of that particular gene. The expression of *AtStr5/AtACR2*, *AtStr17a/HAC1/ATQ1*, and *AtPCSI* was analyzed by developmental and anatomical tools of the Genevestigator program. The developmental tool under this program considered 10 different developmental stage of the life cycle of *Arabidopsis* like the germinated seed, seedling, young rosetta, developed rosetta, bolting, young flower, developed flower, flowers, and siliques mature siliques and senescence. The anatomy tool reveals the specific tissue where the target gene is highly expressed. The Genevestigator program has given the impression that *AtStr5/AtACR2* is highly expressed in all over the life cycle of *Arabidopsis* and phloem tissue the *AtStr17a/HAC1/ATQ1* is highly expressed in the seedling stage in the root part. On the other hand, *AtPCSI* is expressed in all developmental stages except the leaf senescence stage. The plant material was collected for RNA isolation considering the gene expression profile.

Northern blotting was used to visualize the expression of *AtStr5/AtACR2*, *AtStr17a/HAC1/ATQ1*, and *AtPCSI* genes. We had experienced that after Northern blot the NBT/BCIP detection technique was not able to visualize the expression of *AtStr5*, *AtStr17a/HAC1/ATQ1*, and *AtPCSI*. However, the CDP-Star detection system can detect the expression of that gene.

The Northern blot result revealed that the *AtStr5/AtACR2<sup>oe</sup>* line showed an increase fold of expression than the wild-type plants. On the other hand, the *AtPCS1* gene was found to be silenced instead of overexpression; both wild-type and the endogenous gene were remained silenced. This gene silencing could arise for several reasons. One of the possible causes, when the transgene is just ending up next to an endogenous gene in an opposite orientation and transcription initiated at the gene promoter, can read through into the transgene and produce very long chimeric RNA containing both the sense strand of the endogenous gene and antisense strand of the transgene. Double-stranded RNA then formed when antisense part of the long RNA hybridize with the sense RNA produce either by transgene or endogenous gene, the formation of double-stranded RNA is lead for gene silencing. The *AtPCS1* overexpressing line therefore not obtained, although this line was reached in the homozygous state. It could be possible this line can be used as a knockout line for further experiment. The possible overexpressing candidate of *AtPCS1* has to be checked it mRNA level to obtain the overexpression line. The overexpression of *HPTII* gene also achieved for empty vector analysis which will be used as control construct for a future experiment. We could not check the expression of *AtStr5/AtACR2* gene form RNA isolated from leaf samples. As this gene is expressed in the root part of the plant, therefore, we tried to grow the root of *Arabidopsis* in MS media. However, this seems to be not enough for RNA isolation.

The homozygous overexpressing lines of *AtStr5/AtACR2* and *AtStr17a/HAC1/ATQ1* were transformed with the construct pBin-Hyg-TX-*AtPCS1*. The 25 T1 primary dual transform plants of *AtStr5/AtACR2-AtPCS1* and 18 of *AtStr17a/HAC1/ATQ1-AtPCS1* were selected based on kanamycin and hygromycin resistance. The molecular confirmation was also carried out by the presence of *HPTII* gene in those dual overexpressing lines.

## CHAPTER V

### Heterologous overexpression of AtStr5 and AtStr17a in rolB-AtPCS1 overexpressing *Nicotiana tabacum* for arsenic phytoremediation study

#### Abstract

Arsenic (As) toxicity has become a global concern due to the ever-increasing contamination of water, soil, and crops in many regions of the globe. To control the detrimental impact of As, efficient strategy such as phytoremediation is required. Hence, it is crucial to understand the As detoxification mechanism to make this technique fruitful. It has been revealed recently that several genes are participated in As detoxification processes, providing the tools to improve crop species and to optimize phytoremediation, however, so far only a single gene has been manipulated, which has limited progress. Reduction of As from arsenate [As (V)] to arsenite [As (III)] is accomplished by arsenate reductase (AR) and subsequently reduced [As (III)] is bound with phytochelatin (PCs) for complex formation and further vacuolar sequestration. There is evidence that *AR* and *phytochelatin synthase (PCS)* genes are crucial for As detoxification and modulating these two genes lead to improving the phytoremediation process. Therefore, in this study, we made an effort to overexpress the *Arabidopsis thaliana* potential AR (*AtStr5/AtACR2* and *AtStr17a/HAC1/ATQ1*) genes in the transgenic *Nicotiana tabacum* which is already overexpressing *AtPCS1* and *rolB* genes. The *rolB* gene derived from *Agrobacterium rhizogene* and induce the hairy formation in this transgenic plant, which is an adventitious trait, for *in vitro* root growth assay of metal/semimetal tolerance experiments. In this study, we obtained nine *AtStr17a/HAC1/ATQ1* overexpressing lines and one *AtStr5/AtACR2* overexpressing line of *N. tabacum*. It is likely that the overexpression of AR and PCS genes and their concerted action will be increased the As reduction, complex formation, and vacuolar compartmentalization of that As complex, which in turn will assist to develop a useful As phytoremediation technique.

## 1 Introduction

Arsenic (As), a non-essential toxic metalloid which causes a dreadful health hazard to millions of people in the worlds. Water supplies, soils, and sediments contaminated with As are the primary sources of drinking water and food-chain contamination in numerous countries. As toxicity has caused a global epidemic of As poisoning, with many people having developed skin lesions, cancers and other symptoms (Dhankher 2005; Mondal et al. 2006). Prolonged exposure can also cause skin lesions and can intensify the chances of cancer development, especially the possibilities of development of skin, lung, and bladder cancer (Sheena et al. 2009).

As is a non-essential element for plants and other organisms (Khalid et al. 2017), the uptake and accumulation of As by plants depend on the number of factors, including plant species and their habitats, the total As concentration and more importantly, its speciation, which is relied upon As bioavailability in soil (Martínez-Sánchez et al. 2011; Rafiq et al. 2017; Rafiq et al. 2018). In plants, As mainly enters as an inorganic form such as arsenate [As (V)] or arsenite [As (III)] via phosphate (Pi) transporter (Meharg and Macnair 1992; Ullrich-Eberius et al. 1989; Wu et al. 2011) or plasma membrane protein (Bienert et al. 2008; Isayenkov and Maathuis 2008; Ma et al. 2008; Meharg and Jardine 2003). Generally, roots are the first tissue that exposes to As and countering for its growth and proliferation. Subsequently, As can translocate to the shoot, and severely inhibited to plant growth by retarding growth and biomass accumulation, as well as compromising plant reproductive capacity through losses in fertility, yield, and fruit production (Garg and Singla 2011). The various physiological process of the plant is affected by As toxicity, for instance, the cellular membrane of the plant is damaged and causes electrolyte leakage (Singh et al. 2006). This phenomenon can accompany an increased amount of lipid peroxidation, suggestive of oxidative stress due to As toxicity.

Apart from this phenomenon, where most plant species are prone to As toxicity, few plant species are naturally As tolerant and known as As hyper-accumulators plants. Example of As-hyper-accumulators species are *P. vittata* fern (Ma et al. 2001) *P. umbrosia* (Zhao et al. 2002) and *Pityrogramma calomelanos* (Gumaelius et al. 2004), they can be accumulated 5000-22630 mg kg<sup>-1</sup> of As in the fronds (dry weight). Despite the availability of hyper-accumulator species, the low biomass and slow growth rate of most hyper-accumulators are major limitations preventing their use for phytoremediation purposes. Due to the limitations of hyper-accumulators, several approaches have been considered to transfer the ability to accumulate metals into crops with such considerable higher biomass.

Therefore, it is essential to understand the As detoxification pathway, which is accomplished by the coordinated effort of several genes that are involved from As uptake to its accumulation. Therefore, manipulation of a single gene might not be an effective strategy to improve As phytoremediation technique. It is well accepted that once inside into the plant cell, As is reduced from arsenate [As (V)] to arsenite [As (III)] by AR (ACR2) enzymes. In this context, several potential AR genes have been identified in many species as discussed earlier in this thesis. In *Arabidopsis* so far two likely AR genes; *AtACR2/AtStr5* (Dhankher et al. 2006; Dissmeyer et al. 2009; Duan et al. 2005) and *HAC1/ATQ1/AtStr17a* (Chao et al. 2014; Sánchez-Bermejo et al. 2014) have been identified and proposed to be involved in arsenate reduction as a first step of As detoxification process. However, the reduced [As (III)] is 100-fold more toxic than the [As (V)] due to its affinity with sulfhydryl groups in proteins (Cervantes et al. 1994; Mishra and Dubey 2006), resulting in membrane deterioration and subsequent cell death (Meharg and Hartley-Whitaker 2002). To subside the [As (III)] induced toxicity plant have synthesized thiol-reactive cysteine-rich peptides such as phytochelatins (PCs) that can strongly bind with As and convert it to a non-toxic form (Begum et al. 2016; Dixit et al. 2015). The complexation of As with ligands and its vacuolar compartmentation is another mechanism of As detoxification in plants (Chandrakar et al. 2016; Degola et al. 2015). Therefore, it seems to be a promising approach to the manipulation of AR and PCS genes simultaneously that might lead to developing an effective phytoremediation strategy.

In this study, we aimed to overexpress the *Arabidopsis* potential AR genes (*AtACR2/AtStr5*) and (*HAC1/ATQ1/AtStr17a*) into the transgenic *Nicotiana tabacum* plant that is already overexpressing *Arabidopsis phytochelatin synthase (AtPCS1)* gene to obtain more As reduction and more vacuolar sequestration. The heterologous overexpression of *Arabidopsis* AR genes in tobacco will be revealing their AR potentiality precisely. Furthermore, tobacco is a long established model system for plant transformation, and therefore benefits for gene transfer, regeneration procedure and optimized vector system (Stoger et al. 2005). These traits make tobacco a suitable candidate for the production of a transgenic plant in the field of phytoremediation. Moreover, tobacco is not a hyper-accumulator of semimetals/metals though it can extract and accumulate them at considerable level (Zvobgo et al. 2015). Furthermore, tobacco produced a significant amount of biomass and also generated an immense number of seeds in each generation which allows to rapidly scale up the process (Sarret et al. 2006). All these intrinsic attributes make tobacco an excellent candidate for phytoremediation.

Additionally, this transgenic tobacco also contains a *rolB* gene from *Agrobacterium rhizogenes*. The *rolB* expression can also bring some benefit for *in vitro* metal tolerance experiment, as the gene encoding a RolB protein induce adventitious hairy root formation (Nilsson and Olsson 1997). However, the function of the *rolB* gene is not limited to the hairy root formation; there are some other role have been proposed for instance, RolB expression leads to enhance shoot formation, rhizogenesis, and flower formation (Altamura et al., 1994) induce parthenocarpic fruit in tomato (Carmi et al., 2003). Until now, a single opinion of cellular function and localization of this gene does not exist. Different sequences of this gene were revealed in different strains, and encoded proteins were detected in separate compartments of the cell (Pavlova et al. 2014). The *rolB-AtPCS1* overexpressing tobacco was successfully used in metal tolerance experiments, especially for cadmium (Cd) and As tolerance (Pomponi et al. 2006; Zanella et al. 2016). A transgenic plant that is co-overexpressing *AR-PCS* genes might facilitate to enhance As reduction, chelation, and sequestration which are crucial for As phytoremediation process. We intended to investigate whether such overexpression is capable of increasing As tolerance and accumulation both in roots and in shoots either the presence or absence of sulfur. The role of sulfur under stress was elucidated in Chapter 1 of this thesis.

## 2 Material & methods

### 2.1 Plant material

The seeds of transgenic tobacco *rolB-AtPCSI* were obtained from Dr. Maura Cardarelli, Sapienza Università di Roma, and Italy. The plants were *in vitro* grown on 0.5 x MS medium pH 5.7, with 3% sucrose and the antibiotic kanamycin (50 µg ml<sup>-1</sup>) and hygromycin (30 µg ml<sup>-1</sup>). The plants were grown in a growth chamber at 25°C and 16 h/8 h day and night regime and light intensity 120 µmol m<sup>-2</sup> s<sup>-1</sup> (fluorescent lamps, PHILIPS MASTER TL5 HO-54W/840 FLUORA, Holland). Four weeks later, leaf disk (~1 cm<sup>2</sup>) of these plants was used as a source of explants.

### 2.2 *Agrobacterium* strains and culture

The *Agrobacterium tumefaciens* strains GV3101 were used for the transformation of the pBinAR vector that carries the target gene in its T-DNA region. The pBinAR vector contains 770 bp of T-DNA that was controlled by a 35S promoter, which drives the constitutive higher expression of the chimeric gene.

### 2.3 Preparation of the bacteria

The *AtStr5/AtACR2* and *AtStr17a/HAC1/ATQ1* genes were cloned into the pBinAR vector, and specific cloning technique was described in the materials and method part of chapter IV. Therefore, glycerol stocks of pBinAR-*AtStr5/AtACR2* and pBinAR-*AtStr17a/HAC1/ATQ1* strains were directly available for tobacco leaf disc transformation. From the glycerol stock, each strain of bacteria was inoculated to 2YT medium (5 g l<sup>-1</sup> yeast extract, 16 g l<sup>-1</sup> bacto tryptone and 5 g l<sup>-1</sup> NaCl, pH adjusted to 7.0) containing appropriate antibiotics: kanamycin (100 µg ml<sup>-1</sup>) and rifampicin (100 µg ml<sup>-1</sup>). After that, the bacteria were grown overnight (16 h) on a shaker at 180 rpm at 28°C. After centrifugation at 10 min 3130 g, the bacteria were re-suspended with liquid co-cultivation medium. The optical density (OD) of bacteria was measured at 600 nm (OD<sub>600</sub>). The final OD<sub>600</sub> was controlled 0.6-0.8 during transformation.



## 2.4 Transformation, co-cultivation, and regeneration medium

The leaf disks of tobacco were cut into pieces of  $\sim 1 \text{ cm}^2$  with a sterile cork borer and stacked on Petri plates that contain MS medium to avoid the desiccation of explants. The explants were inoculated with the *Agrobacterium* by incubating in a Petri dish containing a bacterial suspension for 5-10 min. Later, the inoculated explants were transferred into the Petri dish (15x100 mm) containing co-cultivation medium (2xMS + glucose  $16 \text{ g l}^{-1}$  pH 5.7). Before transferring the explants, the sterile filter paper was overlaid on the top of the co-cultivation medium. The filter paper was moistened with the liquid co-cultivation medium before placing the inoculated explants. The explants were pre-cultured in a co-cultivation medium in the dark at  $23^\circ\text{C}$  for two days. Subsequently, the explants were blotted on sterile filter paper to remove the bacterial suspension and placed them in a regeneration medium [2x MS + Glucose ( $16 \text{ g l}^{-1}$ ) + NAA ( $0.2 \text{ ml l}^{-1}$ ) + BAP ( $1 \text{ ml l}^{-1}$ ) + kanamycin ( $50 \mu\text{g ml}^{-1}$ ) + hygromycin ( $30 \mu\text{g ml}^{-1}$ ) + Sodium carbenicillin ( $100 \mu\text{g ml}^{-1}$ ) pH 5.7]. Finally, they were placed in a growth chamber ( $25^\circ\text{C}$  temp, 16h light and 8h in the dark). Each week the explants were replaced with a fresh regeneration medium. When the small shoots appeared from the callus, they were excised individually and transferred into the larger container containing rooting medium [2x MS + glucose ( $16 \text{ g l}^{-1}$ ) + kanamycin ( $50 \mu\text{g ml}^{-1}$ ) + hygromycin ( $30 \mu\text{g ml}^{-1}$ )] in the same condition as like regeneration medium.

When all the plantlets had sufficient and established a root system in the rooting media, they were transferred into the soil in the greenhouse. The plants were acclimatized first two weeks by covering them with a plastic dome with no hole. The increased humidity aids plantlets to acclimatize into the new environment.

## 2.5 Molecular analysis

### 2.5.1 DNA isolation

The genomic DNA of T0 and T1 primary transformants were extracted according to the standard DNA isolation procedure (Sambrook et al. 1989). About 100 mg of T0/T1 transformants fresh tissue was crushed to a fine powder using liquid nitrogen and homogenized in 250 µl freshly made extraction mix. About 400 µl freshly made extraction mix was added, and the samples were incubated with for 60 min at 65°C. About 700 µl of chloroform: isoamyl alcohol (24:1) was added to samples, followed by vortexing for 30 Sec. Samples were then centrifuged for 10 min at 9500 g, and the DNA in the supernatant was precipitated with 750 µl of isopropanol and again centrifuged. The precipitate was then washed with 70% ethanol. The pellet dried and mixed with 100 µl TE with 0.5 µg/100 µl RNase and dissolved by incubating at 65°C for 15-30 min. The DNA samples were quantified using a spectrophotometer.

### 2.5.2 PCR amplification and screening of transformed regenerates by analyzing the presence of *AtStr5/AtACR2* and *AtStr17a/ATQ1/HAC1* gene

The transgenic *rolB-AtPCS1* tobacco plants are already double transformed plant, and it contains both the kanamycin and hygromycin resistant genes, therefore after third-time transformation with the pBinAR-*AtStr5/AtACR2* and pBinAR-*AtStr17a/HAC1/ATQ1* construct, the transformants were not the selected based on kanamycin resistance. Since the pBinAR construct contained a kanamycin resistance gene (*NPTII*) for plant selection, a large number of plants were subjected to PCR analysis for transgene selection. The PCR primers were designed in such a way that the forward primer can bind the last few base pairs of the 35S promoter and the first few base pairs of *AtStr5/AtACR2* or *AtStr17a/HAC1/ATQ1* gene. The reverse primer can bind the last part of *AtStr5/AtACR2* or the *AtStr17a/HAC1/ATQ1* gene and the first part of the *octopine synthase (OCS)* terminator. The primers binding ability was verified by amplifying the recombinant plasmid of pBinAR-*AtStr5/AtACR2* and pBinAR-*AtStr17a/HAC1/ATQ1*.

The PCR primer pairs for amplification of the *AtStr5/AtACR2* gene were P1150\_AtStr5/AtACR2-TDNA\_F; TTGGAGAGGACAGGTACCATG and P1152\_AtStr17a/HAC1/ATQ1/AtStr5/AtACR2-TNA\_R; GGCGTCTCGCATATCTCATT and for *AtStr17a/HAC1/ATQ1* gene P1151\_AtStr17a/HAC1/ATQ1-TDNA\_F; GGA GAG GACAGGTACCATGTATACA and P1152\_AtStr17a/HAC1/ATQ1/AtStr5/AtACR2-TDNA\_R; GGCGTCTCGCATATCTCATT. The PCR reaction contained 0.2 mM dNTPs

(Roth, Karlsruhe, Germany), 0.4  $\mu$ M of each primer (Eurofins genomics, Ebersberg, Germany) 0.5  $\mu$ l DreamTaq DNA-Polymerase (ThermoFisher, Germany), 2  $\mu$ l 10x PCR Green buffer and about 1  $\mu$ l template DNA in a final volume of 20  $\mu$ l. The amplification was performed in a programmable PCR cycle using 28 reaction cycles consisting of a 1 min initial denaturation step at 94°C, a 1 min primer annealing step at 52°C and 1 min elongation step at 72°C. The final elongation step was performed for 600 s at 72°C. The amplified PCR product was analyzed on 1% agarose gels.

## 2.6 Southern blotting

The genomic DNA of T0 primary transformants were extracted according to the standard DNA isolation procedure (Sambrook et al. 1989) for Southern blot analysis. DNA was digested overnight with *Hind*III and *Eco*RI in case of the *AtStr17a* overexpressing line and *Eco*RI, *Nco*I, *Xba*I, *Xho*I and *Bam*HI in case of the *AtStr5* overexpressing line, and fractionated by agarose gels electrophoresis, and transferred to nylon membranes (Roth). Digoxigenin labeled probes were synthesized by PCR according to the manufacturer's protocols (Roche) using primers 968A/969A for *AtStr5* and 970/971 (see Table 3, CHAPTER IV). Colorimetric detection was done using nitroblue tetrazolium (NBT) and 5-Bromo-4-chloro-3-indolyl-phosphate (BCIP) as substrates for alkaline phosphatase.

## 3 Results

The coding region of *Arabidopsis AtStr5* and *AtStr17a* were cloned under the control of a CaMV35S promoter (as described in materials and method part of Chapter IV) and used to transform tobacco plants expressing the *rolB* oncogene and *Arabidopsis AtPCS1* gene (Cardarelli et al. 1987; Spena et al. 1987). Nine *rolB-AtPCS1-AtStr17a/HAC1/ATQ1* (**Figure 2A**) and one *rolB-AtPCS1-AtStr5/AtACR2* hygromycin and kanamycin resistant primary transformants (T0), were selected based on the presence of the insert by PCR (**Figure 3A**). The empty pBinAR vector was also used for transformation to use as a control. However, analysis of pBinAR (empty vector) transformed with 40 plantlets did not show any transgene insertion (picture not presented). The seeds from each T0 transgenic plant was harvested separately and grown for next generation (T1). The DNA from each transgenic line (T1) was extracted and subjected to PCR analysis. The PCR result from each *rolB-AtPCS1-AtStr17a/HAC1/ATQ1* was shown negative results that means no amplification of the target genes in these nine transgenic lines which were selected in the first generation (T0) (**Figure 2B**). All the *rolB-AtPCS1-*

*AtStr17a/HAC1/ATQ1* was revealed as chimeric in the first generation. Unfortunately, no cutting was made in the first generation of these transgenic lines. On the other hand, the transgenic *rolB-AtPCS1-AtStr5/AtACR2* were found positive in the next generation (T1). Three cuttings of this plant were maintained and found all have the target *AtStr5/AtACR2* gene (**Figure 3B**). The Southern analysis of these transgenic plants was performed as described in *Arabidopsis* overexpressing experiment. However, the detection was not visible (**Figure 4**).



(A) *In vitro* growing plant



(B) Leaf disc explants in regeneration medium



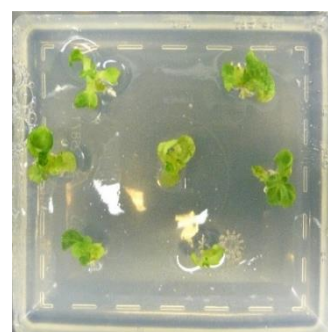
(C) Multiple shoot arising from single callus



(F) Plants are acclimatized in a new environment by gradually removing the plastic dome



(E) Larger seedlings transferred into small pots with soil in a greenhouse, covered with plastic dome (no hole) to generate high humidity condition



(D) Two shoots/callus are transferred in a large plastic container (in growth chamber)



(G) Acclimatized



(H) Transferred into larger pot

**Figure 1.** *N. tabacum* transformation steps (A) One-month-old *in vitro* growing *rolB-AtPCS1* plants. (B) Callus is growing on regeneration medium. (C) The shoot is arising from callus cluster. (D) Shoots are growing in a big plastic container. (E) Platelets are grown in the soil in the greenhouse. (F) Acclimatizing steps. (G) Plants are fully acclimatized (H) Larger plants were growing in 23 cm pots.

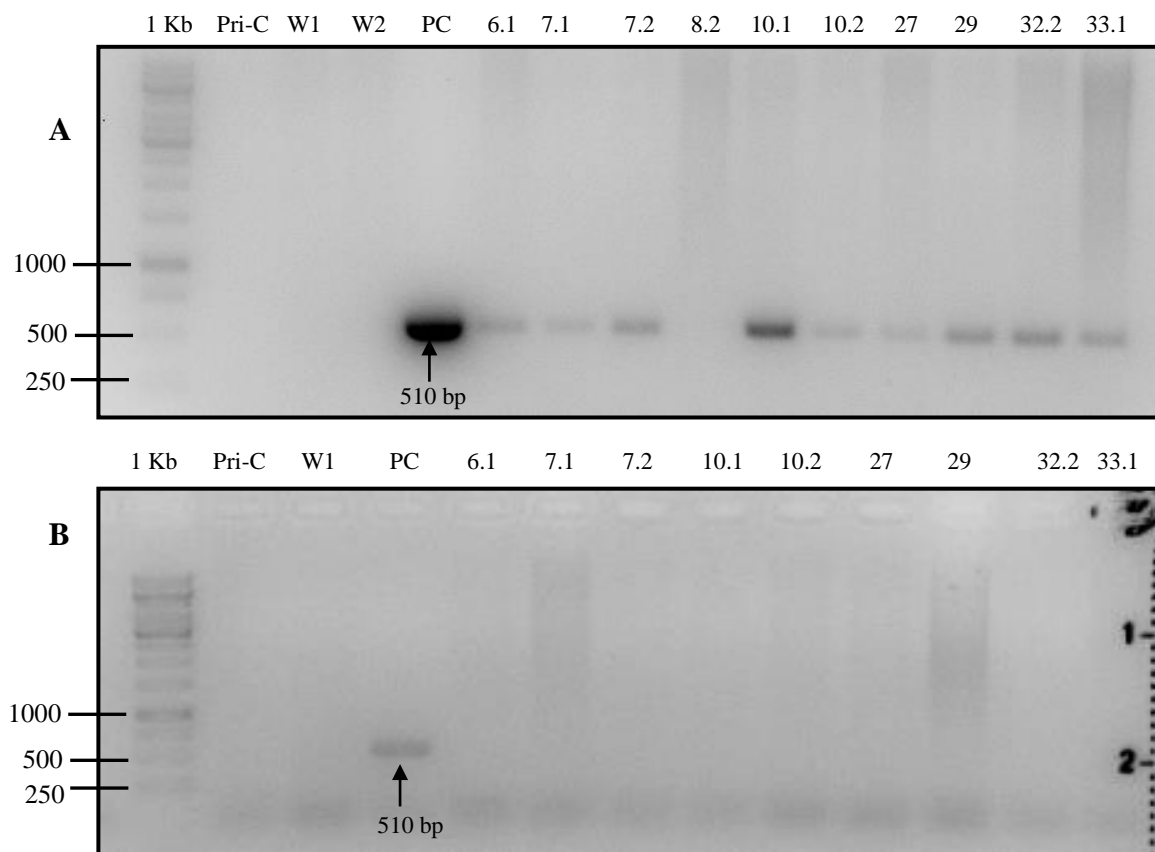


**Figure 2.** The *AtStr17a/HAC1/ATQ1* overexpressing *rolB-AtPCS1* tobacco plants were screened by PCR method. **(A)** The *AtStr17a/HAC1/ATQ1* overexpressing *rolB-AtPCS1* transgenic T0 plants were confirmed by the amplification of 510 bp of PCR product. **(B)** In the next generation, the same *AtStr17a/HAC1/ATQ1* overexpressing *rolB-AtPCS1* transgenic T1 plants were subjected to PCR analysis. However, no PCR yield of the target gene was observed. The primer control (without DNA) and wild-type *rolB-AtPCS1* did not show any amplification in the same PCR process. As a positive control, the plasmid DNA from the recombinant plasmid pBinAR-*AtStr17a/HAC1/ATQ1* was isolated and amplified with the same primer pairs, which produced a 510 bp of PCR product. The lane Pri-con, primer control; W, wild-type; PC, plasmid control; and the different number in each lane indicates the particular plant number.

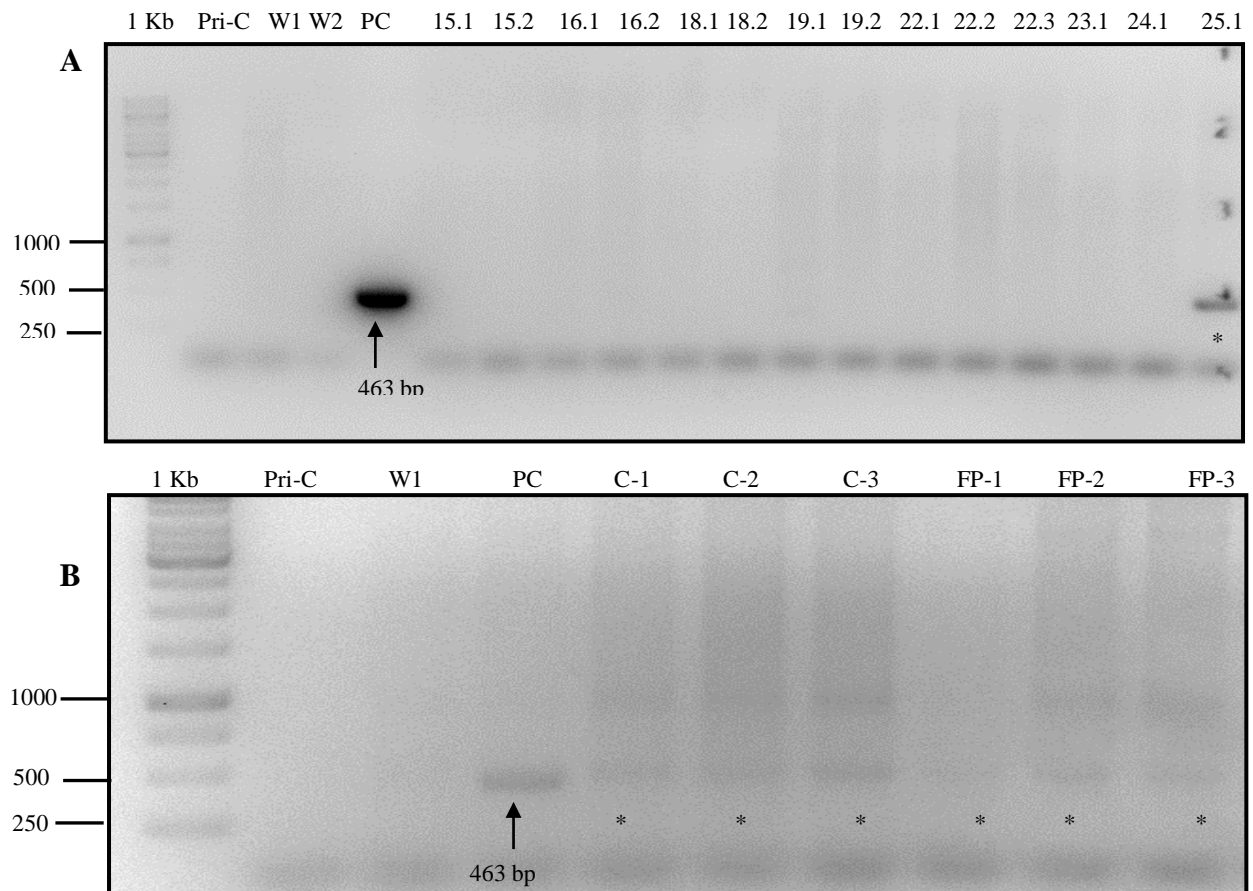


**Figure 3.** The *AtStr5/AtACR2* overexpressing *rolB-AtPCS1* tobacco plants were screened by PCR analysis. **(A)** The *AtStr5/AtACR2* overexpressing *rolB-AtPCS1* transgenic T0 plants were confirmed by the amplification of 463 bp of PCR product. **(B)** In the next generation, the same *AtStr5/AtACR2* overexpressing *rolB-AtPCS1* transgenic T1 plant and three cutting of the same transgenic plant were subjected to PCR analysis, all of them have shown expected amplified product. As a positive control, the plasmid DNA from the recombinant plasmid pBinAR-*AtStr5/AtACR2* was isolated and amplified with the same primer pairs, which produced 463 bp of the PCR product. The lane Pri-con, primer control; W, wild-type; PC, plasmid control; and the different number in each lane indicates the particular plant number.

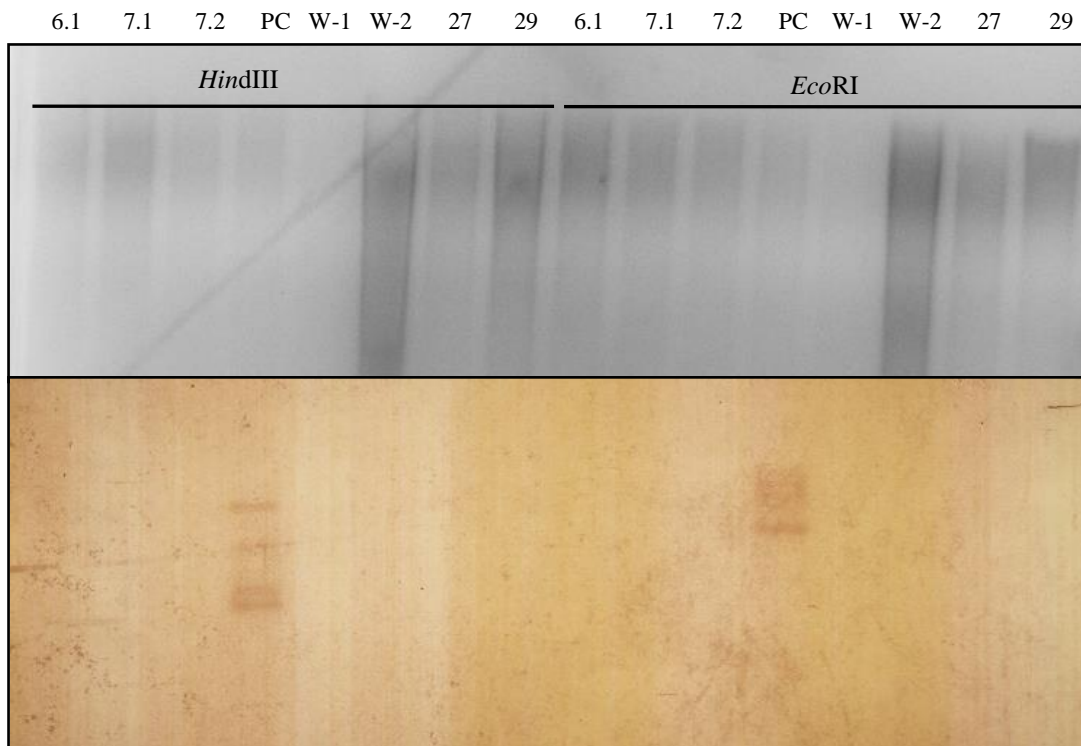


**Figure 4.** Southern blot analysis of T0 overexpressing transformants of *rolB-AtPCS1-AtStr17a/HAC1/ATQ1*. Genomic DNA of each overexpressing, WC, wild-type control (*rolB-AtPCS1*) and PC, positive control (*Arabidopsis AtPCS1* overexpressing line 18) plants was extracted, and 20 µg was digested (with *HindIII* and *EcoRI*) and subjected to Southern blot analysis using a digoxigenin-labeled probe against a gene-specific sequence of *AtStr17a/ HAC1/ATQ1*. Southern blot hybridization result was negative for all the transgenic lines. The lane PC, plasmid control; W, wild-type; and the different number in each lane indicates the particular plant number.



## 4 Discussion

In this study, we attempted to overexpress the *Arabidopsis* potential AR genes *AtStr5/AtACR2* and *AtStr17a/HAC1/ATQ1* in transgenic *N. tabacum* that is already overexpressing *AtPCS1* and has shown increased Cd and As tolerance (Pomponi et al. 2006; Zanella et al. 2016). It has been reported that increase PCs synthesis led to increase As accumulation and tolerance in several species (Dave et al. 2013; Gasic and Korban 2007; Li et al. 2004). Additionally, these same *N. tabacum* plants are also overexpressing a *rolB* gene of *A. rhizogenes* which induce hairy root formation in the infected plants. The root of *rolB* expressing plant proliferates in a culture which may provide a convenient biological system for the assay metal tolerance experiment particularly *N. tabacum* that overexpressing AR and *AtPCS1* gene.

The transgenic plants were developed by following the leaf disc transformation method of tobacco. The PCR based selection was carried out to obtain the primary AR overexpressing transformants of tobacco. Although the transformed plants contain the *NPTII* gene for kanamycin resistance, the kanamycin based selection was not carried out due to the prior presence of *NPTII* and *HPTII* genes in the *rolB-AtPCS1* overexpressing *N. tabacum*. At least 50-80 seedling for each construct were subjected for PCR analysis. The nine T0 overexpressing transformants of *AtStr17a/HAC1/ATQ1/HAC1* gene and one T0 overexpressing transformant of *AtStr5/AtACR2* gene were obtained in the first round of transformation. However, in the T1 generation, all *AtStr17a/HAC1/ATQ1/HAC1* overexpressing transformants were found negative in PCR, which means in the T0 generation all transformed plants were remained in chimeric. In the case of, *AtStr5/AtACR2* overexpressing plant only one transformed plant was obtained and was stable in the T1 generation. It was necessary to make a cutting of each overexpressing lines because in tissue culture systems it is possible to generate chimeric plants. The other potential problem is gene silencing, which could easily arise in the triple transformed plants. The *rolB-AtPCS1* overexpressing *N. tabacum* already contain two times 35S promoter, when it was used to transform with *pBinAR-AtStr5/AtACR2* and *pBinAR-AtStr17a/HAC1/ATQ1* gene, then triple time 35S promoter was present on that plant. Though we did not check the overexpression of AR genes in that plant, it is possible for gene silencing. In such a case we need to screen a vast number of transform plants, then the probability to obtain non-silence plant will be increased. However, due to the PCR selection system, it was not easy to select several numbers of plants, which takes a considerable amount of time, especially when DNA extraction has to be done manually.

On the other hand, the advantages of antibiotic based selection are that it could reduce the number of silencing plants for mRNA study. Because when the kanamycin resistance gene is silenced, then no such a plant can be selected for further analysis, while the PCR method could not make a difference between the silenced and non-silenced of the target gene. However, the PCR method could be risk the non-silence target gene when the kanamycin resistance gene goes for silencing. Southern analyzing of T0 overexpressing transformants of *AtStr5/AtACR2* and *AtStr17a/HAC1/ATQ1* genes were not produced any hybridized band with the *AtStr5* and *AtStr17a* probe. Southern negative hybridization for *AtStr17a/HAC1/ATQ1* overexpressing transformant might be explained that the DNA extracted from the non-transformed part of those chimeric overexpressing plants. Despite the presence of *AtStr5* genes in subsequent generations, the southern hybridization gave negative results. The southern negative consequence of this plant is not known. Screening more transformed plant and redesigning the hybridization probe could solve this issue. Because the primer pairs used for *AtStr5* probe development, when used the same primer pairs for *AtStr5* gene selection in *rolB-AtPCSI N. tabacum*, it was observed that all *rolB-AtPCSI N. tabacum* plants could amplify the *AtStr5* sequence regardless their transformation with this gene.

Therefore, we design the PCR selection primers that were more specific to the exogenous *AtStr5* gene (described in the material and method part) which allows selecting the *AtStr5* transformed plant conveniently from the non-transformed *rolB-AtPCSI* plants, which did not produce the same band in PCR. Developing a new *AtStr5* probe by PCR selection primer pairs of *AtStr5* might solve the southern hybridization problem.

## CHAPTER VI

### 1 General discussion

Sulfurtransferases (Strs) are ubiquitously prevalent in all living organisms. Despite their prevalence across species, the distinct physiological roles of most Strs are not fully understood. In *Arabidopsis* 20 different Strs and Str-like proteins have been identified and classified into six groups based on their amino acid sequence homologies (Bartels et al. 2007; Bauer and Papenbrock 2002). Here we report on the isolation and functional characterization of AtStr5, which contains a single rhodanese (Rhd) domain and is classified into group III of Strs family protein. The AtStr5 comprises a catalytic domain [His-Cys-(X)<sub>5</sub>-R], also shared by the enzyme family of CDC25 phosphatase and arsenate reductase (AR). Thus AtStr5 might be involved in the catalysis of phosphate and arsenate containing substrates *in vitro*. In an earlier study, the AtStr5 was proposed as Arath; CDC25 protein since it can hydrolyze the phosphate-containing substrate *p*NPP, and can stimulate the purified cell division kinase (CDK)-complex *in vitro* (Landrieu et al. 2004a; Landrieu et al. 2004b). However, the CDC25 function of AtStr5 was argued in several studies. Alternatively the AtStr5 has been suggested as an AR enzyme known as AtACR2 (Bleeker et al. 2006; Dhankher et al. 2006; Nahar et al. 2017), which can reduce arsenic (As) from arsenate [As (V)] to arsenite [As (III)] as an essential step in the arsenate detoxification process. However, the AtACR2 function of the AtStr5 protein has been argued recently. Therefore, the physiological function of AtStr5 remains unsolved. The continuing arguable situation and necessities understand the arsenic (As) detoxification mechanism in the plant, drives us to investigate the role of AtStr5 further.

#### 1.1 Sulfurtransferase activity of AtStr5

The difference between AtStr5 and with the other AtStrs is related to their active site loop length; where AtStr5 possess seven amino acid longer catalytic motifs instead of six [His-Cys-(X)<sub>4</sub>-R] in other Strs protein. The elongated active site loop can create a wider catalytic pocket, which can accommodate phosphorus atom which has van der Waal radius is slightly larger than a sulfur atom (1.9 versus 1.85Å) (Bordo and Bork 2002). It could be the possible reason that AtStr5 can accept the different oxyanion binding substrates such as arsenate and phosphate whereas other AtStrs cannot. Nevertheless, in high substrate levels,

few of the AtStr5 enzyme molecules may accept sulfate-rich substrates due to the high structural similarity of sulfate and phosphates and break down from the rest of the chemical moiety. In contrast to the AtStrs that contains six amino acid longer catalytic motifs, the AtStr5 can poorly catalyze sulfur-containing substrates such as 3-MP and TS, and showed higher  $K_m$  values (28.2 mM for 3-MP). From the mutational studies on RhDA of *Azotobacter vinelandii*, it was learned that Str and phosphatase activities do not exist concurrently (Forlani et al. 2003). Therefore, it can be concluded that the rhodanese domain possessing AtStr5 protein is not a Str-protein instead it might be a phosphatase or AR protein.

## 1.2 Phosphatase activity of AtStr5

We demonstrated the phosphatase activity of AtStr5 with the two artificial substrates *p*NPP and 3-OMFP since the natural substrates for many of the dual specificity phosphatases (DS-PTPases) are not known. It has been shown that CDC25-DS-PTPases have higher affinity to 3-OMFP than *p*NPP. To test this incidence for AtStr5, we measured the kinetic comparison of AtStr5 with these two substrates, since AtStr5 was proposed Arath; CDC25 (Landrieu et al. 2004a). It was found that the AtStr5 showed ~3000 fold enhancement of  $k_{cat}/K_m$  (catalytic efficiency) for 3-OMFP over *p*NPP, which indicates 3-OMFP is an ideal substrate for *in vitro* phosphatase activity measurement of an AtStr5, similar to the other DS-PTPases. In the kinetic determination with 3-OMFP, the AtStr5 showed ~1.5-fold lower  $K_m$ , ~11-fold lower  $k_{cat}$  and ~17-fold lower  $k_{cat}/K_m$  values than huCDC25B (measured in a different study, in the same experimental condition). Such a lower turnover rate and lower catalytic efficiency of AtStr5, do not explain that it is a CDC25 protein. It seems to be realistic if such a comparison can make by using the natural substrate. The known natural substrate for CDC25 is CDK. Nevertheless, it cannot be efficiently used *in vitro* enzyme assay due to their availability in a large macromolecular complex and phosphorylated on adjacent threonyl (Thr14) and tyrosyl residues (Tyr15) (Millar and Russell 1992). Additionally, phosphorylated peptides are found to be a poor substrate for CDC25 *in vitro* (Dunphy and Kumagai 1991).

The catalytic [His-Cys72-(X)5-R78] cysteine72 residue of AtStr5 was replaced by alanine72 and found the phosphatase activity is completely abolished, this result is also consistent with other studies, while in huCDC25B enzyme, mutation of cysteine and arginine loss both AR and phosphatase activity (Bhattacharjee et al. 2010; Landrieu et al.

2004a; Landrieu et al. 2004b). The phosphatase activity of other AtStrs for instance; AtStr1, AtStr2, AtStr7, AtStr14, AtStr16, and AtStr17a AtStr18 also tested with 3-OMFP to observe whether the catalytic Cys that present in their catalytic motif is also capable of hydrolyzing the phosphate-rich substrate, however, they did not exhibit any phosphatase activity (Hartmann & Papenbrock, unpublished data; this study). Besides this, the engineered elongation catalytic loop of the *A. vinelandii* Str compromises the ability to catalyze the sulfur transfer reaction and gain phosphatase ability to catalyze the artificial substrate 3-OMFP (Forlani et al. 2003). Thus, it was confirmed that not only the composition but also the length of the active site is crucial for substrate recognition and specificity (Bordo and Bork 2002). Thus, the rhodanese domain with a seven amino acid loop can bind to substrates containing phosphorous or similar arsenic, whereas the rhodanese-like domains with a six amino acid loop interact with substrates containing reactive sulfur or in some cases selenium (Ogasawara et al. 2001).

The AtStr5 was only reported as CDC25 protein in higher plants (Landrieu et al. 2004a; Landrieu et al. 2004b). However, the possibilities of AtStr5 as Arath; CDC25 were overlooked in many physiological studies (Dissmeyer et al. 2009; Spadafora et al. 2010) and raising the issue about the CDC25 function of AtStr5. The most striking points large N-terminal regulatory region is absent in AtStr5, which contains important regulatory elements required for the central function of CDC25 as an integrator of developmental and environmental cues. Therefore, without this important motif that present in human yeast and metazoan raising the question, how AtStr5 carry out the central role in cell cycle control. Although the basic machinery of the cell cycle is common to the plants and other eukaryotes, due to their sessile lifestyle, plants have also developed unique strategies to allow growth and survival under environmentally harsh conditions, for example, endo cell cycle system (Komaki and Sugimoto 2012). Plants generally possess many more genes encoding core cell cycle regulators, compared with animals and yeasts (Breuer et al. 2014; Harashima and Schnittger 2010), and it has been an enigma how their functions are specified or overlapped in development or respond to various environmental changes. Therefore, it is not clear how the plant completes their cell cycle without the absence of the CDC25 protein. Although the AtStr5 affinity towards 3-OMFP indicates its possibilities to be a DS-PTPase, the lower kinetic parameters do not represent its ability to act as CDC25 protein. All the evidence, including our biochemical data, do not support the CDC25 role of AtStr5.

The *in vitro* phosphatase activity of AtStr5 might be explained by the presence of similar oxyanion binding sites in its active site, which is shared by AR and phosphatase enzymes. This phenomenon is not a surprise because many phosphatase enzymes can catalyze arsenate rich substrates *in vitro* such as huCDC25B and huCDC25C which show adventitious AR activity (Bhattacharjee et al. 2010). The vice versa situation can also be observed in bacteria like *arsC* from *Staphylococcus aureus* where plasmid pI258 exhibits low-level phosphatase activity (Ji et al. 1994). However, this similar situation does not prevail to the all known CDC25 and ACR2 enzymes. For example, the proposed eukaryotic ACR2 enzyme, OsACR2 from *Oryza sativa* (Duan et al. 2007) and LmACR2 from the parasitic protozoan *Leishmania major* (Zhou et al. 2006), exhibit both AR and phosphatase activities while ScACR2p from *Saccharomyces cerevisiae* (Bobrowicz et al. 1997; Mukhopadhyay and Rosen 1998) and PvACR2 from the *Pteris vittata* (Ellis et al. 2006), lack phosphatase activity. These ACR2 enzymes exhibit significant variability in their biochemical activities, though each of these following proteins shows similarities in the sequence in their active site region with the CDC25-DS-PTPase class of the protein. Therefore, it is complicated to find the clue why some of the enzymes have shown *in vitro* bi-functionality, and some do not, despite sharing the same catalytic site. In this context, recently identified AR enzyme AtStr17a/HAC1/AtARQ1 in *Arabidopsis* (Chao et al. 2014; Sánchez-Bermejo et al. 2014) also lack the phosphatase activity (from this study). Furthermore, AtStr17a/HAC1/AtARQ1 contains the six amino acid longer active site loop [Cys-(X)<sub>4</sub>-R] and does not represent the plant ACR2 group of reductases, which raise the question whether the length of the catalytic site is important for arsenate recognition.

### 1.3 Subcellular localization of AtStr5

Protein subcellular localization can provide an essential hint behind its physiological function. In GFP mediated intracellular localization study of AtStr5, we found two truncated mutants of this protein was in the cell cytoplasm. However, the localization of the full-length AtStr5 cannot be determined conclusively. Though it's likely to be in a nucleus, results were not reproducible. From the mutant's localization, it can be assumed that AtStr5 is not a genuinely cytoplasmic protein since the expression of truncated mutants were not interrupted to be localized in the cytoplasm. If AtStr5 is a cytoplasmic protein, then it can be localized in the cytoplasm without any hindrance as the truncated mutants. Thus indicated that localization of the full-length AtStr5 protein is controlled by

its N-terminal region, which contains the targeting peptide sequence and somehow this sequence is interrupted and causes a problem for protein expression. Therefore, it indicates the unpredictable localization was due to the biological interference. Moreover, the experimental error was avoided by including positive and negative controls. Another important fact is the large N-terminal regulatory region is absent in AtStr5 unlike huCDC25s, which is controlling the subcellular localization of huCDC25 (Boutros et al. 2007). In such a case, if localization of AtStr5 is controlled by the interaction of other proteins and this interaction may be lost due to the overexpression of AtStr5 in the fusion construct.

According to the predictor cNLS Mapper, the AtStr5 is a dual localized protein potentially in the nucleus and the cytoplasm. The cNLS Mapper, which accurately predicts nuclear localization signals (NLSs) specific to the importin  $\alpha\beta$  pathway by calculating NLS scores (levels of NLS activities), but not by the conventional sequence similarity search or by the machine learning strategy (Kosugi et al. 2008; Kosugi et al. 2009). This cNLS Mapper gives an accurate prediction of yeast species. Analysis of the AtStr5 protein sequence of this program has shown the cutoff score lies between 3 and 4 indicated both nucleus and cytoplasmic localization of the AtStr5 protein. Briefly, a GUS-GFP reporter protein fused to an NLS with a score of 8, 9, or 10 is exclusively localized to the nucleus, that with a score of 7 or 8 partially localized to the nucleus, that with a score of 3, 4, or 5 localized to both the nucleus and the cytoplasm, and that with a score of 1 or 2 localized to the cytoplasm.

The dual localization of AtStr5 can be counted because of its potential AR function in the cell, and so far ARs identified in bacteria and yeast (ScACR2) were found in the cell cytoplasm except the AtStr17a/HAC1/ATQ1 that was found in both the nucleus and cytoplasm (Sánchez-Bermejo et al. 2014). Therefore, for AR activity, the AtStr5 must be located in the cell cytoplasm because after As reduction, the [As(III)-PCs complex formation also occurred in the cell cytoplasm. However, in this experiment, the AtStr5 cannot be found in the cytoplasm possible because of its dual localization (nucleus and the cytoplasm) and its localization is interrupted due to the overexpression of the protein as mention above. However, it can be verified by fusing this predicted NLS sequence to any of cytoplasmic protein, and this NLS can lead the cytoplasmic protein into the particular compartment. It might be a good idea, to avoid the use of the 35S promoter, because

overexpression of protein sometimes masks the signal sequence in the N-terminal region. The consequence can also mislead or silence the target protein.

#### **1.4 Simultaneous overexpression of *AtStr5/AtACR2-AtPCS1* and *AtStr17a/HAC1/ATQ1-AtPCS1* in *A. thaliana* for arsenic phytoremediation study**

The ultimate goal of this study is to improve the As phytoremediation process. Therefore, it is vital to understand the As detoxification mechanism to reach that goal. The As detoxification chemistry in the plant becoming to unwind in the recent era due to the advanced molecular approach and complete genome sequence of *Arabidopsis* and some other crop species. It is known that As is taken up by plant roots by utilizing plant phosphate uptake transporter and while inside the plant cell, the [As (V)] is beginning to reduce into [As (III)] by AR enzymes such as *AtStr5/AtACR2* and *AtStr17a/HAC1/ATQ1*. Nevertheless, it is not the ultimate solution for the plant to get rid of this toxicant because of both the inorganic form of As arises dreadful consequence for plants. Eventually [As (III)] is 100-fold more toxic than [As(V)] (Cervantes et al. 1994; Mishra and Dubey 2006). To get rid of this poisonous effect plant produces chelators such as GSH and PCs that can form complexes with that [As (III)] for vacuolar sequestration. It has already been reported that overexpression of PCS synthase showed promising results in bacteria and plants (Grill et al. 2007). Eventually, overexpression of *A. thaliana phytochelatin synthase 1 (AtPCS1)* yielded in a substantial increase in As resistance with a 20–100 times greater biomass in transgenic plants after exposure to As (Li et al. 2004). The plant has also employed [As (III)]-efflux to extrude back this [As (III)] into the soil from the plant root (Chao et al. 2014).

The single overexpressing lines of *AtStr5* and dual overexpressing lines of *AtStr5-AtPCS1* were developed in this work, to study the physiological function of *AtStr5* concerning its role as *AtACR2*. Similarly, the single and dual overexpressing lines of *AtStr17a* were also produced, as the gene is recently considered another potential AR (*HAC1/ATQ1*) in *Arabidopsis*. As a consequent of AR overexpression, these lines will be able to increase the reduction of arsenate and increase arsenite [As (III)] form would be expected. However, [As (III)] has a very detrimental effect of the plant, hence need to be removed from the cell. The removal of [As (III)] in hyper-accumulator species are accomplished through vacuolar sequestration after by binding with phytochelatins (PCs). However, the AR overexpression can bring an adverse effect to the plant, if the same time the PCs production is not



increasing. In such a situation the dual overexpressing lines of *AtStr5/AtACR2-AtPCS1* and *AtStr17a/HAC1/ATQ1-AtPCS1* can solve this problem by increasing the reduction and PCs production simultaneously. Thus, it is expected that the dual overexpressing lines developed from this work can be efficiently used for As-phytoremediation purposes.

### **1.5 Overexpression of *AtStr5/AtACR2* and *AtStr17a/HAC1/ATQ1* in *rolB-AtPCS1* overexpressing *N. tabacum* for arsenic phytoremediation study**

The endeavor to overexpress the two essential AR genes (*AtStr5/AtACR2* and *AtStr17a/HAC1/ATQ1*) in *AtPCS1* overexpressing *N. tabacum*, led to developing a dual overexpressing line of *AtStr5-AtPCS1* and *AtStr17a-AtPCS1* in tobacco. The heterologous overexpression of *Arabidopsis* AR genes into tobacco could be precisely explored their AR potentiality in different physiological environments. The ultimate goal is transferring the *AtStr5-AtPCS1* and *AtStr17a-AtPCS1* into a plant which has all the attribute for phytoremediation. On that account, tobacco is an excellent candidate for phytoremediation, while it produces a considerable amount of biomass and an immense number of seeds in each generation. Thus, transgenic lines that are developed from this work can be directly used for the As-phytoremediation purpose. In a first attempt, we did not obtain a considerable number of transgenic plants for further verification, such as for southern blotting and m-RNA expression study. However, it is possible to produce a huge number of transgenic plants by repeating the transformation process. It should be mentioned, that the transgenic plants that are developed from this experiment carrying three foreign genes, hence, gene silencing can occur in this plant. Therefore, a huge amount of transgenic plants needs to be screened to obtain the desired one. In this work, only one *AtStr5-AtPCS1* stable line was produced.

On the other hand, the nine *AtStr17a-AtPCS1* overexpressing lines were revealed as chimeric in the 2<sup>nd</sup> generation. However, *AtStr17a-AtPCS1* overexpressing lines can be further developed by repeating the transformation process and selecting a higher number of the transgenic plant. Also, cutting should be made in the first generation to avoid the loss of the transgenic plant entirely because of chimerism.

All the mutants obtained from *Arabidopsis* and tobacco need to be tested under different arsenic and sulfur concentration. It is expected that concerted effort of *AtStr5-AtPCS1* and *AtStr17a-AtPCS1* genes might assist to develop the effective As-phytoremediation system.

## 2 Future prospects

It is beyond to describe that effective arsenic (As) phytoremediation required a detailed understanding of the mechanism of As-detoxification. The enzyme arsenate reductase (AR) is very crucial for the reduction of arsenate [As (V)], which is the initial step of the As-detoxification process. In plants, few potential AR genes have been reported. It seems promising to improve the As-phytoremediation system by modulating those potential ARs. On that account, the *Arabidopsis* potential AR genes *AtStr5* (*AtACR2*) and *AtStr17a* (*HAC1/ATQ1*) were studied in this work to unravel their role in the As-detoxification process. Primarily the function of the former one (*AtStr5/AtACR2*) has gained attention because of its ability to catalyze phosphate, arsenate and sulfur-rich substrates *in vitro*. Notably, the active site of *AtStr5* (*AtACR2*) is shared by the enzyme family of AR and CDC25. Due to sharing the similar structural association and same catalytic motif the function of *AtStr5* protein remains ambiguous. However, the biochemical data obtained from this study pointed out that *AtStr5* function towards arsenate reduction rather than sulfurtransferase (Str) and phosphatase. Furthermore, the mutants developed in this work are an excellent resource to establish its role further and can provide a deeper insight into the As detoxification process.

---

## REFERENCES

- Adams H, Teertstra W, Koster M, Tommassen J (2002) PspE (phage-shock protein E) of *Escherichia coli* is a rhodanese. *FEBS Letters* 518:173-176
- Bartels A (2006) Functional characterization of sulfurtransferase proteins in higher plants. PhD Thesis, Leibniz Universität Hannover
- Bartels A, Mock H-P, Papenbrock J (2007) Differential expression of *Arabidopsis* sulfurtransferases under various growth conditions. *Plant Physiology and Biochemistry* 45:178-187
- Bauer M, Dietrich C, Nowak K, Sierralta WD, Papenbrock J (2004) Intracellular localization of *Arabidopsis* sulfurtransferases. *Plant Physiology* 135:916-926
- Bauer M, Papenbrock J (2002) Identification and characterization of single-domain thiosulfate sulfurtransferases from *Arabidopsis thaliana*. *FEBS Letters* 532:427-431
- Bechtold N, Pelletier G (1998) In planta *Agrobacterium*-mediated transformation of adult *Arabidopsis thaliana* plants by vacuum infiltration. *Arabidopsis Protocols*. Springer, pp 259-266
- Becker D (1990) Binary vectors which allow the exchange of plant selectable markers and reporter genes. *Nucleic Acids Research* 18:203
- Bhattacharjee H, Sheng J, Ajees AA, Mukhopadhyay R, Rosen BP (2010) Adventitious arsenate reductase activity of the catalytic domain of the human Cdc25B and Cdc25C phosphatases. *Biochemistry* 49:802-809
- Bhattacharya P, Samal A, Majumdar J, Santra S (2010) Arsenic contamination in rice, wheat, pulses, and vegetables: a study in an arsenic-affected area of West Bengal, India. *Water, Air, & Soil Pollution* 213:3-13
- Bienert GP, Thorsen M, Schüssler MD, Nilsson HR, Wagner A, Tamás MJ, Jahn TP (2008) A subgroup of plant aquaporins facilitate the bi-directional diffusion of As(OH)<sub>3</sub> and Sb(OH)<sub>3</sub> across membranes. *BMC Biology* 6:26
- Bleeker PM, Hakvoort HW, Bliet M, Souer E, Schat H (2006) Enhanced arsenate reduction by a CDC25-like tyrosine phosphatase explains increased phytochelatin accumulation in arsenate-tolerant *Holcus lanatus*. *The Plant Journal* 45:917-929

- Bobrowicz P, Wysocki R, Owsianik G, Goffeau A, Ułaszewski S (1997) Isolation of three contiguous genes, *ACR1*, *ACR2*, and *ACR3*, involved in resistance to arsenic compounds in the yeast *Saccharomyces cerevisiae*. *Yeast* 13:819-828
- Bondada BR, Ma LQ (2003) Tolerance of heavy metals in vascular plants: arsenic hyperaccumulation by Chinese brake fern (*Pteris vittata* L.). *Pteridology in the New Millennium*. Springer, pp 397-420
- Bordo D, Bork P (2002) The rhodanese/Cdc25 phosphatase superfamily. *EMBO Reports* 3:741-746
- Bordo D, Deriu D, Colnaghi R, Carpen A, Pagani S, Bolognesi M (2000) The crystal structure of a sulfurtransferase from *Azotobacter vinelandii* highlights the evolutionary relationship between the rhodanese and phosphatase enzyme families. *Journal of Molecular Biology* 298:691-704
- Boutros R, Lobjois V, Ducommun B (2007) CDC25 phosphatases in cancer cells: key players? Good targets? *Nature Reviews Cancer* 7:495-507
- Bradford MM (1976) A rapid and sensitive method for the quantitation of microgram quantities of protein utilizing the principle of protein-dye binding. *Analytical Biochemistry* 72:248-254
- Breuer C, Braidwood L, Sugimoto K (2014) Endocycling in the path of plant development. *Current Opinion in Plant Biology* 17:78-85
- Brunetti P, Zanella L, Proia A, De Paolis A, Falasca G, Altamura MM, Sanità di Toppi L, Costantino P, Cardarelli M (2011) Cadmium tolerance and phytochelatin content of *Arabidopsis* seedlings over-expressing the *phytochelatin synthase AtPCS1* gene. *Journal of Experimental Botany* 62:5509-5519
- Burow M, Kessler D, Papenbrock J (2002) Enzymatic activity of the *Arabidopsis* sulfurtransferase resides in the C-terminal domain but is boosted by the N-terminal domain and the linker peptide in the full-length enzyme. *Biological Chemistry* 383:1363-1372
- Capone I, Spano L, Cardarelli M, Bellincampi D, Petit A, Costantino P (1989) Induction and growth properties of carrot roots with different complements of *Agrobacterium rhizogenes* T-DNA. *Plant Molecular Biology* 13:43-52
- Carbonell A, Aarabi M, DeLaune R, Gambrell R, Patrick Jr W (1998) Arsenic in wetland vegetation: availability, phytotoxicity, uptake, and effects on plant growth and nutrition. *The Science of the Total Environment* 217:189-199

- Cardarelli M, Mariotti D, Pomponi M, Spano L, Capone I, Costantino P (1987) *Agrobacterium rhizogenes* T-DNA genes capable of inducing hairy root phenotype. *Molecular and General Genetics MGG* 209:475-480
- Cervantes C, Ji G, Ramirez J, Silver S (1994) Resistance to arsenic compounds in microorganisms. *FEMS Microbiology Reviews* 15:355-367
- Chao D-Y, Chen Y, Chen J, Shi S, Chen Z, Wang C, Danku JM, Zhao F-J, Salt DE (2014) Genome-wide association mapping identifies a new arsenate reductase enzyme critical for limiting arsenic accumulation in plants. *PLoS Biol* 12:e1002009
- Chou W-C, Jie C, Kenedy AA, Jones RJ, Trush MA, Dang CV (2004) Role of NADPH oxidase in arsenic-induced reactive oxygen species formation and cytotoxicity in myeloid leukemia cells. *Proceedings of the National Academy of Sciences of the United States of America* 101:4578-4583
- Cipollone R, Ascenzi P, Visca P (2007) Common themes and variations in the rhodanese superfamily. *IUBMB Life* 59:51-59
- Claire-Lise M, Nathalie V (2012) The use of the model species *Arabidopsis halleri* towards phytoextraction of polluted cadmium soils. *New Biotechnology* 30:9-14
- Claros MG, Vincens P (1996) Computational method to predict mitochondrially imported proteins and their targeting sequences. *The FEBS Journal* 241:779-786
- Clemens S, Kim EJ, Neumann D, Schroeder JI (1999) Tolerance to toxic metals by a gene family of *phytochelatin synthases* from plants and yeast. *The EMBO Journal* 18:3325-3333
- Clemens S, Schroeder JI, Degenkolb T (2001) *Caenorhabditis elegans* expresses a functional phytochelatin synthase. *The FEBS Journal* 268:3640-3643
- Clough SJ, Bent AF (1998) Floral dip: a simplified method for *Agrobacterium*-mediated transformation of *Arabidopsis thaliana*. *The Plant Journal* 16:735-743
- Cobbett C, Goldsbrough P (2002) Phytochelatins and metallothioneins: roles in heavy metal detoxification and homeostasis. *Annual Review of Plant Biology* 53:159-182
- Cobbett CS (1999) A family of *phytochelatin synthase* genes from plant, fungal and animal species. *Trends in Plant Science* 4:335-337
- Cobbett CS (2000) Phytochelatins and their roles in heavy metal detoxification. *Plant Physiology* 123:825-832

- Colnaghi R, Cassinelli G, Drummond M, Forlani F, Pagani S (2001) Properties of the *Escherichia coli* rhodanese-like protein SseA: contribution of the active-site residue Ser240 to sulfur donor recognition. *FEBS Letters* 500:153-156
- Cunningham SD, Berti WR, Huang JW (1995) Phytoremediation of contaminated soils. *Trends in Biotechnology* 13:393-397
- Dave R, Tripathi RD, Dwivedi S, Tripathi P, Dixit G, Sharma YK, Trivedi PK, Corpas FJ, Barroso JB, Chakrabarty D (2013) Arsenate, and arsenite exposure modulate antioxidants and amino acids in contrasting arsenic accumulating rice (*Oryza sativa* L.) genotypes. *Journal of Hazardous Materials* 262:1123-1131
- Denu JM, Zhou G, Wu L, Zhao R, Yuvaniyama J, Saper MA, Dixon JE (1995) The purification and characterization of a human dual-specific protein tyrosine phosphatase. *Journal of Biological Chemistry* 270:3796-3803
- Desbrosses-Fonrouge A-G, Voigt K, Schröder A, Arrivault S, Thomine S, Krämer U (2005) *Arabidopsis thaliana* *MTP1* is a Zn transporter in the vacuolar membrane which mediates Zn detoxification and drives leaf Zn accumulation. *FEBS Letters* 579:4165-4174
- Dhankher OP, Rosen BP, McKinney EC, Meagher RB (2006) Hyperaccumulation of arsenic in the shoots of *Arabidopsis* silenced for *arsenate reductase* (*ACR2*). *Proceedings of the National Academy of Sciences* 103:5413-5418
- Di Toppi LS, Vurro E, De Benedictis M, Falasca G, Zanella L, Musetti R, Lenucci MS, Dalessandro G, Altamura MM (2012) A biphasic response to cadmium stress in carrot: early acclimatory mechanisms give way to root collapse further to prolonged metal exposure. *Plant Physiology and Biochemistry* 58:269-279
- Dissmeyer N, Weimer AK, Pusch S, De Schutter K, Kamei CLA, Nowack MK, Novak B, Duan G-L, Zhu Y-G, De Veylder L (2009) Control of cell proliferation, organ growth, and DNA damage response operate independently of dephosphorylation of the *Arabidopsis* Cdk1 homolog CDKA; 1. *The Plant Cell* 21:3641-3654
- Dixit G, Singh AP, Kumar A, Singh PK, Kumar S, Dwivedi S, Trivedi PK, Pandey V, Norton GJ, Dhankher OP (2015) Sulfur mediated reduction of arsenic toxicity involves efficient thiol metabolism and the antioxidant defense system in rice. *Journal of Hazardous Materials* 298:241-251
- Donadio S, Shafiee A, Hutchinson C (1990) Disruption of a rhodanese-like gene results in cysteine auxotrophy in *Saccharopolyspora erythraea*. *Journal of Bacteriology* 172:350-360
- Donzelli M, Draetta GF (2003) Regulating mammalian checkpoints through Cdc25 inactivation. *EMBO Reports* 4:671-677

- Doucleff M, Terry N (2002) Pumping out the arsenic. Nature Publishing Group
- Drewniak L, Sklodowska A (2013) Arsenic-transforming microbes and their role in biomining processes. *Environmental Science and Pollution Research* 20:7728-7739
- Duan G-L, Hu Y, Liu W-J, Kneer R, Zhao F-J, Zhu Y-G (2011) Evidence for a role of phytochelatins in regulating arsenic accumulation in rice grain. *Environmental and Experimental Botany* 71:416-421
- Duan G-L, Zhu Y-G, Tong Y-P, Cai C, Kneer R (2005) Characterization of arsenate reductase in the extract of roots and fronds of Chinese brake fern, an arsenic hyperaccumulator. *Plant Physiology* 138:461-469
- Duan GL, Zhou Y, Tong YP, Mukhopadhyay R, Rosen BP, Zhu YG (2007) A CDC25 homolog from rice functions as an arsenate reductase. *New Phytologist* 174:311-321
- Duker AA, Carranza E, Hale M (2005) Arsenic Geochemistry and Health. *Environment International* 31:631-641
- Dunphy WG, Kumagai A (1991) The Cdc25 protein contains an intrinsic phosphatase activity. *Cell* 67:189-196
- Eckstein JW, Beer-Romero P, Berdo I (1996) Identification of an essential acidic residue in Cdc25 protein phosphatase and a general three-dimensional model for a core region in protein phosphatases. *Protein Science* 5:5-12
- Ellis DR, Gumaelius L, Indriolo E, Pickering IJ, Banks JA, Salt DE (2006) A novel arsenate reductase from the arsenic hyperaccumulating fern *Pteris vittata*. *Plant Physiology* 141:1544-1554
- Fauman EB, Cogswell JP, Lovejoy B, Rocque WJ, Holmes W, Montana VG, Piwnicka-Worms H, Rink MJ, Saper MA (1998) Crystal structure of the catalytic domain of the human cell cycle control phosphatase, Cdc25A. *Cell* 93:617-625
- Forlani F, Carpen A, Pagani S (2003) Evidence that elongation of the catalytic loop of the *Azotobacter vinelandii* rhodanese changed selectivity from sulfur-to phosphate-containing substrates. *Protein Engineering* 16:515-519
- Gasic K, Korban SS (2007) Transgenic Indian mustard (*Brassica juncea*) plants expressing an *Arabidopsis phytochelatin synthase (AtPCS1)* exhibit enhanced As and Cd tolerance. *Plant Molecular Biology* 64:361-369

Gasteiger E, Hoogland C, Gattiker A, Duvaud Se, Wilkins MR, Appel RD, Bairoch A (2005) Protein identification and analysis tools on the ExPASy server. Springer

Ghosh M, Shen J, Rosen BP (1999) Pathways of As (III) detoxification in *Saccharomyces cerevisiae*. Proceedings of the National Academy of Sciences 96:5001-5006

Gladysheva TB, Oden KL, Rosen BP (1994) Properties of the arsenate reductase of plasmid R773. Biochemistry 33:7288-7293

Gliubich F, Gazerro M, Zanotti G, Delbono S, Bombieri G, Berni R (1996) Active site structural features for chemically modified forms of rhodanese. Journal of Biological Chemistry 271:21054-21061

Glowacka K, Kromdijk J, Leonelli L, Niyogi KK, Clemente TE, Long SP (2016) An evaluation of new and established methods to determine T-DNA copy number and homozygosity in transgenic plants. Plant, Cell & Environment 39:908-917

Gottlin EB, Xu X, Epstein DM, Burke SP, Eckstein JW, Ballou DP, Dixon JE (1996) Kinetic analysis of the catalytic domain of human Cdc25B. Journal of Biological Chemistry 271:27445-27449

Grill E, Mishra S, Srivastava S, Tripathi R (2007) Role of phytochelatins in phytoremediation of heavy metals. Environmental Bioremediation Technologies. Springer, pp 101-146

Grill E, Winnacker E-L, Zenk MH (1985) Phytochelatins: the principal heavy-metal complexing peptides of higher plants. Science (New York, NY) 230:674-676

Ha S-B, Smith AP, Howden R, Dietrich WM, Bugg S, O'Connell MJ, Goldsbrough PB, Cobbett CS (1999) *Phytochelatase synthase* genes from *Arabidopsis* and the yeast *Schizosaccharomyces pombe*. The Plant Cell 11:1153-1163

Harashima H, Schnittger A (2010) The integration of cell division, growth and differentiation. Current Opinion in Plant Biology 13:66-74

Harrison SJ, Mott EK, Parsley K, Aspinall S, Gray JC, Cottage A (2006) A rapid and robust method of identifying transformed *Arabidopsis thaliana* seedlings following floral dip transformation. Plant Methods 2:19

Hatzfeld Y, Saito K (2000) Evidence for the existence of rhodanese (thiosulfate: cyanide sulfurtransferase) in plants: preliminary characterization of two rhodanese cDNAs from *Arabidopsis thaliana*. FEBS Letters 470:147-150



- Helleday T, Nilsson R, Jenssen D (2000) Arsenic [III] and heavy metal ions induce intrachromosomal homologous recombination in the hprt gene of V79 Chinese hamster cells. *Environmental and Molecular Mutagenesis* 35:114-122
- Henne M, König N, Triulzi T, Baroni S, Forlani F, Scheibe R, Pappenbrock J (2015) Sulfurtransferase and thioredoxin specifically interact as demonstrated by bimolecular fluorescence complementation analysis and biochemical tests. *FEBS Open Bio* 5:832-843
- Höfgen R, Willmitzer L (1990) Biochemical and genetic analysis of different patatin isoforms expressed in various organs of potato (*Solanum tuberosum*). *Plant Science* 66:221-230
- Hofmann K, Bucher P, Kajava AV (1998) A model of the Cdc25 phosphatase catalytic domain and Cdk-interaction surface based on the presence of a rhodanese homology domain. *J Mol Biol* 282:195-208
- Hu Z-Y, Zhu Y-G, Li M, Zhang L-G, Cao Z-H, Smith FA (2007) Sulfur (S)-induced enhancement of iron plaque formation in the rhizosphere reduces arsenic accumulation in rice (*Oryza sativa* L.) seedlings. *Environmental Pollution* 147:387-393
- Isayenkov SV, Maathuis FJ (2008) The *Arabidopsis thaliana* aquaglyceroporin *AtNIP7;1* is a pathway for arsenite uptake. *Febs Letters* 582:1625-1628
- Ji G, Garber EA, Armes LG, Chen C-M, Fuchs JA, Silver S (1994) Arsenate reductase of *Staphylococcus aureus* plasmid pI258. *Biochemistry* 33:7294-7299
- Jorgensen R, Snyder C, Jones JDG (1987) T-DNA is organized predominantly in inverted repeat structures in plants transformed with *Agrobacterium tumefaciens* C58 derivatives. *Molecular and General Genetics MGG* 207:471-477
- Karlsson-Rosenthal C, Millar JB (2006) Cdc25: mechanisms of checkpoint inhibition and recovery. *Trends in Cell Biology* 16:285-292
- Katavic V, Haughn GW, Reed D, Martin M, Kunst L (1994) In planta transformation of *Arabidopsis thaliana*. *Molecular and General Genetics MGG* 245:363-370
- Komaki S, Sugimoto K (2012) Control of the plant cell cycle by developmental and environmental cues. *Plant and Cell Physiology* 53:953-964
- Kosugi S, Hasebe M, Entani T, Takayama S, Tomita M, Yanagawa H (2008) Design of peptide inhibitors for the importin  $\alpha/\beta$  nuclear import pathway by activity-based profiling. *Chemistry & Biology* 15:940-949

- Kosugi S, Hasebe M, Tomita M, Yanagawa H (2009) Systematic identification of cell cycle-dependent yeast nucleocytoplasmic shuttling proteins by prediction of composite motifs. *Proceedings of the National Academy of Sciences* 106:10171-10176
- Laemmli UK (1970) Cleavage of structural proteins during the assembly of the head of bacteriophage T4. *Nature* 227:680-685
- Landrieu I, da Costa M, De Veylder L, Dewitte F, Vandepoele K, Hassan S, Wieruszeski J-M, Faure J-D, Van Montagu M, Inzé D (2004a) A small CDC25 dual-specificity tyrosine-phosphatase isoform in *Arabidopsis thaliana*. *Proceedings of the National Academy of Sciences of the United States of America* 101:13380-13385
- Landrieu I, Hassan S, Sauty M, Dewitte F, Wieruszeski J-M, Inzé D, De Veylder L, Lippens G (2004b) Characterization of the *Arabidopsis thaliana* Arath; CDC25 dual-specificity tyrosine phosphatase. *Biochemical and Biophysical Research Communications* 322:734-739
- Lei M, Wan X-m, Li X-w, Chen T-b, Liu Y-r, Huang Z-c (2013) Impacts of sulfur regulation in vivo on arsenic accumulation and tolerance of hyperaccumulator *Pteris vittata*. *Environmental and Experimental Botany* 85:1-6
- Leimkühler S, Rajagopalan K (2001) A sulfurtransferase is required in the transfer of cysteine sulfur in the in vitro synthesis of molybdopterin from precursor Z in *Escherichia coli*. *Journal of Biological Chemistry* 276:22024-22031
- Leonard A, Lauwerys R (1980) Carcinogenicity, teratogenicity and mutagenicity of arsenic. *Mutation Research/Reviews in Genetic Toxicology* 75:49-62
- Li Y, Dhankher O, Carreira L, Balish R, Meagher R (2005) Engineered overexpression of *γ-glutamylcysteine synthetase* in plants confers high-level arsenic and mercury tolerance. *Environ Toxicol Chem* 24:1376-1386
- Li Y, Dhankher OP, Carreira L, Lee D, Chen A, Schroeder JI, Balish RS, Meagher RB (2004) Overexpression of *phytochelatin synthase* in *Arabidopsis* leads to enhanced arsenic tolerance and cadmium hypersensitivity. *Plant and Cell Physiology* 45:1787-1797
- Libiad M, Motl N, Akey DL, Sakamoto N, Fearon ER, Smith JL, Banerjee R (2018) Thiosulfate sulfurtransferase like domain containing 1 protein interacts with thioredoxin. *Journal of Biological Chemistry* 293:2675-2686
- Liu W-J, Wood BA, Raab A, McGrath SP, Zhao F-J, Feldmann J (2010) Complexation of arsenite with phytochelatin reduces arsenite efflux and translocation from roots to shoots in *Arabidopsis*. *Plant Physiology* 152:2211-2221

- Louie M, Kondor N, DeWitt JG (2003) Gene expression in cadmium-tolerant *Datura innoxia*: detection and characterization of cDNAs induced in response to Cd<sup>2+</sup>. *Plant Molecular Biology* 52:81-89
- Luo Y, Christie P, Baker A (2000) Soil solution Zn and pH dynamics in non-rhizosphere soil and in the rhizosphere of *Thlaspi caerulescens* grown in a Zn/Cd-contaminated soil. *Chemosphere* 41:161-164
- Ma JF, Yamaji N, Mitani N, Xu X-Y, Su Y-H, McGrath SP, Zhao F-J (2008) Transporters of arsenite in rice and their role in arsenic accumulation in rice grain. *Proceedings of the National Academy of Sciences* 105:9931-9935
- Mailand N, Falck J, Lukas C, Syljuasen RG, Welcker M, Bartek J, Lukas J (2000) Rapid destruction of human Cdc25A in response to DNA damage. *Science (New York, NY)* 288:1425-1429
- Mailand N, Podtelejnikov AV, Groth A, Mann M, Bartek J, Lukas J (2002) Regulation of G 2/M events by Cdc25A through phosphorylation-dependent modulation of its stability. *The EMBO Journal* 21:5911-5920
- Martin P, DeMel S, Shi J, Gladysheva T, Gatti DL, Rosen BP, Edwards BF (2001) Insights into the structure, solvation, and mechanism of ArsC arsenate reductase, a novel arsenic detoxification enzyme. *Structure* 9:1071-1081
- Matthies A, Rajagopalan K, Mendel RR, Leimkühler S (2004) Evidence for the physiological role of a rhodanese-like protein for the biosynthesis of the molybdenum cofactor in humans. *Proceedings of the National Academy of Sciences of the United States of America* 101:5946-5951
- Meharg A, Macnair M (1992) Suppression of the high-affinity phosphate uptake system: a mechanism of arsenate tolerance in *Holcus lanatus* L. *Journal of Experimental Botany* 43:519-524
- Meharg AA, Jardine L (2003) Arsenite transport into paddy rice (*Oryza sativa*) roots. *New Phytologist* 157:39-44
- Meharg AA, Rahman MM (2003) Arsenic contamination of Bangladesh paddy field soils: implications for rice contribution to arsenic consumption. *Environmental Science & Technology* 37:229-234

Meharg AA, Williams PN, Adomako E, Lawgali YY, Deacon C, Villada A, Cambell RC, Sun G, Zhu Y-G, Feldmann J (2009) Geographical variation in total and inorganic arsenic content of polished (white) rice. *Environmental Science & Technology* 43:1612-1617

Messens J, Hayburn G, Desmyter A, Laus G, Wyns L (1999) The essential catalytic redox couple in arsenate reductase from *Staphylococcus aureus*. *Biochemistry* 38:16857-16865

Meyer T, Burow M, Bauer M, Papenbrock J (2003) *Arabidopsis* sulfurtransferases: investigation of their function during senescence and in cyanide detoxification. *Planta* 217:1-10

Millar J, McGowan CH, Lenaers G, Jones R, Russell P (1991) p80cdc25 mitotic inducer is the tyrosine phosphatase that activates p34cdc2 kinase in fission yeast. *The EMBO Journal* 10:4301-4309

Millar JB, Russell P (1992) The Cdc25 M-phase inducer: an unconventional protein phosphatase. *Cell* 68:407-410

Mishra S, Dubey RS (2006) Inhibition of ribonuclease and protease activities in arsenic-exposed rice seedlings: the role of proline as enzyme protectant. *Journal of Plant Physiology* 163:927-936

Mishra S, Wellenreuther G, Mattusch J, Stärk H-J, Küpper H (2013) Speciation and distribution of arsenic in the non-hyperaccumulator macrophyte *Ceratophyllum demersum*. *Plant Physiology* 163:1396-1408

Motl N, Skiba MA, Kabil O, Smith JL, Banerjee R (2017) Structural and biochemical analyses indicate that a bacterial persulfide dioxygenase-rhodanese fusion protein functions in sulfur assimilation. *Journal of Biological Chemistry* 292:14026-14038

Mueller EG, Palenchar PM, Buck CJ (2001) The role of the cysteine residues of ThiI in the generation of 4-thiouridine in tRNA. *Journal of Biological Chemistry* 276:33588-33595

Mukhopadhyay R, Rosen BP (1998) *Saccharomyces cerevisiae* ACR2 gene encodes an arsenate reductase. *FEMS Microbiology Letters* 168:127-136

Mukhopadhyay R, Rosen BP (2001) The phosphatase C(X)<sub>5</sub>R motif is required for catalytic activity of the *Saccharomyces cerevisiae* Acr2p arsenate reductase. *Journal of Biological Chemistry* 276:34738-34742

Mukhopadhyay R, Rosen BP (2002) Arsenate reductases in prokaryotes and eukaryotes. *Environmental Health Perspectives* 110:745

- Mukhopadhyay R, Shi J, Rosen BP (2000) Purification and Characterization of *Acr2p*, the *Saccharomyces cerevisiae* Arsenate Reductase. *Journal of Biological Chemistry* 275:21149-21157
- Mukhopadhyay R, Zhou Y, Rosen BP (2003) Directed evolution of a yeast arsenate reductase into a protein-tyrosine phosphatase. *Journal of Biological Chemistry* 278:24476-24480
- Murashige T, Skoog F (1962) A revised medium for rapid growth and bioassays with tobacco tissue cultures. *Physiologia Plantarum* 15:473-497
- Nagahara N, Ito T, Minami M (1999) Mercaptopyruvate sulfurtransferase as a defense against cyanide toxication: molecular properties and mode of detoxification. *Histology and Histopathology* 14:1277-1286
- Nagahara N, Okazaki T, Nishino T (1995) Cytosolic mercaptopyruvate sulfurtransferase is evolutionarily related to mitochondrial rhodanese: striking similarity in active site amino acid sequence and the increase in the mercaptopyruvate sulfurtransferase activity of rhodanese by site-directed mutagenesis. *Journal of Biological Chemistry* 270:16230-16235
- Nahar N, Rahman A, Nawani NN, Ghosh S, Mandal A (2017) Phytoremediation of arsenic from the contaminated soil using transgenic tobacco plants expressing *ACR2* gene of *Arabidopsis thaliana*. *Journal of Plant Physiology* 218:121-126
- Nakamura T, Yamaguchi Y, Sano H (2000) Plant mercaptopyruvate sulfurtransferases. *European Journal of Biochemistry* 267:5621-5630
- Nandi DL, Horowitz PM, Westley J (2000) Rhodanese as a thioredoxin oxidase. *The International Journal of Biochemistry & Cell Biology* 32:465-473
- Neelam Redekar and Papenbrock Jutta (2010, unpublished) Arsenate reductase activity of AtStr5
- Nowak K, Luniak N, Meyer S, Schulze J, Mendel R, Hänsch R (2004) Fluorescent proteins in poplar: a useful tool to study promoter function and protein localization. *Plant Biology* 6:65-73
- Ogasawara Y, Lacourciere G, Stadtman TC (2001) Formation of a selenium-substituted rhodanese by reaction with selenite and glutathione: possible role of a protein perselenide in a selenium delivery system. *Proceedings of the National Academy of Sciences* 98:9494-9498

- Okkenhaug G, Zhu Y-G, He J, Li X, Luo L, Mulder J (2012) Antimony (Sb) and arsenic (As) in Sb mining impacted paddy soil from Xikuangshan, China: differences in mechanisms controlling soil sequestration and uptake in rice. *Environmental Science & Technology* 46:3155-3162
- Pagani S, Bonomi F, Cerletti P (1984) Enzymic synthesis of the iron-sulfur cluster of spinach ferredoxin. *The FEBS Journal* 142:361-366
- Palenchar PM, Buck CJ, Cheng H, Larson TJ, Mueller EG (2000) Evidence that ThiI, an enzyme shared between thiamin and 4-thiouridine biosynthesis, may be a sulfurtransferase that proceeds through a persulfide intermediate. *Journal of Biological Chemistry* 275:8283-8286
- Panda S, Upadhyay R, Nath S (2010) Arsenic stress in plants. *Journal of Agronomy and Crop Science* 196:161-174
- Papenbrock J, Grimm B (2001) Regulatory network of tetrapyrrole biosynthesis—studies of intracellular signaling involved in the metabolic and developmental control of plastids. *Planta* 213:667-681
- Papenbrock J, Schmidt A (2000a) Characterization of a sulfurtransferase from *Arabidopsis thaliana*. *European Journal of Biochemistry* 267:145-154
- Papenbrock J, Schmidt A (2000b) Characterization of two sulfurtransferase isozymes from *Arabidopsis thaliana*. *European Journal of Biochemistry* 267:5571-5579
- Picault N, Cazalé A, Beyly A, Cuiné S, Carrier P, Luu D, Forestier C, Peltier G (2006) Chloroplast targeting of phytochelatin synthase in *Arabidopsis*: effects on heavy metal tolerance and accumulation. *Biochimie* 88:1743-1750
- Ploegman JH, Drent G, Kalk KH, Hol W, Heinrikson RL, Keim P, Weng L, Russell J (1978) The covalent and tertiary structure of bovine liver rhodanese. *Nature* 273:124-129
- Ploegman JH, Drent G, Kalk KH, Hol WG (1979) The structure of bovine liver rhodanese: II. The active site in the sulfur-substituted and the sulfur-free enzyme. *Journal of Molecular Biology* 127:149-162
- Pomponi M, Censi V, Di Girolamo V, De Paolis A, di Toppi LS, Aromolo R, Costantino P, Cardarelli M (2006) Overexpression of *Arabidopsis phytochelatin synthase* in tobacco plants enhances Cd<sup>2+</sup> tolerance and accumulation but not translocation to the shoot. *Planta* 223:180-190

- Pot DA, Dixon JE (1992) A thousand and two protein tyrosine phosphatases. *Biochimica et Biophysica Acta (BBA)-Molecular Cell Research* 1136:35-43
- Raab A, Schat H, Meharg AA, Feldmann J (2005) Uptake, translocation and transformation of arsenate and arsenite in sunflower (*Helianthus annuus*): formation of arsenic-phytochelatin complexes during exposure to high arsenic concentrations. *New Phytologist* 168:551-558
- Rausser WE (1990) Phytochelatins. *Annual review of Biochemistry* 59:61-86
- Ray WK, Zeng G, Potters MB, Mansuri AM, Larson TJ (2000a) Characterization of a 12-kilodalton rhodanese encoded by *glpE* of *Escherichia coli* and its interaction with thioredoxin. *Journal of Bacteriology* 182:2277-2284
- Ray WK, Zeng G, Potters MB, Mansuri AM, Larson TJ (2000b) Characterization of a 12-Kilodalton Rhodanese Encoded by *glpE* of *Escherichia coli* and its Interaction with Thioredoxin. *Journal of Bacteriology* 182:2277-2284
- Reumann S, Quan S, Aung K, Yang P, Manandhar-Shrestha K, Holbrook D, Linka N, Switzenberg R, Wilkerson CG, Weber AP (2009) In-depth proteome analysis of *Arabidopsis* leaf peroxisomes combined with in vivo subcellular targeting verification indicates novel metabolic and regulatory functions of peroxisomes. *Plant Physiology* 150:125-143
- Reynolds RA, Yem AW, Wolfe CL, Deibel MR, Chidester CG, Watenpugh KD (1999) Crystal structure of the catalytic subunit of Cdc25B required for G2/M phase transition of the cell cycle. *Journal of Molecular Biology* 293:559-568
- Richly E, Leister D (2004) An improved prediction of chloroplast proteins reveals diversities and commonalities in the chloroplast proteomes of *Arabidopsis* and rice. *Gene* 329:11-16
- Russell J, Weng L, Keim PS, Henrikson R (1978) The covalent structure of bovine liver rhodanese. Isolation and partial structural analysis of cyanogen bromide fragments and the complete sequence of the enzyme. *Journal of Biological Chemistry* 253:8102-8108
- Maniatis T, Fritsch EF, Sambrook J (1982) *Molecular cloning: a laboratory manual*, Cold Spring Harbor laboratory. Cold Spring Harbor, NY
- Sánchez-Bermejo E, Castrillo G, Del Llano B, Navarro C, Zarco-Fernández S, Martínez-Herrera DJ, Leo-del Puerto Y, Muñoz R, Cámara C, Paz-Ares J (2014) Natural variation in arsenate tolerance identifies an arsenate reductase in *Arabidopsis thaliana*. *Nature Communications* 5

- Sarret G, Harada E, Choi Y-E, Isaure M-P, Geoffroy N, Fakra S, Marcus MA, Birschwilks M, Clemens S, Manceau A (2006) Trichomes of tobacco excrete zinc as zinc-substituted calcium carbonate and other zinc-containing compounds. *Plant Physiology* 141:1021-1034
- Schoof R, Yost L, Eickhoff J, Crecelius E, Cragin D, Meachem D (1999) A market basket survey of inorganic arsenic in food. *Food Chem Toxicol* 37:839–846.
- Schultz J, Milpetz F, Bork P, Ponting CP (1998) SMART, a simple modular architecture research tool: identification of signaling domains. *Proceedings of the National Academy of Sciences* 95:5857-5864
- Sheena S, Nordin AB, Tang CG, Sung-Kun K (2009) Phytoremediation for arsenic contamination: Arsenate reductase. *Research Journal of Biotechnology* 4:26-31
- Shen J, Keithly ME, Armstrong RN, Higgins KA, Edmonds KA, Giedroc DP (2015) *Staphylococcus aureus* *CstB* is a novel multidomain persulfide dioxygenase-sulfurtransferase involved in hydrogen sulfide detoxification. *Biochemistry* 54:4542-4554
- Shi J, Vlamis-Gardikas A, Aslund F, Holmgren A, Rosen BP (1999) Reactivity of Glutaredoxins 1, 2, and 3 from *Escherichia coli* shows that Glutaredoxin 2 is the Primary Hydrogen Donor to ArsC-catalyzed Arsenate Reduction. *Journal of Biological Chemistry* 274:36039-36042
- Shukla D, Kesari R, Mishra S, Dwivedi S, Tripathi RD, Nath P, Trivedi PK (2012) Expression of phytochelatin synthase from aquatic macrophyte *Ceratophyllum demersum* L. enhances cadmium and arsenic accumulation in tobacco. *Plant Cell Reports* 31:1687-1699
- Sokolovsky V, Kaldenhoff R, Ricci M, Russo V (1990) Fast and reliable mini-prep RNA extraction from *Neurospora crassa*. *Fungal Genetics Reports* 37:27
- Song W-Y, Park J, Mendoza-Cózatl DG, Suter-Grotemeyer M, Shim D, Hörtensteiner S, Geisler M, Weder B, Rea PA, Rentsch D (2010) Arsenic tolerance in *Arabidopsis* is mediated by two ABCC-type phytochelatin transporters. *Proceedings of the National Academy of Sciences* 107:21187-21192
- Sorrell D, Chrimes D, Dickinson J, Rogers H, Francis D (2005) The *Arabidopsis* CDC25 induces a short cell length when overexpressed in fission yeast: evidence for cell cycle function. *New Phytologist* 165:425-428
- Southern EM (1975) Detection of specific sequences among DNA fragments separated by gel electrophoresis. *Journal of Molecular Biology* 98:503-517



- Spadafora ND, Doonan JH, Herbert RJ, Bitonti MB, Wallace E, Rogers HJ, Francis D (2010) *Arabidopsis* T-DNA insertional lines for CDC25 are hypersensitive to hydroxyurea but not to zeocin or salt stress. *Annals of Botany* 107:1183-1192
- Spallarossa A, Donahue JL, Larson TJ, Bolognesi M, Bordo D (2001) *Escherichia coli* *GlpE* is a prototype sulfurtransferase for the single-domain rhodanese homology superfamily. *Structure* 9:1117-1125
- Spena A, Schmülling T, Koncz C, Schell J (1987) Independent and synergistic activity of rol A, B and C loci in stimulating abnormal growth in plants. *The EMBO Journal* 6:3891-3899
- Srivastava S, D'souza S (2009) Increasing sulfur supply enhances tolerance to arsenic and its accumulation in *Hydrilla verticillata* (Lf) Royle. *Environmental Science & Technology* 43:6308-6313
- Steffens J (1990) The heavy metal-binding peptides of plants. *Annual Review of Plant Biology* 41:553-575
- Stoger E, Sack M, Nicholson L, Fischer R, Christou P (2005) Recent progress in plantibody technology. *Current Pharmaceutical Design* 11:2439-2457
- Stroud JL, Khan MA, Norton GJ, Islam MR, Dasgupta T, Zhu Y-G, Price AH, Meharg AA, McGrath SP, Zhao F-J (2011) Assessing the labile arsenic pool in contaminated paddy soils by isotopic dilution techniques and simple extractions. *Environmental Science & Technology* 45:4262-4269
- Tanz SK, Castleden I, Small ID, Millar AH (2013) Fluorescent protein tagging as a tool to define the subcellular distribution of proteins in plants. *Frontiers in Plant Science* 4:214
- Tinland B (1996) The integration of T-DNA into plant genomes. *Trends in Plant Science* 1:178-184
- Tripathi RD, Tripathi P, Dwivedi S, Kumar A, Mishra A, Chauhan PS, Norton GJ, Nautiyal CS (2014) Roles for root iron plaque in sequestration and uptake of heavy metals and metalloids in aquatic and wetland plants. *Metallomics* 6:1789-1800
- Tzfira T, Li J, Lacroix B, Citovsky V (2004) *Agrobacterium* T-DNA integration: molecules and models. *Trends in Genetics* 20:375-383

- Ullrich-Eberius C, Sanz A, Novacky A (1989) Evaluation of arsenate-and vanadate-associated changes of electrical membrane potential and phosphate transport in *Lemna gibba* G1. *Journal of Experimental Botany*:119-128
- Vagenende V, Yap MG, Trout BL (2009) Mechanisms of protein stabilization and prevention of protein aggregation by glycerol. *Biochemistry* 48:11084-11096
- Vatamaniuk OK, Bucher EA, Ward JT, Rea PA (2001) A New Pathway for Heavy Metal Detoxification in Animals phytochelatin synthase is required for cadmium tolerance in *Caenorhabditis elegans*. *Journal of Biological Chemistry* 276:20817-20820
- Vatamaniuk OK, Mari S, Lu Y-P, Rea PA (1999) *AtPCS1*, a *phytochelatin synthase* from *Arabidopsis*: isolation and in vitro reconstitution. *Proceedings of the National Academy of Sciences* 96:7110-7115
- Vennesland B, Castric P, Conn E, Solomonson L, Volini M, Westley J (1982) Cyanide metabolism. *Federation Proceedings*, p2639
- Westley J (1973) Rhodanese. *Advances in Enzymology and Related Areas of Molecular Biology* 39:736-737
- Williams P, Price A, Raab A, Hossain S, Feldmann J, Meharg AA (2005) Variation in arsenic speciation and concentration in paddy rice related to dietary exposure. *Environmental Science & Technology* 39:5531-5540
- Williams PN, Lei M, Sun G, Huang Q, Lu Y, Deacon C, Meharg AA, Zhu Y-G (2009) Occurrence and partitioning of cadmium, arsenic, and lead in mine-impacted paddy rice: Hunan, China. *Environmental Science & Technology* 43:637-642
- Wojas S, Clemens S, Hennig J, Skłodowska A, Kopera E, Schat H, Bal W, Antosiewicz DM (2008) Overexpression of *phytochelatin synthase* in tobacco: distinctive effects of *AtPCS1* and *CePCS* genes on plant response to cadmium. *Journal of Experimental Botany* 59:2205-2219
- Wood JL, Fiedler H (1953)  $\beta$ -Mercaptopyruvate, a substrate for rhodanese. *Journal of Biological Chemistry* 205:231-234
- Wu G, Kang H, Zhang X, Shao H, Chu L, Ruan C (2010) A critical review on the bio-removal of hazardous heavy metals from contaminated soils: issues, progress, eco-environmental concerns, and opportunities. *Journal of Hazardous Materials* 174:1-8

- Wu Z, Ren H, McGrath SP, Wu P, Zhao F-J (2011) Investigating the contribution of the phosphate transport pathway to arsenic accumulation in rice. *Plant Physiology* 157:498-508
- Yoo S-D, Cho Y-H, Sheen J (2007) *Arabidopsis* mesophyll protoplasts: a versatile cell system for transient gene expression analysis. *Nature Protocols* 2:1565-1572
- Zanella L, Fattorini L, Brunetti P, Roccotiello E, Cornara L, D'Angeli S, Della Rovere F, Cardarelli M, Barbieri M, Sanità di Toppi L, Degola F, Lindberg S, Altamura MM, Falasca G (2016) Overexpression of *AtPCSI* in tobacco increases arsenic and arsenic plus cadmium accumulation and detoxification. *Planta* 243:605-622
- Zegers I, Martins JC, Willem R, Wyns L, Messens J (2001) Arsenate reductase from *S. aureus* plasmid pI258 is a phosphatase drafted for redox duty. *Nature Structural and Molecular Biology* 8:843
- Zenk MH (1996) Heavy metal detoxification in higher plants-a review. *Gene* 179:21-30
- Zhang J, Zhao Q-Z, Duan G-L, Huang Y-C (2011) Influence of sulfur on arsenic accumulation and metabolism in rice seedlings. *Environmental and Experimental Botany* 72:34-40
- Zhao F-J, McGrath SP, Meharg AA (2010) Arsenic as a food chain contaminant: mechanisms of plant uptake and metabolism and mitigation strategies. *Annual Review of Plant Biology* 61:535-559
- Zhou Y, Bhattacharjee H, Mukhopadhyay R (2006) Bifunctional role of the leishmanial antimonate reductase LmACR2 as a protein tyrosine phosphatase. *Molecular and Biochemical Parasitology* 148:161-168
- Zhu Y-G, Williams PN, Meharg AA (2008) Exposure to inorganic arsenic from rice: a global health issue? *Environmental Pollution* 154:169-171
- Zvobgo G, Hu H, Shang S, Shamsi IH, Zhang G (2015) The effects of phosphate on the arsenic uptake and toxicity alleviation in tobacco genotypes with differing arsenic tolerances. *Environmental Toxicology and Chemistry* 34:45-52

## ACKNOWLEDGMENTS

First and foremost, I would like to expand core heartfelt thanks to **Prof. Dr. Jutta Papenbrock**, because of her, a woman like me, blessed the opportunity to be here in Germany, to pursue the prestigious PhD program. She made the journey smooth as she always inspired, profound forbearance, and supported all aspects during my doctoral studies. I reckon without her determination, and sagacious direction this journey would not be possible at all.

I would like to thank **Prof. Dr. Bernd Huchzermeyer** for his support and conviction, moreover taking over the vital role as the second supervisor.

Furthermore, I would like to particularly thank **Pamela von Trzebiatowski** and **Julia Volker** for their technical help in the laboratory, but also for their sincere and amicable nature. I would like to thank **Fabian Soeffker** and **Yvonne Leye** for their friendship and taking care of the plants.

My thanks and appreciation also go to **Dr. Sascha Offermann** for his constructive suggestions.

My sincere gratitude and appreciation go to the financial support of the Deutsche Akademische Austauschdienst (**DAAD-German Academic Exchange Service**) - funding program No. 57048249.

I would like to express most profound thanks to **Dr. Ariel Turcios**, **Yvana Glasenapp**, **Isabell Rupp** and **Johann Hornbacher** and former working group members **Dr. Felix Hirschmann**, **Dr. Christian Boestfleisch** and **Dr. Galal Khames** for their technical support and helping to work in a convenient working environment.

Above ground, I would like to thank my husband **Md Haque**, and my children **Md Shafinnun Haque** and **Md Rhahimun Haque** for their love, pain stacking support and kept me going during the tough time of the work.

# CURRICULUM VITAE

## PERSONAL INFORMATION

---

Most. Shanaj Parvin

Karl Wiechert Allee 15, 30625, Hannover, Germany.

m.parvin@botanik.uni-hannover.de

Nationality: Bangladeshi

Date of Birth: 10.02.1981

Birth Place: Panchagarh, Bangladesh

## EDUCATION

---

- |                   |  |
|-------------------|--|
| 10.2014 – 09.2018 | <b>PhD in Natural Science</b><br>Gottfried Wilhelm Leibniz University Hannover, Hanover, Germany<br>Discipline: Biology<br>PhD thesis title: The functional characterization of AtStr5, a member of the sulfurtransferase/rhodanese family of <i>Arabidopsis thaliana</i> , and its arsenic phytoremediation studies |
| 09.2011 – 08.2013 | <b>Master of Science in Plant Biotechnology</b><br>Specialization: Molecular Plant Breeding and Pathology<br>Wageningen University, Wageningen, The Netherlands  |
| 07.2005 – 07.2007 | <b>Master of Science in Biotechnology, study leave for MSc until 11-07-2007 including master research at the employing institution (BARI).</b><br>Bangladesh Agricultural University, Mymensingh (Bangladesh)  |
| 11.1999 – 06.2005 | <b>Bachelor of Science in Agriculture</b><br>Bangladesh Agricultural University (BAU)<br>2202 Mymensingh (Bangladesh)  |
| 08.1997–08.1999   | <b>Higher Secondary Certificate Examination</b><br>Panchagarh Women's College (Bangladesh)   |
| 01.1988–07.1997   | <b>Secondary School Certificate Examination</b><br>Hara Dighi High School (Bangladesh)   |
-

## LIST OF PUBLICATIONS:

**S. Parvin, E. Haque, M. S. Haque and M. Al-Amin. 2007.** Study of Genetic Diversity of Maize (*Zea mays*) inbred lines through RAPD Markers. Prog. Agric 18 (1): 19-25.

**E. Haque, S. Parvin, M. Al-Amin and M. S. Haque. 2007.** Study of genetic diversity of Brinjal (*Solanum melogena L.*) genotypes by RAPD markers. Prog. Agric 18 (1): 67-74.

**E. Haque, S. Parvin, M. T. Rahman, R. Islam, F. Alam M. S. Abedin and M. S. Rahman. 2009.** Genetic diversity of Potato (*Solanum tuberosum L.*) varieties through RAPD markers. Eco-friendly Agril. J. 2 (5): 559-563.

**F. Akhter, M. S. Parvin, M.E. Haque, M. S. Alam and Maniruzzman 2009.** Rooting and acclimatization of Dendrobium Orchid. Eco-friendly Agril. J. 2 (3): 442-446.

**M. M. Rahim, M. E. Haque, Maniruzzman, M. S. Parvin, A. T. M. T. Islam and R. Islam. 2009.** Biochemical features of winter Tomato genotypes. Intl. J. BioRes. 6 (4): 53-56.

**P. Most and J. Papenbrock. 2015.** Possible roles of plant sulfurtransferases in detoxification of cyanide, reactive oxygen species, selected heavy metals and arsenate. Molecules 20: 1410-1423.